Volume 6, Issue 5, 2024

Print ISSN: 2663-1024
Online ISSN: 2663-1016

EURASIA JOURNAL OF SCIENCE AND TECHNOLOGY

Eurasia Journal of Science and Technology

Volume 6, Issue 5, 2024

Published by Upubscience Publisher

Eurasia Journal of Science and Technology
Print ISSN: 2663-1024 Online ISSN: 2663-1016
Email: info@upubscience.com
Website: http://www.upubscience.com/

Table of Content

Eurasia Journal of Science and Technology
ISSN: 2663-1016
DOI: 10.61784/ejst3028

FAHP-BASED SINGLE-MOUNTED FIRE STRIKE CAPABILITY MODELING STUDY

XiaoYan Cheng[1], GuoZhen Yang[1*], Hui He[2]
[1]Department of Weapon and Control, Army Academy of Armored Forces, Beijing 100072, China.
[2]The Fundermental Department of Army Academy of Armored Forces, Beijing 100072, China.
Corresponding author: GuoZhen Yang, Email: 94180102@qq.com

Abstract: Modern war forms are constantly evolving, and new types of weapons are emerging one after another, but the ground assault force represented by tanks and armored vehicles is still the main combat equipment. This paper focuses on the tanks and armored vehicles with fire strike capability, builds the index system of single-mounted fire strike capability, determines the weight of the indexes by using fuzzy analytic hierarchy process (FAHP), establishes the assessment model of the single-mounted fire strike capability of the ground assault force, improves and optimizes the real-war maneuver, makes the maneuver effect close to the real war, and provides support for the realization of the autonomous search, decision-making and striking against the enemy targets.
Keywords: FAHP; Single-mounted firepower; Assessment indicator system; Strike capability

1 INTROCUDTION

Modernized war patterns are constantly evolving, and quantitative maneuver of the combat process is needed before the initiation of combat. Single-mounted weapon system is the basic unit of simulation, and its data accuracy is directly related to the accuracy of the results of the maneuver, so the maneuver should be a combat single-mounted autonomy to attempt the combat mission as the goal, to achieve the effect of autonomous search and decision-making to strike the enemy target. In this paper, based on the effect of single-mounted weapon system strikes in the actual war environment, the degree of destruction caused to the target from the discovery of the target to the launch of one or more rounds of artillery shells within a unit of time, as a basis for evaluating the strength of single-mounted fire striking capability of the ground assault force, the fuzzy analytic hierarchy process (FAHP) is used to evaluate the various stages of tank combat from discovering the target to tracking and aiming at the target to destroying the target, to establish a set of assessment models of the single-mounted fire striking capability of the ground assault force, to enhance the realism of combat simulation, and to assist the commanders of the basement armored detachments in simulating the war process and decision-making [1-2].

2 SINGLE-MOUNTED FIREPOWER STRIKE CAPABILITY AND ITS CHARACTERISTICS

Single-mounted fire strike capability is a modern military force with strong fire destructive capability, coordinated operation capability, rapid reaction capability battlefield adaptability, and is one of the important forces in modern war. Specifically, single-mounted fire strike capability refers to the ground assault force in different combat environments, the use of a single vehicle's artillery, machine guns, information equipment, reconnaissance equipment, fire control systems, protective devices, maneuvering devices, and other types of weaponry on the target to implement the ability to fire strike, which mainly contains the fire destruction capability, coordinated operation capability, rapid reaction capability, battlefield adaptability, as shown in Figure 1.

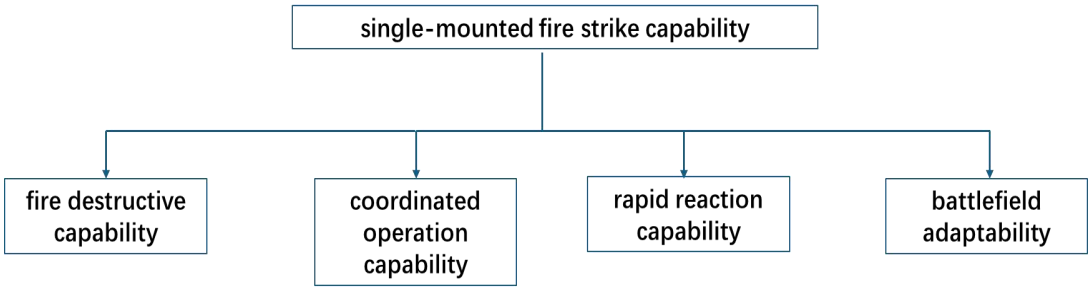

Figure 1 Schematic of Single-Mounted Fire Strike Capability

3 INDICATOR SYSTEM FOR ASSESSING THE FIRE-STRIKE CAPABILITY OF SINGLE-MOUNTED WEAPON SYSTEMS

Single-mounted equipment refers to the main weaponry on a single vehicle of the ground assault force, which directly determines the fire-strike capability of a single vehicle. The establishment of the indicator system is the fundamental

work of assessing the fire strike capability, as the evaluation standard of the single-mounted fire strike capability of the ground assault force, it has an important status in the assessment, which is directly related to the rationality and accuracy of the assessment results. Therefore, when constructing the index system, it needs to be subdivided into multiple aspects in order to comprehensively integrate the single-mounted strike capability [3-4].

This paper takes tanks as the main body to study the single-loaded fire strike capability, tanks as the main fire assault equipment on the ground at present, the factors affecting the fire strike capability of the region, personnel, environment, equipment situation, etc., but the general analysis, the main determining factors are the three aspects of projectile striking effect, shooting time, and probability of destruction. Therefore, the first-level evaluation index of firepower striking capability can be divided into projectile striking effect, shooting response time, and probability of destruction. Each level of evaluation indicators can be divided into a number of sub-indicators, i.e., secondary evaluation indicators (see Figure 2), of which the first-level evaluation indicators of the effectiveness of projectile strikes can be divided into the type of artillery shells, caliber of artillery, protection capabilities, environmental factors; the first-level evaluation indicators of the firing response time can be divided into the detection capability, the fire control system, the tracking ability; the first-level evaluation indicators of the probability of destruction can be divided into: the shooting mode, the distance, the quality of the combatants, the mobility ability. The probability of destruction can be divided into: firing mode, distance, quality of combatants, maneuvering ability.

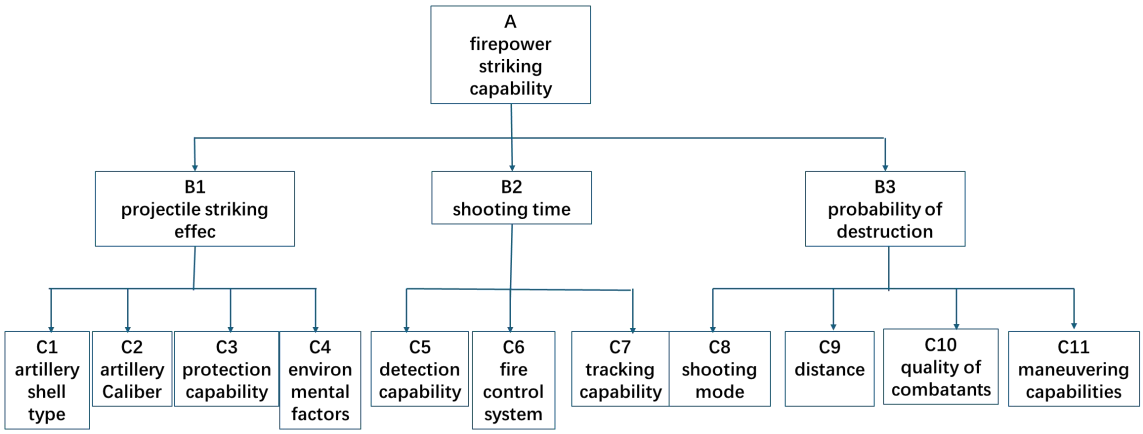

Figure 2 Indicator System for Single-Mounted Fire Capability

4 SINGLE-MOUNTED FIRE STRIKE CAPABILITY ASSESSMENT MODEL BASED ON FAHP

FAHP is a decision analysis method that combines qualitative and quantitative, and is widely used in decision problem analysis, prioritization, and performance evaluation in various fields. The FAHP-based operation loop capability analysis integrates the detection, decision-making, and striking in the operation loop into the process of striking the target caused by a single-mounted weapon system, and a comprehensive and objective evaluation is used to assess the capability of single-mounted fire strikes. In the single-mounted fire strike capability model, to determine the weight of each factor on the target, the following methods can generally be used:

(1) Establish single-mounted fire strike capability indicator system: according to the operational requirements and single-loaded fire strike capability indicator system, the single-loaded fire strike capability indicator system is divided into three levels, as shown in Figure 2.

(2) Determine the weight of each level of indicators: according to the single-mounted fire strike capability indicator system, establish the single-mounted fire strike capability evaluation indicator system, for the target A, through the two-by-two comparison of the factors B_1, B_2, B_3 and select the scale as in Table 1, the establishment of the matrix A-B; similarly for the B_1, B_2, B_3, respectively, the establishment of the judging matrix B_1-C, B_2-C, B_3-C, where, a_{ij} denotes the relative importance of the ith factor to the jth factor.

Table 1 Scales and Their Meanings

Scale	Meaning
1	Both elements are of equal importance
3	One element is slightly more important than the other
5	One element is significantly more important than the other
7	One element is more strongly important than the other
9	One element is more important than the other extreme
2，4，6，8	If the difference between the two elements is in between, take the middle value

reciprocal	If the ratio of the importance of elements i and j is a_{ij}, then the ratio of the importance of elements *i* and *j* is $a_{ij}=1/a_{ji}$

(3) Calculate the weights of the factors based on the fuzzy judgment matrix and normalize the w_i

$$w_i = \frac{\left(\prod_{j=1}^{n} r_{ij}\right)^{\frac{1}{n}}}{\sum_{i=1}^{n}\left(\prod_{j=1}^{n} r_{ij}\right)^{\frac{1}{n}}}$$

The consistency test is calculated based on the characteristic root $\lambda_{\max} = \frac{R_w W}{W}$ of the judgment matrix to verify whether the calculated weights are in line with the objective reality, and the judgment criterion is: $CI = \frac{\lambda_{\max} - n}{n\text{-}1}$,when the consistency ratio $CR = \frac{CI}{RI}$ <0.1, it means that the relative importance of each factor to the goal is consistent, so that the consistency test is passed. RI is the random consistency index, which is a pre-calculated value depending on the number of guidelines.

(4) Determine the weight of each factor: according to the principle of fuzzy comprehensive judgment, establish the single-level judgment matrix in the single-unit fire strike capability index system, that is, the comprehensive judgment matrix of the single target.

(5) Calculate fuzzy sets $B_x = W_x \cdot R_x$, let $R = (B_1, B_2, B_3)^T$

(6) Further single-mounted fire strike capability target tier evaluations: $H=W \cdot R$

(7) According to the impact system of evaluation indicators, you can establish the evaluation set V, such as Table 2, according to V = {100,90,80,60,0}, to find the comprehensive evaluation score: $S=H \cdot V^T$, according to the score to determine the single-loaded fire strike capability.

Table 2 Single-mounted Fire Strike Capability Evaluation Set

Degree of target damage	Attack and destroy	Loss of firepower and mobility at the same time	Loss of firepower capability	Loss of mobility	In good conditi on
Damage index	100	90	80	60	0

5 SIMULATION CASE ANALYSIS

5.1 Case Analysis

In a position attack red-blue confrontation process, the Blue Army in the front of the position sent a certain type of infantry fighting vehicle to carry out reconnaissance alert strike mission. At a certain moment, the enemy vehicle stands still in the bunker, scouting the battlefield situation, obtaining data through sensors, including artillery type, caliber, effective range, speed, carrying ammunition, position and other information.

The concrete evaluation method is divided into three steps: single index analysis to determine the impact of factors on the degree of damage alone; The multi-factor comprehensive influence result is analyzed, and the formula is summarized to link each influence factor and comprehensively evaluate the single-load firepower strike capability.

5.2 Single-mounted Fire Strike Capability Assessment

According to the degree of influence of evaluation indicators, the evaluation set can be established: $V = \{v_1, v_2, ..., v_m\}$, m is the total number of evaluation grades. Referring to the domestic and foreign common evaluation grading, we can define the evaluation set of single-mounted fire strike capability of ground assault force as follows: V = {intact, loss of fire and mobility, loss of fire capability, loss of mobility, intact}.

Experts in the field of armored chassis, firepower, and systems are invited to study and judge the evaluation indexes of the ground assault force at all levels. Each factor level has a certain influence on the evaluation indicators of the evaluation set, which can be expressed by the affiliation function R_i. Define the affiliation of factor u_i to evaluation level v_j as r_{ij}, then the single factor evaluation set of u_i is $R_i = (r_{i1}, r_{i2}, \cdots r_{im})$. Judging each factor, the fuzzy relationship matrix $R=(r_{ij})_{m\times n}$, i=1, 2, ⋯, m; j=1, 2, ⋯, n can be constructed from the factor set U to the evaluation set V. Based on

the evaluation index system of Fig. 1, the weights of each index are determined, and the resulting judgment matrix is shown in Tables 3 to 6.

Table 3 Judgment Matrix of A-B and Corresponding Weight Vector W

A	B_1	B_2	B_3	W
B_1	1	2	1/3	0.249
B_2	1/2	1	1/3	0.157
B_3	3	3	1	0.594
λ max =3.05 CR=0.027<0.1				

Table 4 Judgment Matrix of B_1-C and Corresponding Weight Vector W_1

B_1	C_1	C_2	C_3	C_4	W_1
C_1	1	3	4	5	0.540
C_2	1/3	1	3	3	0.255
C_3	1/4	1/3	1	1/2	0.088
C_4	1/5	1/3	2	1	0.117
λ max =4.15 CR=0.049<0.1					

Table 5 Judgment Matrix of B_2-C and Corresponding Weight Vector W_2

B_2	C_5	C_6	C_7	W_2
C_5	1	4	3	0.630
C_6	1/4	1	2	0.219
C_7	1/3	1/2	1	0.152
λ max =3.11 CR=0.053<0.1				

Table 6 Judgment Matrix of B_3-C and Corresponding Weight Vector W_3

B_3	C_8	C_9	C_{10}	C_{11}	W_3
C_8	1	2	3	3	0.453
C_9	1/2	1	2	3	0.289
C_{10}	1/3	1/3	1	1/2	0.107
C_{11}	1/3	1/3	2	1	0.151
λ max =4.04 CR=0.012<0.1					

According to the calculation results, it can be seen that the consistency ratio of each judgment matrix CR < 0.1, which fully meets the consistency test requirements. The single-factor indicators affecting the single-mounted fire strike capability are evaluated by 10 experts respectively, and the corresponding affiliation r_{ij} is calculated. r_{ij} is the ratio of the number of times the indicator u_i is rated as v_j to the total number of experts, and the evaluation results are shown in Table 7.

Table 7 Expert Evaluation Results

r_{ij}	C1	C2	C3	C4	C5	C6	C7	C8	C9	C10	C11
100	0.2	0.3	0.1	0	0	0.3	0.3	0.3	0.5	0.1	0.4
90	0.3	0.4	0.2	0.2	0.2	0.4	0.3	0.5	0.4	0.4	0.4
80	0.3	0.2	0.3	0.4	0.5	0.2	0.2	0.2	0.1	0.3	0.1
60	0.2	0.1	0.3	0.2	0.2	0.1	0.2	0	0	0.1	0.1
0	0	0	0.1	0.2	0.1	0	0	0	0	0	0

Based on the evaluation of each factor by the expert members, a fuzzy evaluation judgment matrix is obtained:

$$R_1=\begin{bmatrix}0.2 & 0.3 & 0.3 & 0.2 & 0\\ 0.3 & 0.4 & 0.2 & 0.1 & 0\\ 0.1 & 0.2 & 0.3 & 0.3 & 0.1\\ 0 & 0.2 & 0.4 & 0.2 & 0.2\end{bmatrix}$$

$$R_2=\begin{bmatrix}0 & 0.2 & 0.5 & 0.2 & 0.1\\ 0.3 & 0.4 & 0.2 & 0.1 & 0\\ 0.3 & 0.3 & 0.2 & 0.2 & 0\end{bmatrix}$$

$$R_3=\begin{bmatrix}0.3 & 0.5 & 0.2 & 0 & 0\\ 0.5 & 0.4 & 0.1 & 0 & 0\\ 0.1 & 0.1 & 0.3 & 0.1 & 0\\ 0.4 & 0.4 & 0.1 & 0.1 & 0\end{bmatrix}$$

Fuzzy sets for each indicator layer:

$$B1=W1 \cdot R1=(0.193 \quad 0.305 \quad 0.289 \quad 0.016 \quad 0.012)$$

$$B2=W2 \cdot R2=(0.286 \quad 0.260 \quad 0.389 \quad 0.178 \quad 0.063)$$

$$B3=W3 \cdot R3=(0.352 \quad 0.445 \quad 0.167 \quad 0.042 \quad 0)$$

Get:

$$R=\begin{bmatrix}B_1\\ B_2\\ B_3\end{bmatrix}=\begin{bmatrix}0.193 & 0.305 & 0.289 & 0.016 & 0.012\\ 0.286 & 0.260 & 0.389 & 0.178 & 0.063\\ 0.352 & 0.445 & 0.067 & 0.042 & 0\end{bmatrix}$$

Based on the results of the Tier 1 evaluation, further single-mounted fire strike capability target tier evaluations were conducted:

$H=W \cdot R=(0.326 \quad 0.354 \quad 0.216 \quad 0.094 \quad 0.013)$

$V=\{100, \ 90, \ 80, \ 60, \ 0\}$

Finding the comprehensive evaluation score: $S=H-VT=75.67$

According to the evaluation results, in accordance with the principle of maximum affiliation, it can be seen that the single-loaded fire-strike capability of the ground assault equipment is evaluated to be able to cause the enemy to lose its fire-strike capability, which indicates that the fire-strike capability of the evaluated ground assault equipment is high.

6 CONCLUSION

This paper establishes a single-mounted fire strike capability assessment model of ground assault force based on FAHP, which is an effective military assessment tool for scientific assessment and control of military systems and can be used to improve the combat simulation software such as weapon projection and computer simulation, which can make the results of the projection closer to the actual combat and assist the commanders to make correct decisions, which can help to improve the combat effectiveness. At the same time, this model is based on tanks and armored vehicles to study the single-armor fire strike capability, after the model is established, through experimental analysis and modification of its parameters, it can assess the purpose of the air, sea and long-range fire strike capability, and this model is combined with artificial intelligence to realize the weapon system autonomy to carry out combat tasks, and to promote the weaponry to the intelligent progress.

COMPETING INTERESTS

The authors have no relevant financial or non-financial interests to disclose.

REFERENCE

[1] Zhou Liyao, Liu Xiaofang, Wang Yaguang, et al. Assessment of missile equipment fire strike capability based on improved FAHP. 2022.
[2] Zhao Manyun, Zhang Lei. Composite FAHP's assessment method of missile brigade's overall NBC defense capability. Firepower and Command and Control, 2022, 47(11): 5.
[3] Li Suying, Tian Ya, Wu Yongli. Research on risk assessment of railroad engineering projects based on FAHP model. Journal of Railway Engineering, 2019, 36(7): 8.
[4] Zhang Yaolong, Ruan Yongjun, Li Zhen. Research on the assessment of synthetic brigade's equipment guarantee capability based on topable cloud. Command Control and Simulation, 2021, 43(6): 71-77.

Eurasia Journal of Science and Technology
ISSN: 2663-1016
DOI: 10.61784/ejst3030

APPLICATION OF STATISTICS IN THE APPLICATION OF CELL THERAPY RESEARCH

RongMing Zhou
JIU ZHI TANG MAKER (Beijing) Cell Technology Co., Ltd, Beijing 102600, China.
Corresponding Email: nicetomeetyouhere@163.com

Abstract: This article explores the application of statistics in cell therapy research, especially in the fields of immunotherapy and neural repair. The article emphasizes the key role of statistical methods in evaluating treatment effects, managing risks, and designing rational clinical trials. Through tools such as survival analysis, hypothesis testing, and statistical models, researchers can intuitively assess patients' survival and progression-free survival, as well as predict treatment effects and adverse reactions. The article also discusses the challenges of randomized controlled trial design, multicenter studies, and the importance of data management and analysis. Finally, the article points out the value and prospects of statistics in cell therapy research, while also proposing the limitations of current research and future directions.
Keywords: Cell therapy; Statistical application; Survival analysis; Hypothesis testing; Randomized controlled trial

1 INTRODUCTION

1.1 Research Background

Cell therapy is an important breakthrough in modern biomedical, especially in the fields of immunotherapy and nerve repair. The chimeric antigen receptor T cell (Car-T) therapy and stem cell therapy represent the two mainstream directions of cell therapy, especially when treating complex diseases such as cancer and nervous system diseases. However, with the deepening of research, the clinical transformation of cell therapy faces many challenges, including the uncertainty of the curative effect, the complexity of the treatment standards, and the management of adverse reactions [1].
Statistical methods provide important support for solving these problems. Through accurate data analysis, statistical help researchers evaluate the efficacy, management risks, and design more reasonable clinical trials. This not only improves the scientific and repeatability of research, but also promotes the smooth transition from laboratory to the clinical transition from laboratory.

1.2 Research Objectives

This review aims to explore the application of statistics in cell therapy research, focusing on the critical role of statistical methods in various phases of cell therapy. By reviewing current literature, this paper will introduce the application of common statistical tools such as survival analysis, hypothesis testing, and statistical models in cell therapy, evaluating their contributions to clinical trial design, efficacy assessment, and data management, thereby providing a reference for future cell therapy research.

2 STATISTICAL APPLICATIONS IN CELL THERAPY

2.1 Survival Analysis

In cell therapy research, survival analysis is a crucial statistical method primarily used to evaluate patient survival and progression-free survival (PFS) after treatment[2]. The Kaplan-Meier curve is a common tool that intuitively displays the survival outcomes of patients in different treatment groups by plotting cumulative probability curves of survival time. For example, in studies of chimeric antigen receptor T-cell (CAR-T) therapy for relapsed or refractory multiple myeloma, the Kaplan-Meier curve is used to assess overall survival (OS) and progression-free survival after CAR-T cell treatment[3]. Through this method of analysis, researchers can intuitively understand the survival differences among various patient groups after treatment.
In addition, the Cox proportional hazards regression model is often applied in survival analysis to evaluate the impact of various factors, such as age, baseline health status, and CAR-T cell expansion, on patient survival time. Through this model, researchers can analyze which factors are significantly associated with long-term survival in cell therapy, providing important references for the development of personalized treatment plans [4].

2.2 Hypothesis Testing

Hypothesis testing is widely applied in evaluating the efficacy of cell therapy, particularly when comparing the efficacy differences of various treatment regimens. Common hypothesis testing methods include the T-test and the Chi-square

test. The T-test is primarily used for comparing intergroup differences of continuous variables (such as blood indicators or cell counts), while the Chi-square test is used for comparing differences in categorical variables (such as the rate of efficacy achievement) [5].

In cell therapy research, researchers often use the T-test to assess changes in biomarkers in patients' blood before and after treatment, such as changes in the concentration of inflammatory factors (IL-6, TNF-α). Through these statistical tests, researchers can determine whether the treatment significantly improved the physiological state of patients. Additionally, the Chi-square test is frequently used to analyze the proportions of patients achieving complete or partial remission after receiving cell therapy, thereby evaluating the efficacy differences of different treatment methods [6].

2.3 Statistical Models

Statistical models play a vital role in cell therapy research, especially in efficacy prediction and risk assessment. Linear regression and logistic regression are the most commonly used statistical models for analyzing the multidimensional influencing factors of cell therapy efficacy [7]. The linear regression model is used to analyze the relationship between continuous variables, while the logistic regression model is widely applied to analyze categorical outcomes, such as whether patients experience adverse reactions or whether the treatment meets the target.

In CAR-T therapy, logistic regression models are used to predict whether patients will experience severe adverse reactions such as cytokine release syndrome (CRS). Researchers construct risk models by analyzing patients' baseline characteristics and cell levels before and after treatment to help predict and intervene in potential severe adverse reactions in advance. The application of these models enhances the safety of treatment and helps optimize treatment strategies.

3 CLINICAL TRIAL DESIGN IN STATISTICS

3.1 Randomized Controlled Trial Design

Randomized controlled trials (RCTs) are considered the "gold standard" for evaluating efficacy in cell therapy research. Through RCTs, researchers can randomly assign patients to either a treatment group or a control group, avoiding potential biases and ensuring a scientific assessment of treatment effects. RCTs have been widely applied in CAR-T cell therapy and neural repair treatments [8]. For example, in studies of CAR-T therapy for relapsed multiple myeloma, patients are assigned to different treatment groups through a rigorous randomization process, and the progression-free survival (PFS) and overall survival (OS) of patients are evaluated using statistical tools such as Kaplan-Meier survival curves. However, despite being the main tool for efficacy assessment, RCTs in cell therapy often face numerous challenges. First, cell therapy involves complex individual patient differences, making standardized treatment difficult. Second, adverse reactions in cell therapy, such as cytokine release syndrome (CRS), have not been fully understood in terms of their impact on treatment effectiveness and patient safety, adding to the complexity of RCTs [9].

3.2 Challenges of Multi-Center Studies

Multi-center clinical trials are an important means for validating the effects of cell therapy. Particularly in neural repair and CAR-T treatment research, more trials are spanning multiple research centers to increase sample size and improve the generalizability of results. However, multi-center studies also face some unique statistical challenges. Due to significant variations in data collection and processing methods between different centers, there may be heterogeneity in study outcomes. To reduce this heterogeneity, researchers often use stratified randomization in the trial design to ensure balanced patient distribution across centers [10]. Additionally, data integration and analysis often require advanced statistical methods.If broad generalized linear mixed models (GLMM) are used to address systemic differences between various centers[11].

Additionally, the complexity of cell therapy further exacerbates the challenges of multi-center trials. There is significant variation in patient responses to treatment, and rigorous quality control of cell products and standardization of therapeutic procedures are required. Even within the same research center, different cell therapy protocols or experimental designs can significantly impact the outcomes. Therefore, in multi-center research, researchers need to ensure the rigor of trial design and utilize effective statistical analysis tools to handle complex heterogeneity[12].

4 CASE STUDIES IN STATISTICAL ANALYSIS

4.1 Statistical Analysis of CAR-T Therapy

Chimeric Antigen Receptor T-cell (CAR-T) therapy is one of the cutting-edge technologies in cellular immunotherapy, especially showing remarkable efficacy in treating hematological malignancies such as acute B-lymphoblastic leukemia (B-ALL) and multiple myeloma. In these studies, statistical methods play a crucial role in efficacy evaluation and adverse reaction monitoring.

In BCMA-targeted CAR-T therapy research, Kaplan-Meier survival curves are used to evaluate patients' progression-free survival (PFS) and overall survival (OS), revealing differences in survival rates among patients in different treatment groups through survival analysis[13]. Additionally, the Cox proportional hazards model is employed

to analyze the relationship between patients' baseline indicators, changes in cytokines pre- and post-treatment, and efficacy. For example, studies indicate a positive correlation between the expansion of CAR-T cells in peripheral blood and patient efficacy.

Moreover, adverse reactions in CAR-T therapy, such as Cytokine Release Syndrome (CRS), are predicted using statistical models. Researchers use logistic regression models to evaluate the impact of baseline data on the incidence of adverse reactions.

To identify factors significantly associated with CRS risk through multivariate analysis, which helps optimize treatment plans and improve safety.

4.2 Statistical Applications in Neurological Treatments

In cell therapy for neurological diseases, cell types like mesenchymal stem cells and olfactory ensheathing cells are widely used for the repair of neural injuries. Statistical methods are applied to evaluate the efficacy and safety of these treatments [14]. For instance, in studies of neurological disorders such as spinal cord injuries and stroke sequelae, Kaplan-Meier curves are used to analyze the recovery of neural functions in patients, while Cox regression models are employed to assess multiple factors affecting treatment outcomes, including cell type, dosage, and disease duration [15].

Although some studies show the potential of cell therapy in neurological diseases, some multicenter randomized controlled trials (RCTs) have failed to demonstrate significant efficacy. For example, certain stem cell therapies have shown improvement in neural functions in small sample studies but did not significantly improve quality of life or neural functions in large multicenter studies. This suggests that further optimization of treatment plans and standardization of treatment processes may be key to enhancing efficacy [16].

5 DATA MANAGEMENT AND ANALYSIS

5.1 The Importance of Data Collection

In the research of cell therapy, data collection is a crucial aspect that determines the success of clinical trials. Scientific and systematic data collection and management ensure more accurate evaluation of treatment efficacy and help in timely detection of adverse reactions [17]. For complex therapies like CAR-T, researchers need to comprehensively collect diverse information such as patients' baseline data, cell expansion during treatment, and immune responses. This data not only aids researchers in evaluating short-term efficacy but also provides essential insights for analyzing long-term efficacy and survival rates [18].

Modern data collection tools, such as Electronic Data Capture (EDC) systems, have greatly improved the accuracy and completeness of data. Furthermore, data collection in multicenter studies requires special attention to standardization. Different centers may have varying data collection methods, and it is crucial to ensure that standards and data formats are consistent across all centers to facilitate subsequent data integration and analysis [19].

5.2 Data Modeling and Analysis

Data modeling is a critical step in the analysis of cell therapy data, helping researchers extract valuable information from complex clinical data. Common modeling methods include linear regression, logistic regression, and survival analysis models. Through these statistical models, researchers can predict patients' treatment responses, efficacy, and potential adverse reactions.

In CAR-T therapy, data modeling is used not only for efficacy prediction but also for assessing treatment safety. For example, researchers use logistic regression models to predict which patients have a higher risk of cytokine release syndrome (CRS) and intervene early to reduce the treatment risk. In the context of cell therapy for neurological diseases, data modeling is also used to analyze the relationships between different cell types, doses, and efficacy, helping to optimize treatment plans [20].

6 CONCLUSION

6.1 The Value and Prospects of Statistics

Statistics hold critical value in cell therapy research. Through survival analysis, hypothesis testing, and statistical models, researchers can accurately evaluate the efficacy of cell therapies, optimize clinical trial design, and improve treatment safety [21]. For instance, Kaplan-Meier curves provide an intuitive illustration of progression-free survival and overall survival, aiding researchers in quickly identifying differences between treatment groups.

In addition, statistical tools such as Cox regression models are also used to analyze the impact of multiple factors on treatment outcomes, providing theoretical support for personalized therapy. As the application of cell therapy continues to expand, such as CAR-T cell therapy and neural repair therapy, the role of statistics will become more widespread [22]. In the future, combining machine learning and big data technologies, statistics will further enhance data processing capabilities in cell therapy, thereby promoting improvement in treatment effectiveness and ensuring safety.

6.2 Limitations and Prospects of the Study

Although statistics provide strong support for cell therapy research, some challenges remain. First, different statistical models are suitable for different types of research, and inappropriate model selection may lead to errors. Second, in multi-center studies, the issue of data heterogeneity between different centers is still a major challenge, requiring more flexible statistical models to solve [23].

Future research should further optimize the application of statistics in cell therapy, especially in adverse reaction prediction and data integration. Additionally, researchers should also focus on how to use emerging statistical techniques and tools to handle increasingly complex clinical data to improve the efficiency and efficacy of cell therapy [24].

By continuing to advance high-quality randomized controlled trials and more precise statistical analyses, statistics will provide stronger support for the future development of cell therapy.

COMPETING INTERESTS

The authors have no relevant financial or non-financial interests to disclose.

REFERENCES

[1] Zu Cheng, Wang Kexin, Zhang Qiqi, et al. Clinical observation of BCMA-targeted chimeric antigen receptor T cell therapy for relapsed/refractory multiple myeloma with hemophagocytic syndrome. Journal of Zhejiang University (Medical Edition), 2022, 51(02):160-166.

[2] Chen Y, Jian T, Shen Y. Immune Checkpoint Inhibitors in Lung Cancer// Wuhan Zhicheng Times Cultural Development Co., Ltd.. Proceedings of 2nd International Conference on Biomedical Engineering, Healthcare and Disease Prevention (BEHDP 2022). Capital Medical University; Guizhou Medical University; Shenzhen College of International Education, 2023: 10.

[3] Guo Huanxu, Fan Dan, Zhang Jingyi, et al. Comparative efficacy of first-line immunosuppression and hematopoietic stem cell transplantation in treating hepatitis-associated aplastic anemia. Journal of Clinical Hematology, 2024, 37(05): 343-348.

[4] Wang Hongjuan, Hu Wen, Ding Yuan, et al. Meta-analysis of efficacy of autologous cell transplantation in the treatment of stable vitiligo. Chinese Journal of Dermatovenerology of Integrated Traditional and Western Medicine, 2024, 23(01): 22-29.

[5] Liu Yukai, Liu Qi, Ma Cong, et al. Effect of anti-CD19 chimeric antigen receptor T-cell therapy on pediatric acute B-lymphoblastic leukemia. Chinese Medical Innovation, 2023, 20(16): 43-47.

[6] Zhang Zhanqiang, Zhang Gailing, Li Wenqian, et al. Relationship between platelet count and the efficacy of CD19-CAR-T cell therapy in refractory/relapsed acute B lymphoblastic leukemia. Journal of Clinical Hematology, 2022, 35(09): 674-676+679.

[7] Huang Hongyun, Chen Lin, Mao Gengsheng, et al. Progress in clinical cell therapy in neurorestoratology. Chinese Journal of Cellular and Stem Cell Research (Electronic Edition), 2022, 12(01): 1-7.

[8] Wu Qiaozhu, Tian Chunfang. Research progress in the treatment of intrauterine adhesion. Guide to Women and Children's Health, 2024, 3(18): 23-26+30.

[9] Guo X, Sheng X. Drug discovery of PD-L1 inhibitor Atezolizumab// Wuhan Zhicheng Times Cultural Development Co., Ltd.. Proceedings of 2nd International Conference on Biomedical Engineering, Healthcare and Disease Prevention (BEHDP 2022). The university of Strathclyde;The University of Melbourne, 2023: 8.

[10] Xu Xiaoming, Xia Yunlong, Xia Linying, et al. Advances in Non-Pharmacological Treatment of Heart Failure with Preserved Ejection Fraction. Chinese Journal of Interventional Cardiology, 2024, 32 (09): 528-534.

[11] Zhang Weijie, Zhang Hong. Research Progress on the Relationship between Iron Deficiency and Heart Failure. Journal of Cardiovascular and Cerebrovascular Diseases with Integrated Traditional and Western Medicine, 2024, 22 (18): 3343-3346.

[12] Li Zhe, Guo Guangling, Li Ping, et al. Network Meta-Analysis of the Efficacy of Mesenchymal Stem Cells from Different Sources in the Treatment of Animal Models of Premature Ovarian Failure. Chinese Journal of Tissue Engineering Research, 2024 1-12.

[13] Zhao Na, He Sheng, Shi Linan. Effects of 40 Hz Rhythmic Stimulation on Alzheimer's Disease and Cognitive Function. Progress in Biochemistry and Biophysics, 2024, 1-15.

[14] Guo X, Sheng X. Drug discovery of PD-L1 inhibitor Atezolizumab// Wuhan Zhicheng Times Cultural Development Co., Ltd.. Proceedings of 2nd International Conference on Biomedical Engineering, Healthcare and Disease Prevention (BEHDP 2022). The university of Strathclyde;The University of Melbourne, 2023: 8.

[15] Yu Haiyin, Li Xiaoning. Research Progress on Acupuncture Promoting Cell Proliferation and Differentiation after Spinal Cord Injury. Journal of Clinical Acupuncture, 2024, 40 (09): 96-101.

[16] Peng Jianhong, He Jiahua, Liao Leen, et al. Advances in the Clinical Application of Precision Medicine Testing in Hepatic Metastasis of Colorectal Cancer. Chinese ScienceBulletin, 2024, 1-11.

[17] Cao Xiaoshan, Yang Beibei, Cong Binbin, et al. Advances in the Treatment of Brain Metastases in Triple-Negative Breast Cancer. Chinese Journal of Cancer, 2024, 34 (08): 777-784.

[18] Xu Haoran, Zhao Xiaoyi, Nie He, et al. Immunotherapy for Colorectal Cancer. Progress in Biochemistry and Biophysics, 2024, 1-22.

[19] Liu Qing, Su Tingting, Gao Jiaming, et al. Effects of Tianshan Chaopiao on Adipogenic and Osteogenic Differentiation of Adipose-Derived Stem Cells. Journal of Tongji University (Medical Science), 2024, 45 (04): 471-479.
[20] Lin Meiyu, Zhao Xilong, Gao Jing, et al. Mechanisms and Progress of the Anti-Aging Effects of Stem Cells on Ovarian Granulosa Cells. Chinese Journal of Tissue Engineering Research, 2024, 1-8.
[21] Ying Yu-jia, Tang Yong-min. Analysis of Prognostic Factors and Progress in Treatment of Infant Acute Lymphoblastic Leukemia. Chinese Journal of Pediatric Hematology and Oncology, 2024, 29 (04): 299-302.
[22] Liu Qiang, Liu Hua-qian, Liu Li, et al. Current Status and Prospects of Mesenchymal Stem Cell-Targeted Therapy for Premature Ovarian Insufficiency. Chinese Journal of Cell Biology, 2024, 46 (08): 1567-1579.
[23] Wang Xin-xin, He Ji-hui, Li Gang, et al. Effects of Triclosan on Biological Characteristics of Dental Pulp Stem Cells. Prevention and Treatment of Oral Diseases, 2024, 1-15.
[24] Zheng Zi-ling, Li Yuanyuan, Shan Yuan-hong. Advances in Research on Genetic Doping and Its Detection Technologies// International Bandy Federation (FIB), International Strength and Conditioning Association (ISCA), Macao Strength and Conditioning Association (MSCA), Chinese Bandy Association (CBF). The Proceedings of the 2023 Inaugural International Sports Science Conference by the Chinese Radio Orienteering and Direction Finding Association (CRSOA). Shanghai University of Sport; Shanghai Anti-doping Laboratory, Shanghai University of Sport, 2023: 22.

Eurasia Journal of Science and Technology
ISSN: 2663-1016
DOI: 10.61784/ejst3031

PERFORMANCE INVESTIGATION ON DEODORIZATION MATERIALS

LingYan Zhu, DaSen Luo, Teng Wu, Rong Xia, YeMing Sun*
Electrolux (Hangzhou) Domestic Appliances Co Ltd., Hangzhou 310000, Zhejiang, China.
Corresponding Author: YeMing Sun, Email: Ryan.Sun@electrolux.com

Abstract: The paper aims to create a design logical on gas removal material application for deodorization functions. Since the gas removal material varies by different type and different mechanism. Such as active carbon, silicon ball, photocatalyst and so on. Then we designed the performance test according to existing JEM standard, which is to evaluate air purifier performance on odor removal. Through the prototype design to add different purification materials one by one and test its performance to get the conclusion. Which is the active carbon materials have better removal efficiency of polar substance pollutants (formaldehyde and acetic acid), but the capability for non-polar VOCs removal (Ammonia) is weak. So compound active carbon materials maybe is a better choice for IAQ purification research to purify kinds of gas pollutant molecules.
Keywords: Deodorization; Active carbon; Photocatalyst; Air purifier

1 INTRODUCTION

Indoor air quality(IAQ) always being a hot topic that people focused on. For particle matter, such as PM1.0, PM2.5 and PM 10, we already have mature solution both on industry and domestic home appliances. We had PP, PET and PTFE materials to capture the particle matter due to mechanical and electrical effect[1]. But when referred to gas especially on odor, the mechanical will be much more complicated. Adsorb by active carbon is a direct and rapid way to removal the gas in the air. Adsorption has been classified as two types, which is physical adsorption[2] and chemical adsorption[3]. Physical adsorption is reversible and rapid, so it is easily to generate secondly pollutant due to the desorption[4]. Chemical adsorption is irreversible. Even it still has the situation on desorption[4], but the component desorbed is not the same as it is. Chemical adsorption is strong but not as fast as physical adsorption[3]. At the same time, the carbon filter itself has lifetime, not only with physical adsorption, but also with chemical adsorption.
Meanwhile, Titanium dioxide (TiO2) has attracted great attentions due to its low cost, minimal toxicity, advanced chemical stability, excellent performance and safety. It has been investigated to apply on purification area as photocatalyst Since Fujishima and Honda first used TiO2 for photolysis of water to produce hydrogen in 1972[5]. With the support of external light irradiance, electrons (e-) and holes (h+) generated, which migrate to the surface of TiO2. The electrons (e-) and holes (h+) can not only react with toxic and harmful organic substances, but also directly or indirectly convert the surrounding oxygen and water into ·OH with strong oxidation capacity by using its own oxidation reduction property, thus degrading toxic substances[6]. The whole reaction system is environmental friendly, but the reaction process is not fast and need to triggered by UV light.
This paper is to have a comparison test is to compare deodorization performance of different samples (Active Carbon, Silicon) with TiO2 in a DEMO, which is a prototype from Italy R&D. Get determination on the air purification prototype design on required carbon amount without or together with TiO2.

2 METHOD

2.1 Prototype Description

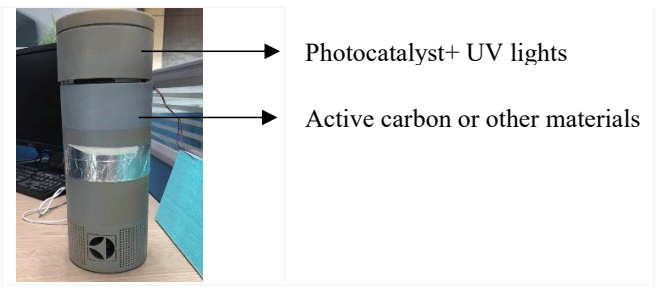

Figure 1 Prototype Display

2.1.1 Air purifier

Modified Air Purifier prototype which can use different materials as its filter which indicated in figure 1.

2.1.2 Filtration material

The filtration material we chosen for test is listed below and showed in figure 2.

1) VOC removal Active Carbon

Ingredient: Active carbon with formula additive which is special for VOC removal

2) Formaldehyde removal Active Carbon

Ingredient: Active carbon with formula additive which is special for formaldehyde removal

3) Common Active Carbon

Ingredient: Active carbon base without additive

4) Compound Active Carbon

Ingredient: Active carbon, attapulgite, diatom ooze, sepiolite. The last there kinds additive material are porous mineral material, which has large specific surface area, so they can absorb the gaseous pollutant and heavy metal in the gas. They have kinds of application in industrial purification, for example in edible oil purification, water purification etc.

Compound active carbon is the mixture of active carbon, attapulgite, diatom ooze, sepiolite. It is made of brightness ball, with diameter around 2mm.

5) Formaldehyde removal silicon ball

Ingredient: Silicon material is sphere ball base with vegetable source additive which can decompose organic pollutant.

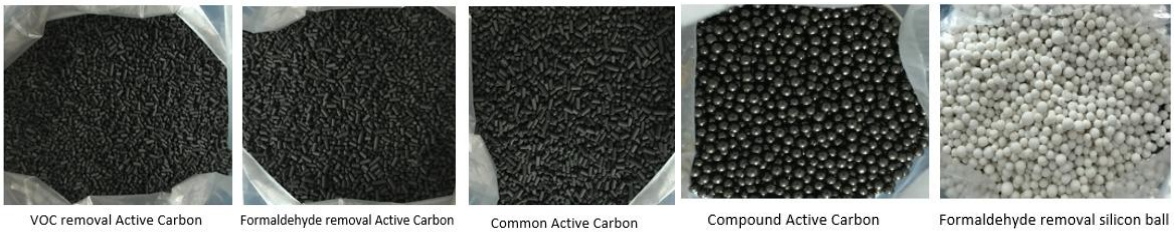

Figure 2 Overview of Filtration Materials

6) Phototype catalyst only, we called it PECO.

7) PECO +active carbon

2.1.3 Honeycomb filter base support on PECO module

Honeycomb filter base support is to install different filtration material for performance test showed in figure 3.

Filtration Area Size: 100mm*83mm*20mm.

Figure 3 Honeycomb Filter Base Support

2.2 Test Method

2.2.1 Test item

Formaldehyde removal rate, Acetic Acid removal rate and Ammonia removal rate.

2.2.2 Test equipment

1m3 test chamber with inject inlet and detect inlet showed in figure 4.

Figure 4 1m³ Chamber Overview

Gastec Detector Tube Systems to detect the concentration of deleterious gas showed in figure 5.

Figure 5 Concentration Detection Tube

2.2.3 Deleterious gas preparation

Initial concentration should be in the scope of related test tube. Table 1 is the initial amount of pollutant added.

Table 1 Pollutant Drop Amount

VOC MATTER	Drop Amount	Initial Pollutant Amount / g
Formaldehyde	3	0.145
Acetic acid	3	0.057
Ammonia	14	0.740

2.2.4 Test time

0 ~ 60min.

Start counting when the concentration is in equilibrium level after injection.

2.2.5 Test standards

JEM1467-2015

3 RESULT

3.1 Determination of Filter Samples Amount

In the honeycomb filter on the air purify prototype, filter material can be filled with max.40g of active carbon particles, but the air flow drop will be larger. For same weight, different material has different thickness due to particle size and shape. The relation of weight and thickness for each sample are tested as Table 2.

Table 2 Filtration Material Description

No.	Filtration material	Test Sample Weight and Thickness		
		20g	30g	40g
1	VOC removal Active Carbon	10mm	15mm	20mm
2	Formaldehyde Removal Active Carbon	10mm	15mm	20mm
3	Common Active Carbon	10mm	15mm	20mm

4	Compound Active Carbon	8mm	12mm	15mm
5	VOC Removal Silicon Ball	8mm	12mm	15mm

Use No.1 VOC removal active carbon as benchmark to determine what weight can be used as benchmark weight for this comparison study at the first step. The data on figure 6 shows that the best amount of filter material is 30g, which has similar curve trend with PECO photocatalyst module. So 30g is determined as benchmark amount in the next study.

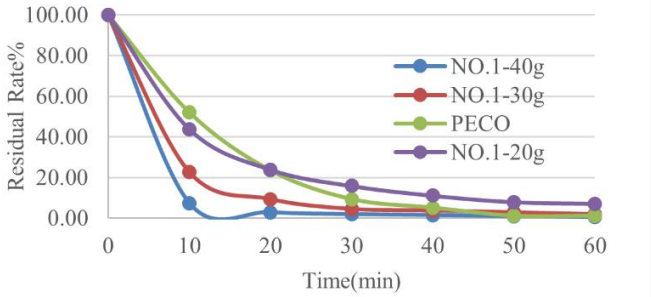

Figure 6 Acetate Removal Rate by No. Sample

3.2 Performance Test

3.2.1 Acetate removal efficiency

Table 3 Acetate Removal Test Result

Sampling Time	Removal Rate / %						
	NO.1	NO.2	NO.3	NO.4	No.5	PECO(TiO2)	PECO+NO.3
0min	0.00	0.00	0.00	0.00	0.00	0.00	0.00
10min	77.40	65.52	76.00	37.91	70.93	48.01	77.86
20min	90.72	86.21	84.80	65.13	90.22	76.52	92.08
30min	95.54	93.10	92.00	77.87	93.29	90.66	96.27
40min	96.29	94.48	94.80	82.98	95.43	94.87	97.20
50min	97.21	94.82	97.20	85.53	96.35	98.84	98.13
60min	98.14	95.85	97.60	88.94	97.57	98.84	98.60

Based on the table 3, we make the data curve to show the removal efficiency intuitively in figure 7.
Acetate Removal performance for 5 different materials Except for sample relatively equals to PECO filter. The performance of PECO+ active carbon didn't improve much compared to pure active carbon. The reason may be active carbon already excellent in formaldehyde and acetic acid removal. But maybe the combination of PECO will be good in extending lifetime of carbon[7].

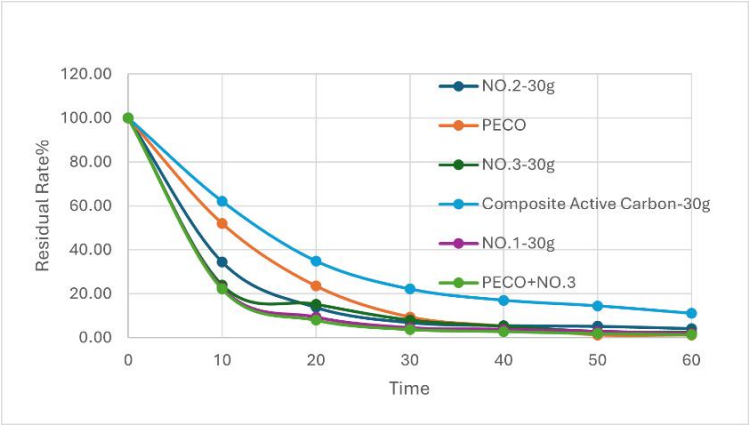

Figure 7 Actetate Removal Test Result

3.2.2 Ammonia removal efficiency

Performance for 5 different materials, all the samples that weigh 30g. The data shows in table 4, sample no.5 (silicon ball) has better than PECO photocatalyst, but the performance of other samples is far worse than PECO photocatalyst. So PECO and No.5 material is better than other solutions for Ammonia removal.

Table 4 Ammonia Removal Test Result

Sampling time	Removal Rate / %						
	NO.1	NO.2	NO.3	NO.4	No.5	PECO(TiO2)	PECO+NO.3
0min	0.00	0.00	0.00	0.00	0.00	0.00	0.00
10min	14.37	18.90	5.23	15.79	53.33	16.17	23.25
20min	15.71	20.96	9.07	19.30	66.67	25.41	29.49
30min	15.71	22.93	18.03	28.00	75.00	30.74	36.85
40min	17.14	22.93	19.31	29.76	81.65	32.07	42.92
50min	/	/	/	/	83.32	40.00	47.78
60min	/	/	/	/	83.32	46.18	51.42

Based on the table, we make the data curve to show the removal efficiency intuitively in figure 8.

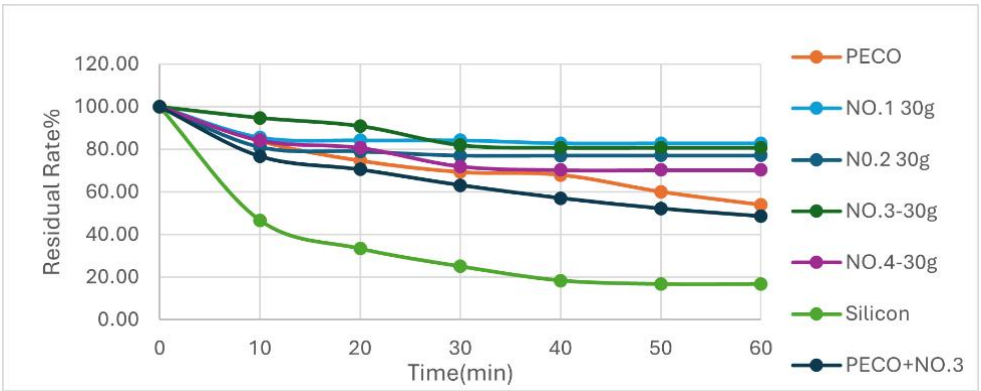

Figure 8 Ammonia Removal Test Result

In order to further understand the difference among PECO, carbon, PECO+carbon. We extended testing time from 60min to 180min.

Table 5 Ammonia Removal Test Result with Extend Testing Time

Sampling time	Removal Rate / %		
	PECO	Carbon	PECO+Carbon
0min	0.00	0.00	0.00
30min	39.21	5.43	31.47
60min	53.89	12.09	40.38
90min	63.71	17.19	51.71
120min	73.50	22.29	62.93
150min	78.43	22.29	70.35
180min	84.48	22.20	77.76

Based on the table 5, we make the data curve to show the removal efficiency intuitively in figure 9.

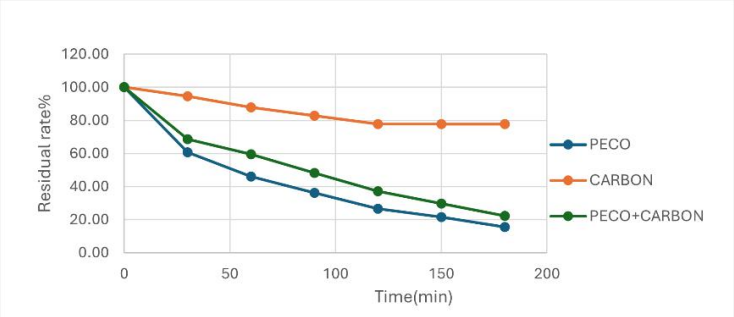

Figure 9 Long Term Ammonia Removal Test Result

The addition of PECO increased the Ammonia removal rate greatly. But due to the air resistance, the performance of PECO+carbon is lower than PECO itself.

Molecule polarity is one of molecule attribute based on molecule configuration and electric charge in chemical science field[8]. In this rule, molecules are classified as polar and non-polar. In the group of molecules of polar, they attract each other, and exclude non-polar molecules in the same time. For non-polar molecules group, they are same. In purification process, if both filter material and pollutant are in the same group, pollutant will be absorbed easily[8]. Ammonia is non-polar molecules, which means the filter material are non-molecule groups.

3.2.3 Formaldehyde removal efficiency

Based on the table 6, we make the data curve to show the removal efficiency intuitively in figure 10.

Table 6 Formaldehyde Removal Test Result

Sampling time	Removal rate / %						
	NO.1	NO.2	NO.3	NO.4	No.5	PECO(TiO2)	PECO+NO.3
0min	0.00	0.00	0.00	0.00	0.00	0.0	0.00
10min	50.09	73.88	71.43	22.35	71.43	16.7	70.53
20min	64.01	86.94	91.41	33.33	89.29	50.0	89.95
30min	72.32	95.10	94.62	37.62	94.64	66.7	96.06
40min	/	98.03	97.31	48.76	99.10	90.0	97.89
50min	77.86	99.67	99.10	55.44	99.64	93.8	98.80
60min	80.39	99.67	99.46	59.80	99.64	96.9	98.81

For 5 different material, with formaldehyde removal, sample no.2, 3, 5 have similar performance with PECO photocatalyst. Sample no.1 (VOC removal type) and No.4 (bare carbon material) have worse performance for formaldehyde. The performance of PECO+ active carbon didn't improve much compared to pure active carbon. The reason may be active carbon already excellent in formaldehyde and acetic acid removal. But maybe the combination of PECO will be good in extending lifetime of carbon[7].

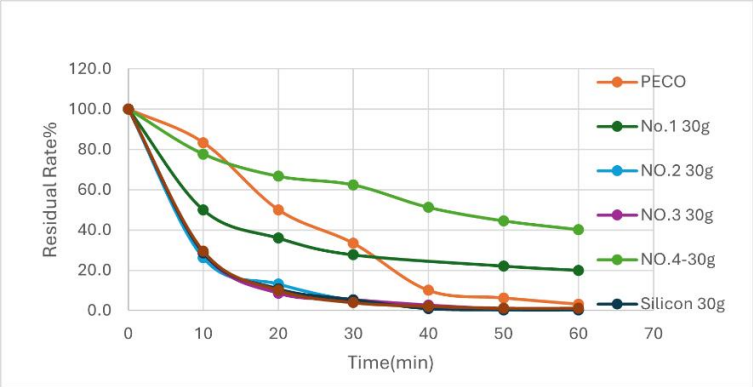

Figure 10 Formaldehyde Removal Test Result

4 CONCLUSION

All the samples have good removal efficiency as PECO photocatalyst, except sample no.4 (compound active carbon) is worse than PECO. Which means bare carbon material is not efficient stand alone

In all, the study shows that active carbon materials have better removal efficiency formaldehyde and acetic acid pollutants, but the capability for VOCs removal (such as Ammonia) is weak. So combination with carbon material together with PECO is good but requires optimization for amount of carbon usage or combined solution will extend the carbon filter lifetime.

Molecule polarity is one of molecule attribute based on molecule configuration and electric charge in chemical science field[8]. In this rule, molecules are classified as polar and non-polar. In the group of molecules of polar, they attract each other, and exclude non-polar molecules in the same time. For non-polar molecules group, they are same. In purification process, if both filter material and pollutant are in the same group, pollutant will be absorbed easily. Ammonia is non-polar molecules, formaldehyde and acetate are polar molecule. In the test, the data shows the regular of polarity.

The study shows that active carbon materials have better removal efficiency of polar substance pollutants (formaldehyde and acetic acid), but the capability for non-polar VOCs removal (Ammonia) is weak. So compound active carbon materials maybe is a better choice for IAQ purification research to purify kinds of gas pollutant molecules.

COMPETING INTERESTS

The authors have no relevant financial or non-financial interests to disclose.

REFERENCES

[1] Liu, G, Xiao, M, Zhang, X, et al. A review of air filtration technologies for sustainable and healthy building ventilation. Sustainable Cities and Society, 2017, 32: 375-396.

[2] Zhang X Y, Gao B, Creamer A E, et al. Adsorption of VOCs onto engineered carbon materials: A review. Journal of Hazardous Materials, 2017, 338: 102-123.

[3] Li L, Liu S Q, Liu J X. Surface modification of co conut shell based activated carbon for the im provement of hydrophobic VOC removal. Journal of Hazardous Materials, 2011, 192(2): 683-690.

[4] Luengas A, Barona A, Hort C, et al. A review of indoor air treatment technologies. Reviews in Environmental Science and Bio/Technology, 2015, 14: 499-522.

[5] Fujishima A, Honda K. Electrochemical photolysis of water at a semiconductor electrode. Nature, 1972, 238(5358): 37 -8.

[6] Peller J, Wiest O, Kamat PV. Synergy of combining sonolysis and photocatalysis in the degradation and mineralization of chlorinated aromatic compounds. Environmental Science & Technology, 2003, 37(9): 1926-1932.

[7] Jo W K, Yang C H. Granular-activated carbon adsorption followed by annular-type photocatalytic system for control of indoor aromatic compounds. Separation and Purification Technology, 2009, 66: 438-442.

[8] Pak S H, Jeon M J, Jeon Y W. Study of sulfuric acid treatment of activated carbon used to enhance mixed VOC removal. International Biodeterio ration & Biodegradation, 2016, 113: 195-200.

Eurasia Journal of Science and Technology
ISSN: 2663-1016
DOI: https://doi.org/10.61784/ejst3032

STUDY ON FACTORS OF CO_2 GAS CHANNELING

XinRui Wang[1], RuHao Liu[2*]
[1]*School of Earth Science, Northeast Petroleum University, Daqing, 163318, China.*
[2]*Institute of Unconventional Oil and Gas Development, Chongqing University of Science and Technology, Chongqing 401331, China.*
Corresponding Author: RuHao Liu, Email: lrh_1992@163.com

Abstract: CO_2 flooding has certain development prospects in improving recovery efficiency of low permeability reservoir, but there are some problems such as gas channeling, poor gas injection development effect, and low understanding of influencing factors of gas channeling. As an injection well in the study area W20, gas discovery occurs in nearby Wells, resulting in increased pressure and decreased oil production. The factors of CO_2 gas channeling are analyzed from the aspects of sand body distribution, microfacies type, reservoir heterogeneity and fracture development scale. The law is verified according to the actual work area. The research shows that the distribution of sand body is the main gas channeling channel, and different microfacies types have different gas channeling capabilities. The vertical heterogeneity of the reservoir controls the gas channeling capability inside the sand body, and the development of fractures controls the gas distribution. The research results provide a theoretical basis for the selection of gas injection Wells and the improvement of gas injection development results.
Keywords: CO_2 displacement; Numerical simulation; Tight reservoir; Volumetric fracturing

1 INTRODUCTION

CO_2 gas has the characteristics of low viscosity and easy compression, and its injection capacity is higher than that of water injection, so it is easy to establish an effective displacement system. When the reservoir pressure is higher than the miscible pressure, CO_2 gas can form miscible with crude oil and improve the recovery rate [1-2]. Therefore, CO_2 flooding technology is an important means to develop ultra-low permeability reservoirs [3-4]. Due to the influence of reservoir heterogeneity, fluid characteristics, injection and production development parameters and other factors, gas channeling is easy to occur in the process of CO_2 flooding, which seriously affects the gas injection development effect [5]. At present, the existing research results of gas channeling are few, mainly based on the actual production data of the mine, although the judgment results are more accurate, but correct
The low degree of understanding of the influencing factors of gas channeling can not achieve the purpose of real-time early warning and prevention, which reduces the effect of oil displacement and increases the cost. The numerical simulation of different gas channeling factors was carried out in this study. Through the numerical simulation results, the main factors affecting CO_2 gas migration and gas channeling were further identified.

2 INFLUENCING FACTORS OF CO_2 GAS CHANNELING

2.1 Sand Body Distribution

Sand body, as the main oil supply channel, is closely related to the distribution of oil and gas. At the same time, sand body serves as the main migration channel of gas drive in the process of CO_2 gas injection due to the larger porosity and permeability characteristics compared with mudstone. In view of the distribution of sand body, selecting the location of CO_2 drive injection well can effectively improve oil recovery on the one hand. On the other hand, it can also effectively avoid gas channeling and affect injection and production.
A mechanism model for sand body distribution is established (**Figure 1**), and it is found that mudstone, as an effective sand body shield, also has a strong shielding effect on the diffusion range of carbon dioxide gas during the process of carbon dioxide injection. Due to the connectivity of sand bodies, carbon dioxide gas exists in the top sand body, but its distribution pattern is affected by mudstone shield, and the middle right sand body is affected by mudstone shield. No gas display exists. Therefore, the connectivity of sand bodies provides the main migration channel for gas diffusion (**Figure 2**).

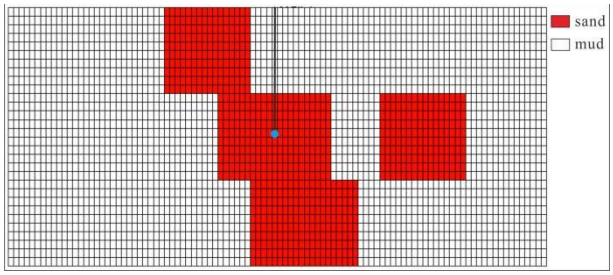

Figure 1 Profile of Sand Body Distribution

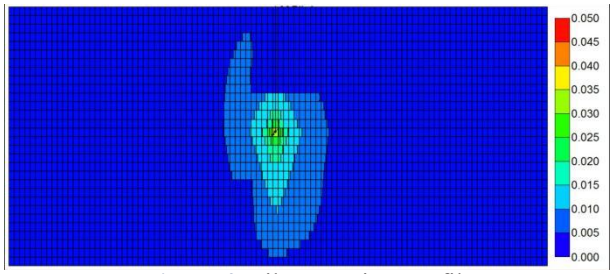

Figure 2 Oil Saturation Profile

2.2 Types of Sedimentary Microfacies

Sedimentary microfacies control the geometry and distribution of the reservoir sand body on the macro level, and determine the precursor of the reservoir physical properties on the micro level. Different sedimentary microfacies types also have different levels of physical properties and pore structures. When carbon dioxide flooding is carried out, the diffusion capacity of carbon dioxide in the reservoir is also different due to the difference of pore structure types of different microfacies.

The mechanism model of CO_2 diffusion area under different microfacies types was established. In the study area, the porosity distribution of channel sand body was 0.062~0.241%, with a median value of 0.077%; the permeability distribution was 0.09~2.45mD, with a median value of 0.11mD; and the porosity distribution of overflowed bank sand body was 0.044%~0.071%, with a median value of 0.053%. The permeability distribution ranged from 0.051 to 0.1047mD with a median of 0.073mD.

According to the pore permeability characteristics of different microphase types, it is found that the diffusion range of carbon dioxide in the channel sand body is larger than that in the overflow bank sand body at the same injection amount. According to different sedimentary microfacies types, the better the reservoir physical properties, the faster the gas diffusion rate and the shorter the breakthrough time (**Figure 3)**.

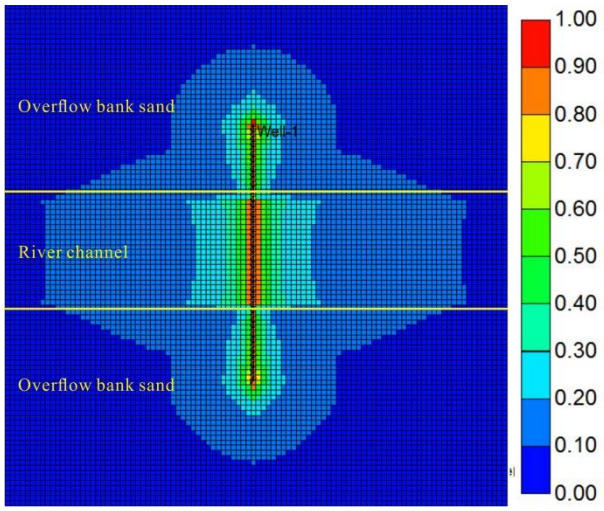

Figure 3 Oil Saturation Distribution of Different Microphase Types

2.3 Heterogeneity

In heterogeneous reservoirs, the injected CO_2 preferentially enters the high permeability zone. As a result, when the oil in the low permeability zone is not completely swept, the CO_2 has burst from the high permeability zone into the production well, resulting in viscous pointing, which reduces the oil displacement efficiency. Therefore, the less heterogeneous the reservoir rock, the better,

In the study area, the sand body has vertical heterogeneity, the channel sand body is mostly in a positive rhythmic form, and the physical property of the bottom sand body is better than that of the top sand body. During carbon dioxide injection, the gas affected by the structure is the first to preferentially replace the upper part. However, the permeability of the bottom sand body is higher, and carbon dioxide gas has been widely diffused from the bottom high permeability part before the top low permeability reservoir is completely displaced.

The mechanism models were established by injecting the upper middle part of the sand body in different ways, and the analysis showed that: When the horizontal well is drilled into the upper part of the sand body, the gas drive location of the carbon dioxide sand body is relatively average; when the sand body is drilled into the middle part of the sand body, the distribution is trapezoidal, and the production degree of the top sand body is weaker than that of the bottom sand body; when the horizontal well is drilled into the bottom sand body, the production degree of the top low permeability reservoir is very low. Therefore, when the sand body is drilled into the top sand body during gas drive, it has a good displacement effect(**Figure 4)**.

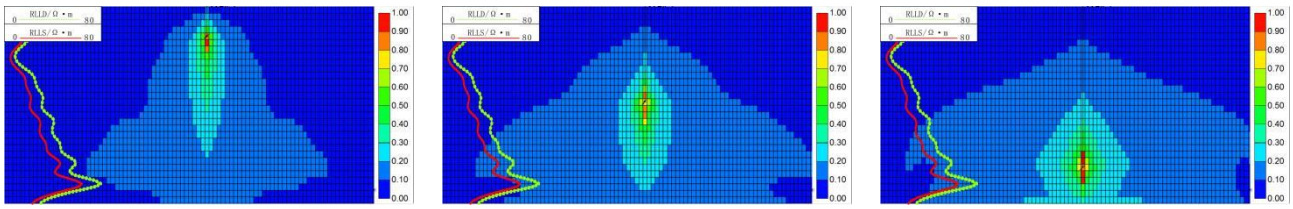

Figure 4 Profile of Gas Saturation Distribution at Different Locations of Horizontal Well Drilling

2.4 Scale of Artificial Fracture Development

Whether it is artificial fracture or natural fracture, its large pores and strong seepage capacity, for medium and low permeability oil fields, most of the water injection development, the water injected into the reservoir through the fracture to both sides of the drive, the fracture of the water injection interval can improve the water flooding effect, but also bring some difficulties to the stable exploitation of the oil field, resulting in early flooding water channeling, affecting the oil field recovery. For gas injection production in tight reservoirs, gas has a stronger diffusion ability than water, and gas has a stronger gas channeling ability along fractures. The mechanism model of horizontal well fracturing and non-fracturing is established to study the gas distribution law after gas injection.

Through comparison, it is found that cracks have a strong seepage capacity, and gas enters into cracks quickly after injection and spreads along the direction of cracks. The overall distribution is zigzag along the direction of cracks, and vertically affected by cracks, the distribution is uniform. The gas is mainly distributed along the cracks (Figure 5, 6).

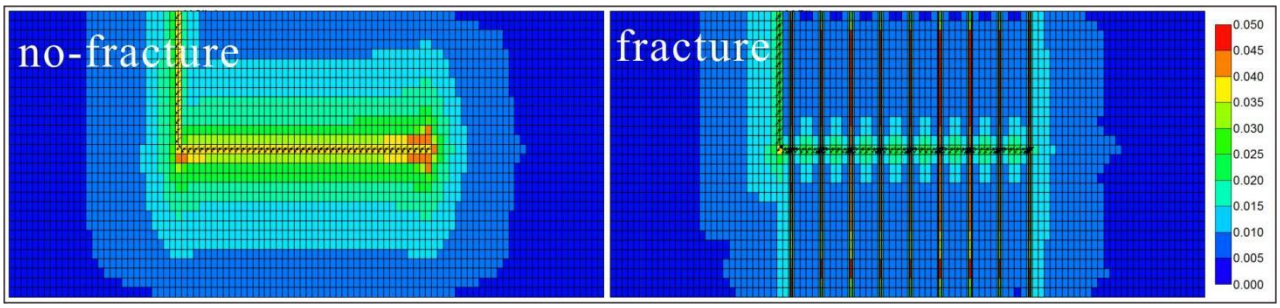

Figure 5 Horizontal Well Fracturing Oil Saturation Distribution Plan

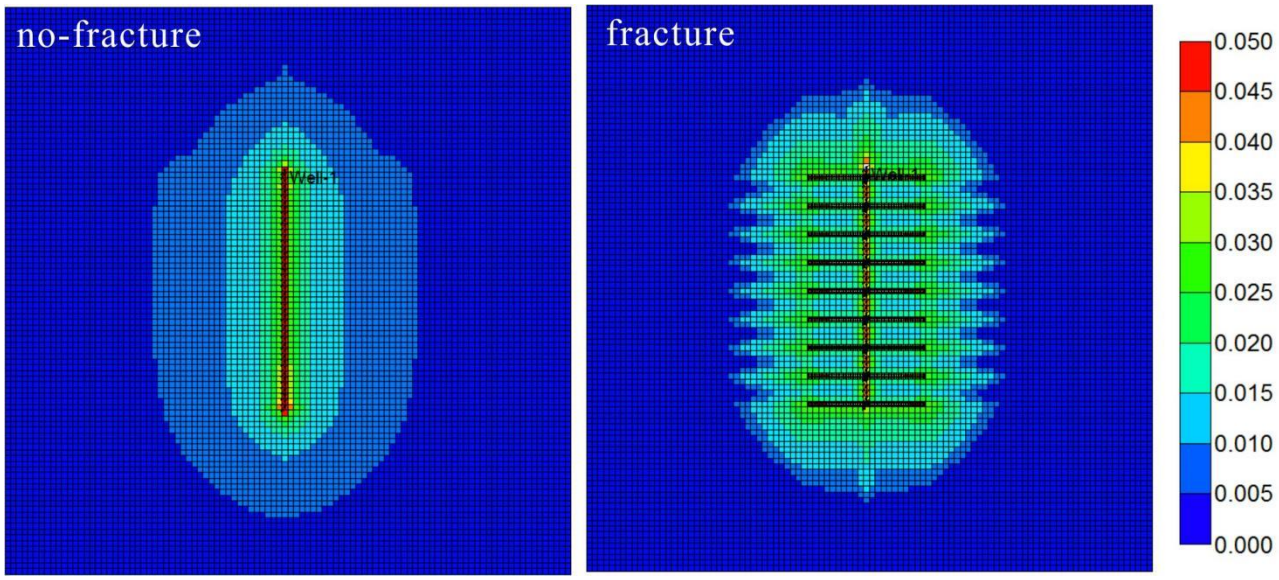

Figure 6 Horizontal Well Fracturing Oil Saturation Distribution Profile

3 INFLUENCING FACTORS OF CO_2 GAS CHANNELING

The study area is located in the Fuyu oil reservoir in the southern Songliao Basin, which is dominated by low-ultra-low permeability delta plain-delta front sandstone. The Fuyu oil reservoir in the southern Songliao Basin is a tight reservoir with a burial depth greater than 1750m, porosity less than 12% and permeability less than 1.0 × 10-3 μ m2.

At present, carbon dioxide flooding is being carried out in the horizontal well area to improve production. In the carbon dioxide injection in well w20, it is found that w1-5, w14 and wpf2 all have gas discovery phenomena. A numerical simulation model is established to analyze the gas channeling phenomenon in the study area. Grid step size 40m*40m, carbon dioxide gas injection amount based on the actual, the average daily injection amount is 180m3.

As shown in Figure 7, combined with the sedimentary microfacies distribution diagram and gas saturation distribution diagram of the study area, well w20, as a carbon dioxide injection well, was drilled into four small layers. After gas injection, the gas diffusion range was mainly affected by the location of sand body, and the distribution of mudstone effectively controlled the gas diffusion direction.

As shown in Figure 8, the time variation curves of gas saturation in different Wells are analyzed. After artificial fracturing, the fractures of WFP2 vertical well are connected with the second cluster of fractures of w20 well, and gas development preferentially occurs after CO_2 injection. Affected by the occlusion between the shunt of the three small layers, the gas diffusion site decreases, and the gas of W1-5 Wells comes from the four small layers, and that of W14 Wells comes from the two small layers. Therefore, well W1-5 is preferred to well W14 for gas development.

As shown in Figure 9, combined with the time curve of gas saturation of each small layer, the analysis shows that due to the influence of the shunt between the three small layers of well w20, the gas diffusion ability is weakened, and the gas saturation of the three small layers is lower than that of the five small layers. When carbon dioxide flooding is carried out, it is necessary to take into account the vertical sand body overlaying relationship, and effective mudstone blocking horizon can effectively control the carbon dioxide displacement range and improve the oil displacement efficiency of the target horizon.

Horizontal Wells in the study area have been substantially fractured, and fractures not only improve the mining efficiency, but also act as the main gas dispersion channel in gas drive. Compared with the diffusion velocity between fractures and non-fractures in the study area, the gas migration velocity in the fracture range is four times that in the non -fracture range. Therefore, in the process of gas displacement, in order to reduce the impact of gas channeling, the gas migration velocity is four times that in the non-fracture range. In addition to the fractures formed by artificial fracturing, the natural fracture development zone should be moderately avoided.

Layer 1. Channel sand body and overflow bank sand body are developed in small beds. Due to the different physical properties of the sedimentary microfacies of the two, gas preferentially diffused along the channel sand body and then in the overflow bank sand body during gas injection, and the channel gas diffusion ability is better than that of overflow bank sand.

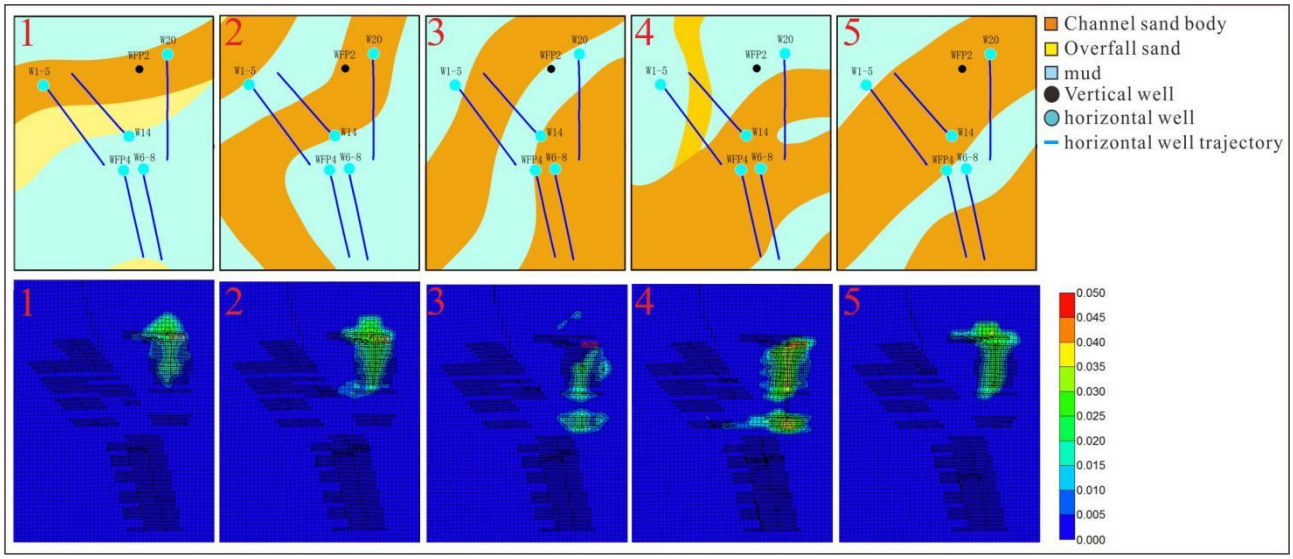

Figure 7 Horizontal Well Fracturing Oil Saturation Distribution Profile

Figure 8 Oil Saturation Curves of Different Wells

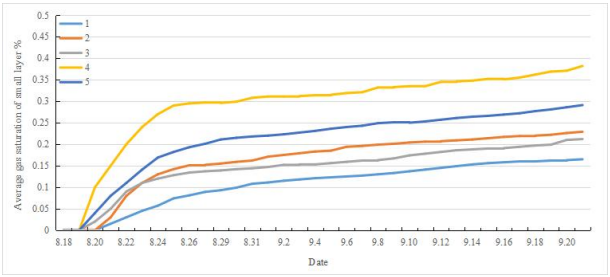

Figure 9 Oil Saturation Curves of Different Layers

4 CONCLUSION

1. Sand body distribution is the main migration channel after carbon dioxide injection. Determining the sand body distribution near the injection well can effectively control the diffusion range of carbon dioxide gas and avoid the abnormal increase of pressure in nearby Wells caused by gas diffusion, so as to effectively improve oil recovery.

2. Different microfacies types will lead to changes in the diffusion capacity of gases. When the differential distribution of sedimentary microfacies is effectively utilized, the diffusion range of gases can be further controlled to achieve the purpose of local effective displacement.

3. In the positive rhythm channel, when horizontal Wells meet the part or middle of the channel, the effect of carbon dioxide gas is better than that of drilling the bottom sand body due to vertical heterogeneity, which can effectively reduce the problem of remaining oil enrichment at the top of the sand body.
4. As a fast channel for gas migration, gas injection Wells should minimize communication with neighboring fractures during fracturing, resulting in reduced gas injection effect.

COMPETING INTERESTS

The authors have no relevant financial or non-financial interests to disclose.

REFERENCES

[1] Gao Huimei, He Ying, Zhou Xisheng. CO_2 injection to enhance oil recoveryTechnical research progress. Special Oil and Gas Reservoirs, 2009, 16 (1): 6-12.
[2] Zhou Yu, Wang Rui, Gou Feifei, et al. Mechanism of CO_2 flooding in high water cut reservoirs. Acta Petrolei Sinica, 2016, 37(1) : 143-150.
[3] Zhang Xing, Yang Shenglai, Wen Bo, et al. Experimental Study on starting pressure gradient of CO_2 miscible flooding in low permeability reservoir. Petroleum Geology & Experiment, 2013, 35(5): 583-586.
[4] He Jia, Zhou Xisheng, Li Min, et al. Study on CO_2 displacement injection method in ultra-low permeability reservoir. Journal of Oil and Gas Technology, 2010, 32(6): 131-134.
[5] Peng Songshui. Study on CO_2 displacement gas channeling in ultra-low permeability reservoir of Shengli Zhenglizhuang Oilfield. Journal of Oil and Gas Technology, 2013, 35(3): 147-149.

Eurasia Journal of Science and Technology
ISSN: 2663-1016
DOI: https://doi.org/10.61784/ejst3033

TRANSCRIPTOME ANALYSIS OF THIACLOPRID-RESISTANT MYZUS PERSICAE REVEALS THE OVEREXPRESSION OF METABOLIC DETOXIFICATION GENES

JinFeng Hu*, XianZhi Zhou, Lei Lin
Fujian Engineering Research Center for Green Pest Management, Key Laboratory for Monitoring and Integrated Management of Crop Pests, Institute of Plant Protection, Fujian Academy of Agricultural Sciences, Fuzhou, China.
Corresponding author: JinFeng Hu, Email: hujinfeng007@sina.com

Abstract: The green peach aphid *Myzus persicae* (Sulzer, 1776) (GPA) is an economic pest that damages many agricultural crops and has evolved resistance to various classes of insecticides, including neonicotinoids. Thiacloprid is a broad-spectrum neonicotinoid with low toxicity to bees. After fifty selection cycles from a susceptible strain (FAA-S), a strain (THG-R) with 1,201.2-fold resistance to thiacloprid was obtained under laboratory conditions. The THG-R strain exhibited a high level of cross-resistance to imidacloprid (894.3-fold), moderate levels of cross-resistance to acetamiprid (48.7-fold), dinotefuran (44.7-fold), flupyradifurone (24.9-fold), and sulfoxaflor (14.6-fold), and low levels of cross-resistance to thiamethoxam (9.4-fold) and clothianidin (6.4-fold). Synergism and activity tests indicated the possible involvement of cytochrome P450 in the detoxification resistance to thiacloprid. Transcriptome profiling of the THG-R and FAA-S strains identified 72 differentially expressed genes (DEGs) related to insecticide detoxification, including 15 upregulated and 57 downregulated genes. Resistance was not conferred by known detoxification mechanisms of resistance to neonicotinoid insecticides and sulfoxaflor, but rather by overexpression of the P450 genes *CYP6CY3* and *CYP380c40* and UDP-glucuronosyltransferase (UGT) gene UGT344P2. The adenosine triphosphate (ATP)-binding cassette transporters (ABCs) *Mplethal(2)03659.1* and thioesterase *MpThem6* were highly overexpressed (30.3-fold and 7-fold, respectively) in the THG-R strain. These findings provided another possible enhanced metabolic route responsible for neonicotinoid resistance in GPA.
Keywords: *Myzus persicae*; Thiacloprid; Resistance development; Cross-resistance; Detoxification mechanism

1 INTRODUCTION

The green peach aphid *Myzus persicae* (Sulzer, 1776) (GPA) is one of the most economically important agricultural pests. It can feed on more than 400 plant species belonging to 50 families, including potato, tobacco, and eggplant. The GPA is notorious because it can act as a vector to transmit 115 different plant viruses, accounting for 67.7% of the aphid-vector viruses [1]. Insecticides are the foundation of the management of the GPA in China and other countries. More than 70 active ingredients across a range of modes of action (MOA) groups have been registered for use to control GPA globally [2]. However, heavy repeated applications of insecticides have led to field populations of GPA developing resistance to most used insecticides, such as organophosphates, carbamates, pyrethroids, and pyridine azomethine derivatives [3-5].

Neonicotinoids are systemic insecticides that act on the nicotinic acetylcholine receptors (nAChR) of insects and have become the most widely used pesticides in the world [6]. The major neonicotinoids in commercial pesticides are acetamiprid, clothianidin, dinotefuran, imidacloprid, thiacloprid, and thiamethoxam [2]. Pest resistance to neonicotinoids remains a growing concern, with GPA resistance to imidacloprid in fields in Japan reported in 1996 [7]. Based on the Arthropod Pesticide Resistance Database (APRD) [8], 132 cases of neonicotinoid resistance involve the GPA, with only *Bemisia tabaci* and *Nilaparvata lugens* exhibiting more cases of resistance. Field monitoring data have shown that GPA has developed resistance to imidacloprid [9, 10], thiamethoxam [9], and acetamiprid [10]. The first chloronicotinyl insecticide, thiacloprid [(Z)-3-(6-chloro-3-pyridylmethyl)-1,3-thiazolidin-2-ylidenecyanamide] was discovered by Bayer and commercialized in 2000 with a much broader spectrum of pests targeted and lower acute toxicity to bees than other neonicotinoids [11,12]. Thiacloprid entered the Chinese market in 2014 and has been registered to control GPA in cabbage, potato, and peach. To date, neonicotinoids have remained an effective control measure against GPA in China [4], although recent resistance monitoring work has indicated a lack of efficacy of imidacloprid in some districts [5]. Previous studies have mainly focused on the mechanism of imidacloprid resistance development in GPA [9,13,14], but the existing knowledge of thiacloprid is limited to its cross-resistance with other neonicotinoids.

Metabolic resistance is much more common in insects resistant to neonicotinoids, highlighting the role of cytochrome P450 as the principal agent. The overexpression of P450 genes has been widely reported to be responsible for neonicotinoid resistance in insects, such as *Drosophila melanogaster* (*CYP6G1*) [15], *B. tabaci* (*CYP6CM1*, *CYP4C64*) [16], *Aphis gossypii* (*CYP6CY14, CYP6CY22*, and *CYP6UN1*) [17], and *N. lugens* (*CYP6AY1*, *CYP6ER1*, *CYP4CE1*, and *CYP6CW1*) [18]. Biochemical surveys have also indicated an increase in the activities of detoxification enzymes, such as cytochrome P450 monooxygenases (P450), glutathione S-transferases (GSTs), and carboxylesterases (CarEs) in

imidacloprid-resistant aphids [4]. In GPA, the enhanced expression of a P450 gene, *CYP6CY3*, associated with imidacloprid resistance is much more common in individuals in the field than the R81T mutation of nAChR, and the molecular mechanisms of *CYP6CY3*-mediated resistance to some neonicotinoids have been well documented [19]. In recent years, new techniques and advances in genomic research revealed other metabolic enzymes that were also attributed to neonicotinoid resistance. For example, the overexpression of uridine diphosphate (UDP)-glycosyltransferases (UGTs) is associated with sulfoxaflor resistance in GPA [20] and thiamethoxam resistance in *A. gossypii* [21].

Under laboratory conditions, we obtained a high thiacloprid-resistant strain of GPA by successively screening a susceptible strain with thiacloprid. In the present study, we investigated the cross-resistance spectrum between thiacloprid and other insecticides. The present study has also identified genome-wide transcriptional changes between the thiacloprid-susceptible and resistant GPA strains. Genes involved in insecticide metabolic and detoxification, including P450, UGTs, adenosine triphosphate (ATP)-binding cassette transporters (ABCs), GSTs. and esterase, were identified, which provided insights into the metabolic mechanisms of GPS to thiacloprid. This information could be used to slow-down and eventually overcome pest resistance to thiacloprid.

2 MATERIALS AND METHODS

2.1 Insects

Two GPA strains, (FAA-S and THG-R), were used in the study. The THG-R strain was reared in the laboratory without exposure to insecticides after being collected from *Arabidopsis thaliana* in the Jianxin District of Fuzhou, China, in 2008 and was susceptible to neonicotinoids. The THG-R strain was established from the FAA-S strain by successive screening with thiacloprid for more than 50 generations in the laboratory. More than 50,000 adults were selected with direct spraying in each generation. Both GPA strains were reared on pakchoi cabbage seedlings, *Brassica chinensis*, under controlled conditions of 19−22°C, 60% relative humidity, and a photoperiod of 16:8 h (light:dark).

2.2 Pesticides, SYNERGISTS, and Other Chemicals

The insecticides used for bioassays included thiacloprid (97.5% purity; Bayer AG, Germany), imidacloprid (97% purity; Bayer AG, Germany), flupyradifurone (96% purity; Bayer AG, Germany), acetamiprid (99% purity; Ningbo Sanjiang Yinong Chemical Co., Ltd., China), thiamethoxam (98%purity; Syngenta Group, Switzerland), clothianidin (98% purity; Hailir Chemicals Co., Ltd., China), dinotefuran (96% purity; Hebei Veyong Bio-chemical Co., Ltd., China), sulfoxaflor (95.9% purity; Corteva Agriscience Chile Ltda. of China, China) and triflumezopyrim (95.9% purity; Corteva Agriscience Chile Ltda. of China, China). Synergists piperonyl butoxide (PBO; reagent grade), S,S,S-tributyl phosphorotrithioate (DEF; reagent grade), and diethyl maleate (DEM; reagent grade) and Chemicals, were purchased from Sigma-Aldrich Shanghai Trading Co., Ltd., United States.

Ethylenediaminetetraacetic acid (EDTA), albumin bovine (BSA), p-nitrophenol, reduced glutathione (GSH), coenzyme NADPH and sodium dodecyl sulfate (SDS) were from Shanghai Aladdin Bio-Chem Technology Co., LTD (Shanghai, China). Eserine, p-nitroanisole, fast blue B salt, α-naphthyl acetate (α-NA), n-phenylthiourea (PTU), coomassie brilliant blue G250, 1-chloro-2,4-dinitrochlorobenzene (CDNB), phenylmethylsulfonyl fluoride (PMSF), DL-dithiothreitol (DTT), Triton X-100 and other chemicals were also purchased from Sigma-Aldrich Shanghai Trading Co., Ltd., United States

2.3 Susceptible Test Methods

The leaf-dip method was used to measure the toxicity of insecticides, as recommended by the Insecticide Resistance Action Committee (IRAC) [2]. Five to seven concentrations of insecticides were prepared using 0.1% Triton-100 and four replicates were conducted for each treatment. Clean leaf-discs of *Brassica oleracea* L. were cut using metal tubes and dipped in the test liquid for 10 s. The air-dried leaf-discs were placed onto 1% agar plate (20 mm depth) in a petri dish (30 mm diameter and 40 mm depth). Twenty apterous adults were then transferred onto each of the leaf discs using a paint brush and each unit was covered with a close-fitting, ventilated lid. Mortality was assessed after 3 d. Aphids that could not right themselves within 10 s once turned on their back were considered to be dead.

The effects of three synergists (piperonyl butoxide (PBO), S,S,S-tributyl phosphorotrithioate (DEF), and diethyl maleate (DEM)) in combination with thiacloprid against GPA were evaluated using the bioassay method mentioned above. The highest doses of PBO, DEF, and DEM for the susceptible strain that led to zero mortality were 0.8, 0.5, and 1 g L^{-1}, respectively, using the bioassay method. Apterous adult aphids were exposed to leaf discs that were treated with PBO, DEF, or DEM and the thiacloprid mixtures.

2.4 Determination of P450s, GST, and Carboxylesterase Activity

The monooxygenase enzyme (MFO) activity was measured according to Shang's method [22]. Sixty adult aphids were homogenized in 2.0 mL ice-cold phosphate-buffered saline (PBS, 0.04 mol L^{-1}, pH 7.8). The supernatant obtained by centrifuging 10,000 × *g* for 10 min at 4°C was added to a reaction unit containing NADPH and nitroanisole (0.05 mol L^{-1} in acetone) as a substrate. Hydrochloric acid (HCl, 1 mol L^{-1}) was added to terminate the reaction after incubation

for 30 min at 37°C. Then, the reaction unit was extracted by a sodium hydroxide (NaOH) and chloroform solution. Finally, the optical density (OD) of the enzyme source was recorded at 400 nm using a microplate reader. The specific activity was obtained according to a nitrophenol standard curve and the protein concentration of the enzyme source.

Carboxylesterase activity was determined using α-naphthyl acetate (α-NA) as the substrate according to the method reported by Van Asperen [23], with some modifications. Sixty adult aphids were homogenized in 2.0 mL of ice-cold PBS (0.04 mol L^{-1}, pH 7.0) and centrifuged at 4°C at 10,000 × *g* for 10 min. The supernatant fluid was used as the enzyme source. The supernatant fluid was kept on ice before the analysis. After the substrates a-NA (3×10^{-4} mol L^{-1}) and physostigmine (10^{-4} mol L^{-1}) were incubated with the enzyme source for 10 min at 37°C, the color developing agent [mass fraction 5%, SDS; mass fraction, 1% fast blue B salt = 5:2 (v/v)] was added. Absorbance at 600 nm (450 nm) was recorded at the same time in a microplate reader (SPECTRA max PLUS384, Molecular Devices, San Jose, CA, USA). The specific activity of CarEs was calculated based on an a-naphthol standard curve and the protein concentration of the enzyme source.

The activity of GSTs was determined according to a slightly modified published method involving 1-chloro-2, 4-dinitrobenzene (CDNB) [24]. Sixty adult aphids were homogenized in 2.0 mL ice-cold PBS (0.04 mol L^{-1}, pH 7.5), and the supernatant solution was used after being centrifuged at 10,000 × *g* for 10 min at 4°C. Briefly, a 300 μL reaction mixture containing 100 μL diluted enzyme solution, 100 μL CDNB (1.2 mM) substrate solution and 100 μL glutathione (GSH) (6 mM) was prepared, after which the absorbance was measured at 340 nm using the kinetic model for 10 min. The results were determined based on the protein concentration of an enzyme source and the specific activity was converted from an OD value.

The protein contents of the enzyme solutions were determined by the Bradford method [25]. Serial dilutions of a bovine serum albumin (BSA) solution and samples were measured together and the protein content of the samples was calculated by a standard curve based on the BSA solutions. The diluted enzyme solutions (50 μL) were mixed with Coomassie Blue (200 μL). After incubating at 25°C for 10 min, the absorbance at 595 nm was measured. All experiments were repeated three times, and the average values were obtained from the triple-replicated data.

2.5 Sample Collection and RNA Isolation

About 1800 aphids (300 mg, all instars, winged and wingless nymphs, and adults) from susceptible and thiacloprid-resistant strains were collected and the total RNA was extracted with TRIzol™ reagent (Invitrogen, Carlsbad, CA, USA) according to the product protocol. The RNA integrity was assessed using the RNA Nano 6000 assay kit from the Bioanalyzer 2100 system (Agilent Technologies, Santa Clara, CA, USA).

2.6 Library Preparation for Transcriptome Sequencing

The sequencing library was prepared by Novogene Co., Ltd. (Beijing, China) and sequenced on an Illumina Novaseq platform. Briefly, mRNA isolated from the FAA-S and THG-R strains, with three replicates per strain, was purified from the total RNA using poly-T oligo-attached magnetic beads. First strand cDNA was synthesized using a random hexamer primer and M-MuLV Reverse Transcriptase (RNase H-). Second strand cDNA synthesis was subsequently performed using DNA Polymerase I and RNase H. After the adenylation of 3′ ends of DNA fragments, an adaptor with a hairpin loop structure was ligated to prepare for hybridization. Finally, the polymerase chain reaction (PCR) products were purified (AMPure XP system, Beckman Coulter, Brea, CA, USA) and the library quality was assessed on the Agilent Bioanalyzer 2100 system.

2.7 Read Mapping and Expression Quantification

The clean reads were mapped to the GDP clone O genome using Hisat2 v2.0.5, and the mapped reads were counted using Htseq v0.11.2 [26] based on the MyzpeCyc clone O database. The expected number of Fragments Per Kilobase of Transcript Sequence per Million base pairs sequenced (FPKM) was used to estimate gene expression levels [27].

2.8 Differential Expression Analysis and Annotation

The DEG-Seq 2R package (1.20.0) was used to identify significant differentially expressed genes (DEGs). Genes with an adjusted P-value < 0.05 and a fold-change > 2 found by DEG-Seq 2R were assigned as differentially expressed. The functional annotation and classification of the DEGs were performed using the gene ontology (GO) database, and biological pathway annotations were obtained using the Kyoto Encyclopedia of Genes and Genomes (KEGG) database by the clusterProfiler R package.

2.9 Quantitative Real-Time PCR (qRT-PCR) Analysis

A qRT-PCR analysis was performed to validate the expression profiles of selected metabolic detoxification genes, including DEGs and other detoxification genes that were reported to be associated with insecticide resistance in GPA, such as the cytochrome P450 genes, g7429, g25170, CYP6CY3 (KF218356.1) and CYP380C40 (OM677847)), GSTs, E4 (X74554.1), ABCs (g10538, g20740, and g10536), and the UDP-glucuronosyltransferase (UGT) genes ((UGT344P2 (OM677846), g20497, g20587, g20497, and g3205), and β-actin, EF1α as the internal control. The primers used in the

qRT-PCR are summarized in Table 1. The qRT-PCR reactions were conducted on a qTOWER 2.0/2.2 qRT-PCR thermal cycler (Analytik Jena, Jena, Germany) using 2 × SYBR® Green Master Mix (DBI). Three replicates were set using independent samples for each qRT-PCR experiment. The relative gene expression was calculated automatically using the qPCRsoft 3.2 software. The relative gene expression $2^{\wedge-\triangle\triangle Ct}$ method was used to calculate the relative fold gene expression of samples [28].

Table 1 Primers Used for the qRT-PCR Validation of DEGs

Gene name	Forward primer (5′-3′)	Reverse primer (5′-3′)
β-actin	GGTGTCTCACACACAGTGCC	CGGCGGTGGTGGTGAAGCTG
EF1α	CCGATGTCTATGTCTGCTAAGG	CATGATTTGAGCCTCGCCAA
GAPDH	GCGGTTTCGACGTGTCAGTTTG	CCGGAGCCCACAATGCACAC
CYP6CY3	CGGGGTGACGATCATCTATT	GGGTGGTCTTTTGACAAAGC Ss
E4	AAACTTTCCTTTTACACCGTT	TCTAAGCCAAGAAATGTTGAAA
GST	ACCCATGAGATTCCTTCTGTCC	TTCCAACACAGGCACTTTGC
CYP380C40	GCCAGTGATACTCAGAGAACT	AGCGACATTTTCTGGGCTGAA
UGT344P2	AATGGTTTCCTCAGCGTGAAA	GGCTGATCATAGAACATGGG
g10536	TGGACGCTGGTACAATAGTT	TTGAGAATCTGTTGACATCTGC
g20740	CGTGTTTGACCATCCATT	GCCACATAATACCGCTTAA
g10538	CTTGGCTAGAGCAATTATACGA	TACCGTACCAGCGTCAAT
g24259	GATCGTGCTTCTGTACTG	CGAGTTGTTCATGTGGAA
g25170	ACTCAGACAACTCCAAGATG	GGATTCGGATACAACTCAGG
g7429	GAAGCTACGCAGGATTACCA	TCCATCACCAAACGGCATAT
g20587	TGGAACTCATTAACGACGAA	CATTGTGACGATGTATGTACTC
g20497	ACGCCTCAAGAGTCTGTT	AGTGCTTCGGATTTCAAGTG
g3205	ATAAGGCAATGATCCAGAGTCG	GCTCCATCGTTCCGAATGA

2.10 Data Analysis

A probit analysis was conducted using the Data Processing System (DPS) software [29] to calculate the slope, LC_{50}, 95% confidence interval (CI) value, and the χ^2 value of each insecticide. Resistance ratios (RRs) were calculated using the results for a Lab-HN strain as the factor divisor. The insecticide resistance levels were classified according to Zhang et al. [30] i.e., susceptible (RR ≤ 5.0), low level of resistance (5.0 < RR ≤ 10.0), moderate level of resistance (10.0 < RR ≤ 100.0), and high level of resistance (RR > 100.0). Statistics analysis was also performed using he Data Processing System (DPS) software [29].

3 RESULTS

3.1 Thiacloprid Resistance Selection and Cross-Resistance Spectrum

The THG-R strain was obtained from the susceptible FAA-S strain after more than 50 generations of continuous selection with thiacloprid. A toxicity test indicated that the THG-R strain developed a very high level of resistance to thiacloprid (1201.2-fold, LC_{50} = 2270 mg·L^{-1}) compared to the FAA-S strain (LC_{50} = 1.89 mg·L^{-1}) (Table 1). The results of a cross-resistance test between thiacloprid and other insecticides for the THG-R strain of GPA are also shown in Table 2. Compared to the sensitive strain (SS), the cross-resistance ratios of the resistant strain (RS) for imidacloprid, acetamiprid, thiamethoxam, clothianidin, dinotefuran, sulfoxaflor, flupyradifurone, and Triflumezopyrim were 894.3-, 48.7-, 9.4-, 6.4-, 44.7-, 14.6-, 24.9-, and 2.36-fold, respectively, which indicated a high cross-resistance between thiacloprid with imidacloprid, a moderate cross-resistance with acetamiprid, dinotefuran, sulfoxaflor, and flupyradifurone, and a low cross-resistance with thiamethoxam and clothianidin. There was no cross-resistance between thiacloprid and triflumezopyrim in the THG-R strain.

Table 2 Resistance and Cross-Resistance of the FAA-S and THG-R Strains of GPA to Seven Insecticides

Insecticides	Strains	No.	Slope (SE)	LC_{50} (95% CI) Mg·L^{-1}	χ^2	RR[a]
Thiacloprid	FAA-S	480	4 (0.33)	1.89 (1.74-2.06)	3.32 (df=3)	
	THG-R	560	1.43 (0.13)	2270 (1861-2802)	2.52 (df=4)	1201.2
Imidacloprid	FAA-S	560	2.68 (0.21)	1.09 (0.97-1.22)	2.12 (df=4)	
	THG-R	560	1.44 (0.13)	974.74 (654.22-978.07)	4.19 (df=4)	894.3
Acetamiprid	FAA-S	480	2.02 (0.19)	2.63 (2.23-3.08)	3.85 (df=3)	
	THG-R	560	1.8 (0.15)	128.11 (108.5-152.03)	3.52 (df=4)	48.7
Thiamethoxam	FAA-S	560	4.71 (0.36)	2.57 (2.4-3.74)	5.5 (df=4)	
	THG-R	480	1.82 (0.18)	24.06 (20.18-28.67)	2.75 (df=3)	9.4
Clothianidin	FAA-S	560	3.5 (0.3)	3.21 (2.93-3.51)	4.19 (df=4)	

Dinotefuran	THG-R	480	1.93 (0.19)	20.41 (17.2-24.2)	3.91 (df=3)	6.4
	FAA-S	480	3.31 (0.26)	4.13 (3.76-4.53)	4.62 (df=3)	
Sulfoxaflor	THG-R	560	1.86 (0.15)	184.76 (157.04-217.85)	5.69 (df=4)	44.7
	FAA-S	480	2.68 (0.24)	1.34 (1.17-1.51)	2.61 (df=3)	
Flupyradifurone	THG-R	480	1.96 (0.18)	19.55 (16.6-23.28)	1.55 (df=3)	14.6
	FAA-S	480	3.26 (0.31)	1.98 (1.77-2.20)	2.76 (df=3)	
Triflumezopyrim	THG-R	480	2.03 (0.19)	49.38 (42.07-58.02)	5.06 (df=3)	24.9
	FAA-S	480	2.05 (0.19)	27.25 (23.28-32.05)	4.51 (df=3)	
	THG-R	480	2.02 (0.19)	64.24 (54.76-76.14)	2.18 (df=3)	2.5

[a]RR = the resistance ratio, obtained by the LC_{50} of each insecticide for the THG-R strain divided by the LC_{50} for the FAA-S strain.

3.2 Synergism of the Enzyme Inhibitors

The synergism results (Table 3) of the enzyme inhibitors showed that PBO exhibited significant synergistic action on the THG-R strain, with synergistic ratios of 2-fold, but no significant synergistic action on the FAA-S strain, with synergistic ratios of 1.03-fold. There was no significant synergistic action of DEF on the two strains, with low synergistic ratios of 1.02- and 1.26-fold, respectively. There was a significant synergistic action of DEM on the THG-R strain with a synergistic ratio of 1.86-fold, but no significant synergistic action on the FAA-S strain, with a synergistic ratio of 1.06-fold.

Table 3 Synergism of Three Enzyme Inhibitors on Thiacloprid Toxicity to the THG-R Strain of GPA

Insecticides	Treatment	No.	Slope±SE	LC_{50} (95% CI)	χ^2	Synergistic ratios (SR)
FAA-S	THC	480	4(0.33)	1.89(1.74-2.06)	3.32(df=3)	
	THC+PBO	480	3.82(0.32)	1.83(1.67-1.99)	3.61(df=3)	1.03
	THC+DEF	480	3.71(0.32)	1.85(1.69-2.02)	3.36(df=3)	1.02
	THC+DEM	480	4.01(0.33)	1.78(1.63-1.94)	3.39(df=3)	1.06
THG-R	THC	560	1.43(0.13)	2270.26(1861.38-2802.38)	2.52(df=4)	
	THC+PBO	560	1.56(0.14)	1142.75(948.56-1381.1)	4.59(df=4)	2
	THC+DEF	560	1.45(0.13)	1799.16(1482.75-2205.3)	0.86(df=4)	1.26
	THC+DEM	560	1.78(0.15)	1220.61(1032.17-1450.8)	5.88(df=4)	1.86

3.3 Detoxification of Enzyme Activities

The specific activities of detoxification enzymes (CarEs, MFO, and GSTs) in the FAA-S and THG-R strains were determined to analyze the biochemical mechanism of resistance in GPA to thiacloprid (Table 4). Compared to the FAA-S strain, the P450 activity in the THG-R strain increased significantly by 1.91-fold ($p < 0.01$) and the GST activity in the THG-R strain also significantly increased by 1.79-fold ($p < 0.05$). However, there was no significant difference in CarEs activity between the FAA-S and THG-R strains. According to the enzyme activity and synergism results, P450 may contribute to the metabolic resistance of GPA to thiacloprid.

Table 4 Detoxifying Enzyme Activities in the FAA-S and THG-R Strains of GPA

Metabolic enzyme	Strains	Activity	Ratio[b]
Specific activity of CarE[a] (μ mol μg^{-1} 10 min^{-1})	FAA-S	6.7±1.02	
	THG-R	8.17±2.01	1.22
Specific activity of GSTs[a] (n mol 0μg^{-1} min^{-1})	FAA-S	0.0047±0.00055	
	THG-R	0.0084±0.0026*	1.79
Specific activity of MFO[a] (n mol μg^{-1} 30 min^{-1})	FAA-S	0.34±0.052	
	THG-R	0.66±0.14**[a]	1.91

[a]Values within a column followed by different letters are significantly different (*significant at the 0.05 level and **significant at the 0.01 level using Tukey's test. [b]Ratio: activity of an enzyme in the THG-R strain / activity of an enzyme in the FAA-S strain.

3.4 Summary of the RNA-seq Data

The GPA gene expression in the THG-R strain and FAA-S strain (control) was quantified by RNA-seq and a total of 38.27 GB clean sequence data were obtained. The guanine-cytosine (GC) content was 40.07–43.41%, and the Q20 and Q30 values were ≥96.82% and ≥91.37%, respectively. The average total mapping ratio and average unique mapping ratio were 86.28 and 82.82%, respectively (Table 5).

Table 5 Summary of the RNA-seq Data

Sample	Raw reads	Clean bases (Gb)	Q20 (%)	Q20 (%)	GC (%)	Total reads	Total map	Unique map
FAA-S1	44,928,742	6.74G	96.95	91.76	40.73	43,616,450	39,529,693(90.63%)	37,511,121(86.0%)
FAA-S2	43,566,522	6.53G	97.02	91.83	38.49	42,309,780	37,711,668(89.13%)	36,182,851(85.52%)
FAA-S3	44,473,064	6.67G	96.82	91.37	36.81	43,284,852	36,691,863(84.77%)	35,268,102(81.48%)
THG-R1	42,067,498	6.31G	98.11	94.37	36.4	41,613,804	33,803,075(81.23%)	32,639,599(78.43%)

THG-R2	40,871,230	6.13G	98.15	94.46	40.02	40,035,794	36,427,134(90.99%)	35,126,460(87.74%)
THG-R3	39,251,802	5.89G	97.98	93.94	36.06	38,643,186	31,272,750(80.93%)	30,034,784(77.72%)

FAA-S1, S2 and S2: three repeats from a susceptible GPA strain raised under control conditions with no pesticide contact; THG-R1, R2 and R3: three repeats from the FAA-S strain screened continuously by thiaclopid for more than 50 generation; Q20: the percentage of bases with a Phred value > 20; Q30: the percentage of bases with a Phred value > 30. Total reads: the number of clean reads after quality control; Total map: the number and percentage of clean reads mapped with the reference genome; Unique map: the number and percentage of clean reads mapped with the unique locus of the reference genome.

3.5 Differentially Expressed Genes between the FAA-S and THG-R Strains

A total of 18,581 genes were merged and assembled based on all the mapped reads from the four strains using Stringtie (1.3.3b) [31]. The distributions of the expression levels of all genes were similar between the FAA-S and THG-R strains. Using the DEG-Seq 2R package (1.20.0), a total of 1,670 DEGs were identified between the FAA-S and THG-R GPA transcriptomes. More than 62.1% of the genes (1,037) were overexpressed (log_2foldchange > 1) and approximately 37.9% of the genes (633) were downregulated in the THG-R strain (Figure 1).

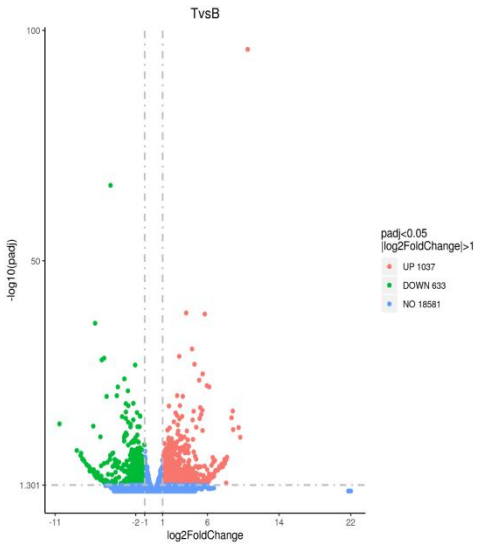

Figure 1 The DEGs between the GPA FAA-S and THG-R Strains

All DEGs were classified into three main GO categories: biological processes, cellular components, and molecular functions (Figure 2). For biological processes, the categories most represented were cellular processes (GO: 0008151, 643 out of 1,464 DEGs; 43.9%) and metabolic processes (GO: 0008152, 584 out of 1,464 DEGs; 25.3%) (Figure 2B). For cellular components, the genes involved in organelle parts (GO: 00043226, 90 out of 229 DEGs; 39.3%) and intracellular anatomical structure (GO: 0005622, 77 out of 229 DEGs; 33.6%) were the most abundant (Figure 2C). For molecular functions, catalytic activity (GO: 0003824, 796 out of 1,746 DEGs, 45.6%), transporter activity (GO:0005215, 383 out of 1,746 DEGs, 21.9%), and binding (GO: 0005488, 326 out of 1,746 DEGs, 18.7%) were the most highly represented categories (Figure 2D).

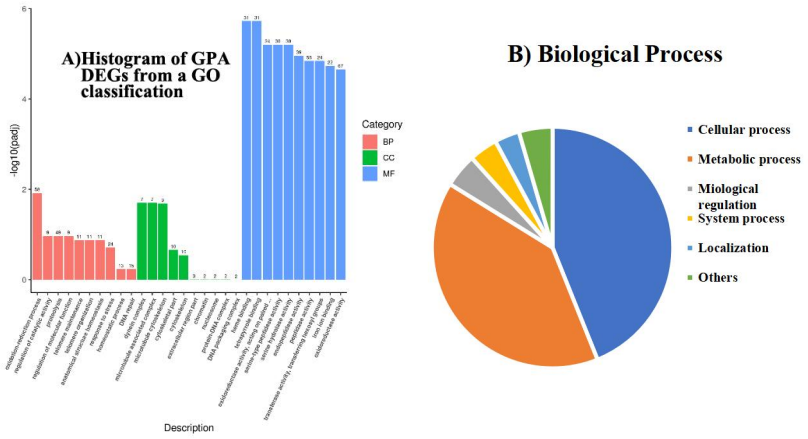

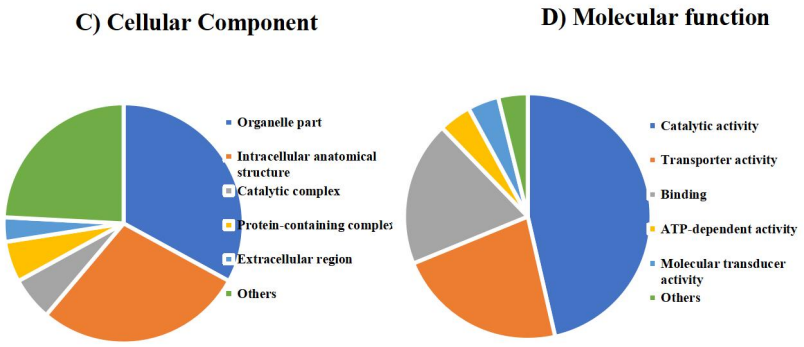

Figure 2 A GO Analysis of the DEGs of the GPA Transcriptome Annotated to UniGene cDNA Reference Data. The Analysis was Performed with Blast2GO-PRO. A) Histogram of GPA Differentially Expressed Sequences from a GO Classification. Three Main Ontologies (Biological Processes, Cellular Components, and Molecular Functions) are Shown on the X-axis. The Y-axis Indicates the Percentage of Total Genes, and the Right y-axis is the Number of Genes in each Category. B) The Distribution of Transcripts in the Biological Processes Category. C) The Distribution of Transcripts in the Cellular Components Category. D) The Distribution of Transcripts in the Molecular Functions Category.

A total of 547 DEGs were mapped onto 103 KEGG pathways (Figure 3). The largest category was lysosome, which contained 26 annotated DEGs (10.1%), followed by drug metabolism-cytochrome P450, pentose, and glucuronate interconversions, The metabolism of xenobiotics by cytochrome P450, fatty acid metabolism, and drug metabolism-other enzymes had 22 DEGs (8.1%), respectively.

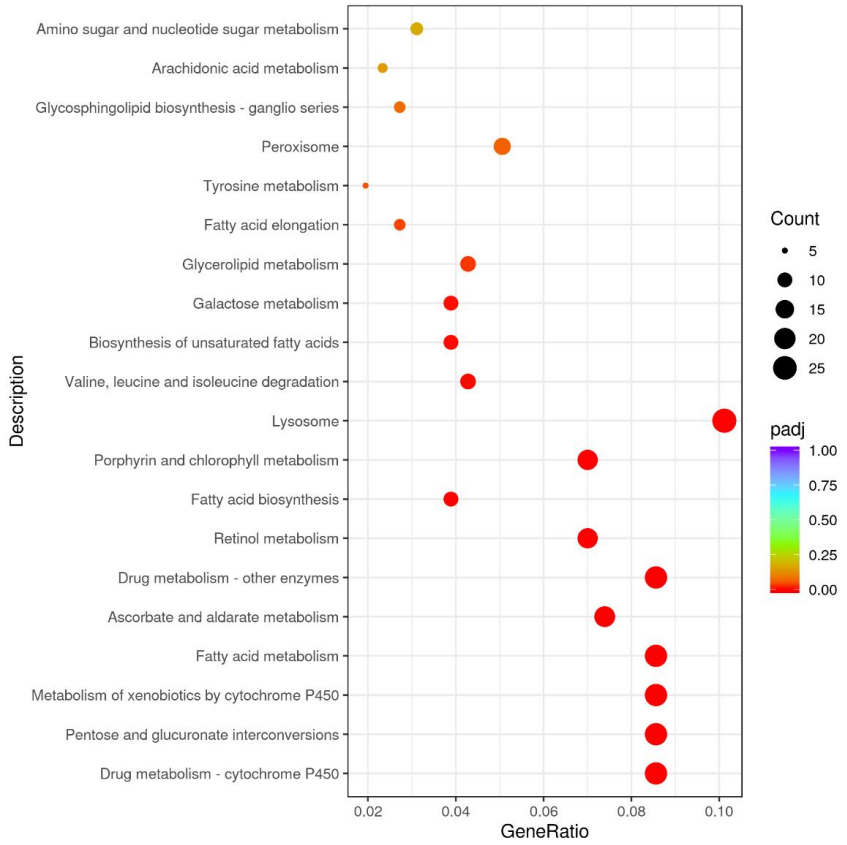

Figure 3 The Results of a KEGG Pathway Enrichment Analysis

3.6 Analysis of the Putative Genes Involved in the Regulatory Mechanism of Insecticide Detoxification

Among all the DEGs, 72 genes were identified that were involved in insecticide detoxification (Figure 4), including 15 upregulated detoxification genes and 57 downregulated detoxification genes. These overexpression genes are listed in Table 5, including five genes related to UGTs (*MpUgt2c1.3* (g20587), *MpUgt2c1.1* (g3205), *MpUgt2c1.2* (g10743),

MpUgt2b9 (g21618), and *MpUgt344j3* (g20497)); two genes related to P450s (cytochrome-P450) (*MpCyp4c1* (g25170) and *MpCyp6a14* (g7429)); two genes related to esterases (*MpPde11a* (g18568) and *MpThem6* (g24259)); and six genes related to ABCs (ATP-binding cassette transporters) (*Mplethal(2)03659.1* (g10536), *MpAbcg23.3* (g20740), *MpAbcg23.1* (g4805), *MpAbcg23.2* (g26047), *MpAbcb1b* (g21645), and *Mplethal(2)03659.2* (g10538)). The distribution of these upgraded detoxification genes on GPA chromosomes is shown in Figure 5.

Table 5 Selected Genes of the Detoxification Enzymes Identified by a Microarray as Significantly Differentially Transcribed between the THG-R and FAA-S Strains

Family	protein ID	blast result	name	Rename abbr.
ABCs	g10536.p1	XP_022166670.1	probable multidrug resistance-associated protein lethal(2)03659 isoform X2	*Mplethal(2)03659.1*
ABCs	g20740.p1	XP_022180695.1	ABC transporter G family member 23-like	*MpAbcg23.3*
ABCs	g4805.p1	XP_022180629.1	ABC transporter G family member 23-like isoform X1	*MpAbcg23.1*
ABCs	g26047.p1	XP_022175210.1	ABC transporter G family member 23-like	*MpAbcg23.2*
ABCs	g21645.p1	XP_022176197.1	multidrug resistance protein 1B-like isoform X1	*MpAbcb1b*
ABCs	g10538.p1	XP_022166683.1	probable multidrug resistance-associated protein lethal(2)03659	*Mplethal(2)03659.2*
Esterases	g18568.p1	XP_022168710.1	dual 3',5'-cyclic-AMP and -GMP phosphodiesterase 11A-like	*MpPde11a*
Esterases	g24259.p1	XP_022182351.1	protein THEM6-like	*MpThem6*
P450s	g25170.p1	XP_022175934.1	cytochrome P450 4C1-like	*MpCyp4c1*
P450s	g7429.p1	XP_022171832.1	probable cytochrome P450 6a14	*MpCyp6a14*
UDPGT	g20587.p1	XP_022182837.1	UDP-glucuronosyltransferase 2C1-like	*MpUgt2c1.3*
UDPGT	g3205.p1	XP_001949897.2	UDP-glucuronosyltransferase 2C1	*MpUgt2c1.1*
UDPGT	g10743.p1	XP_022166626.1	UDP-glucuronosyltransferase 2C1-like	*MpUgt2c1.2*
UDPGT	g21618.p1	XP_022162085.1	UDP-glucuronosyltransferase 2B9-like isoform X9	*MpUgt2b9*
UDPGT	g20497.p1	ATN96079.1	UDP-glucuronosyl transferase 344J3	*MpUgt344j3*

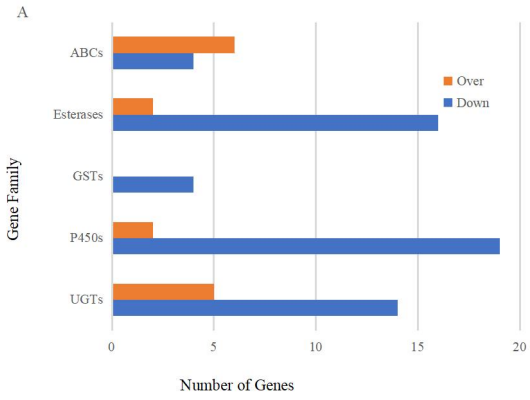

Figure 4 The DEGs between the THG-R and FAA-S Strains (Control) of *Myzus persicae*. A) The Number of Genes Encoding ABC Transporters, Esterases, GSTs, P450s, and UGTs that were Commonly Differentially Expressed between Thiacloprid Resistant and Susceptible Strains

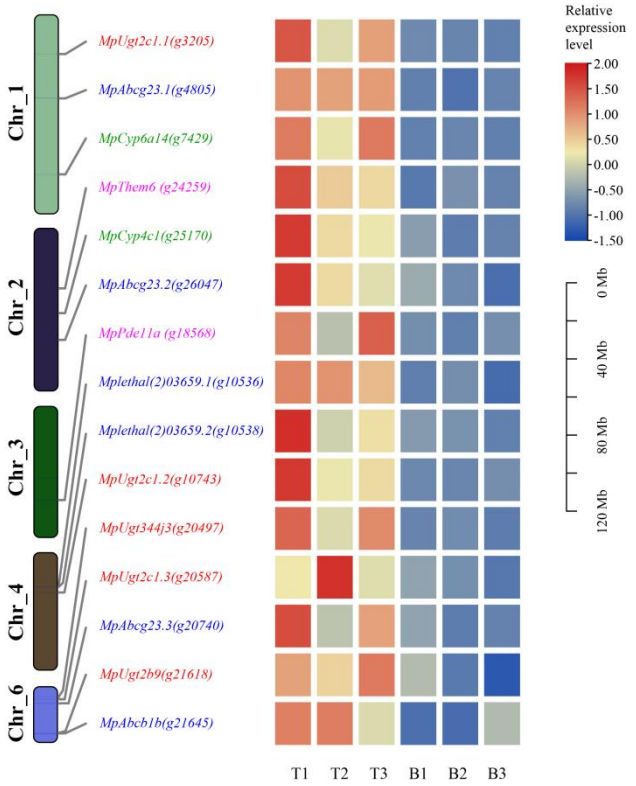

Figure 5 Distribution of the Detoxification Genes on *Myzus persicae* Chromosomes and Expression Heat Map (T: THG-R, B: FAA-S)

UDPGT Family Genes Shown in Red, ABC Transporter Family Shown in blue, P450 Family Shown in Green, Esterase Family Shown in Purple. These Genes were Distributed in each Chromosome, Except Chr_5. Gene Expression Levels are Indicated with a Rainbow Color Scale from Blue (Low Expression) to Red (High Expression)

3.7 Expression Levels of Insecticide Detoxification Genes in the FAA-S and THG-R Strains

Among the upregulated detoxification genes, *Mplethal(2)03659.1* was the most highly overexpressed (fold-change = 33.8), followed by *MpUgt2c1.3* (fold-change = 22.2) (Figure 6), *MpThem6* (fold-change = 4.1), *Mplethal(2)03659.2* (fold-change = 3.5), *MpUgt344j3* (fold-change = 3.4), *MpAbcg23.3* (fold-change = 3.3) and *MpUgt2c1.1* (3-fold), while the P450 genes *MpCyp4c1* and *MpCyp6a14* exhibited 2.9- and 2.7-fold-changes. For the other six upgraded detoxification genes, the fold-changes were below 2.7 (Fig. 6). The downregulated genes included all four sequences encoding GSTs with a negative fold-change of -1 to -2, and 19 sequences encoding cytochrome P450s, including *MpCyp380c40* with a fold-change of -1.5 to 2.5.

To further clarify the association between the overexpression of detoxification genes and the thiacloprid resistance mechanism of THG-R (Figure 7), we determined and compared the differences in the expression levels of nine upgraded detoxification enzyme genes (fold-change ≥ 2.7) in a transcript analysis and five other genes (*CYP6CY3*, *CYP380C40*, *FE4*, *GST*, *UGT344P2*) that were previously reported to be involved in resistance to Group 4 insecticides between the THG-R and FAA-S strain. The high expression levels of *MpUgt2c1.3*, MpThem6, and *Mplethal(2)03659.1* were 2.4-, 7-, and 30.3-fold, respectively. In contrast, the expression levels of *CYP380C40*, *MpCyp6a14*, and *FE4* were downregulated in the THG-R compared with the FAA-S.

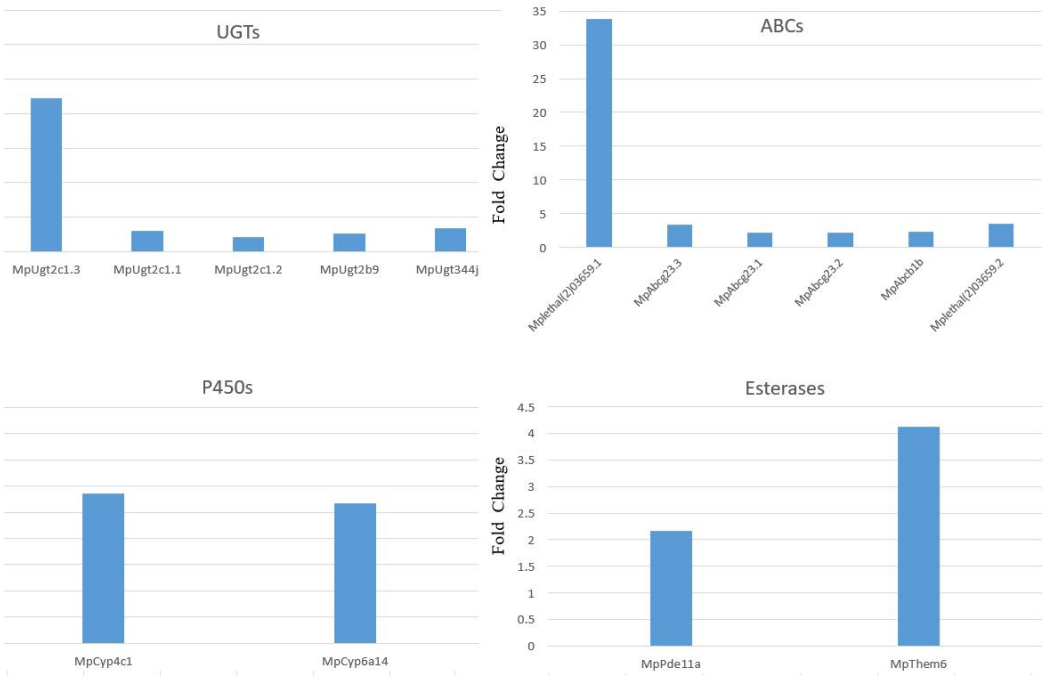

Figure 6 The Fold-Changes of Selected Genes Identified by a Microarray as Significantly Differentially Transcribed between the THG-R and FAA-S Strains

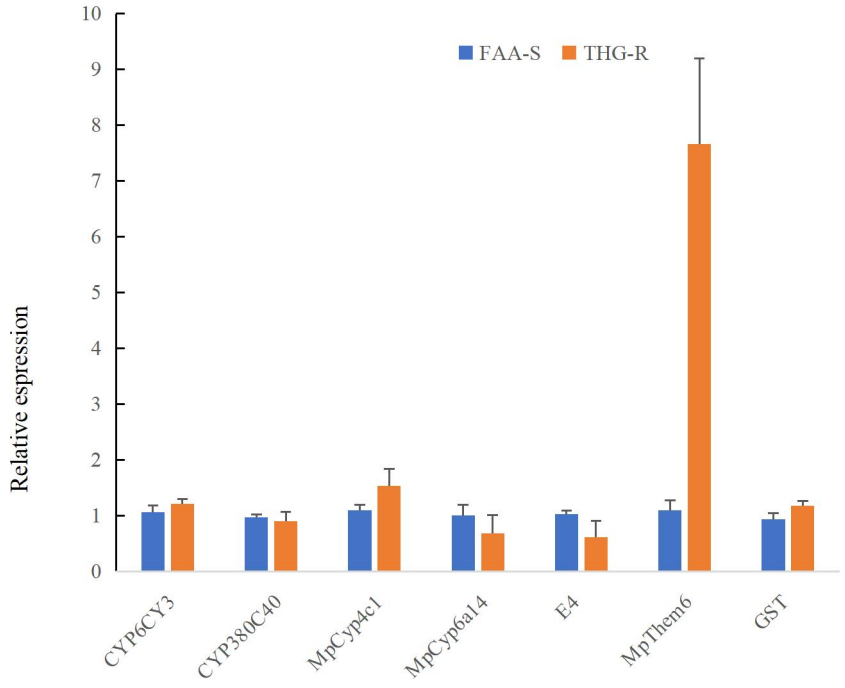

A) cytochrome P450, Carboxylesterase & Glutathione S-transferases

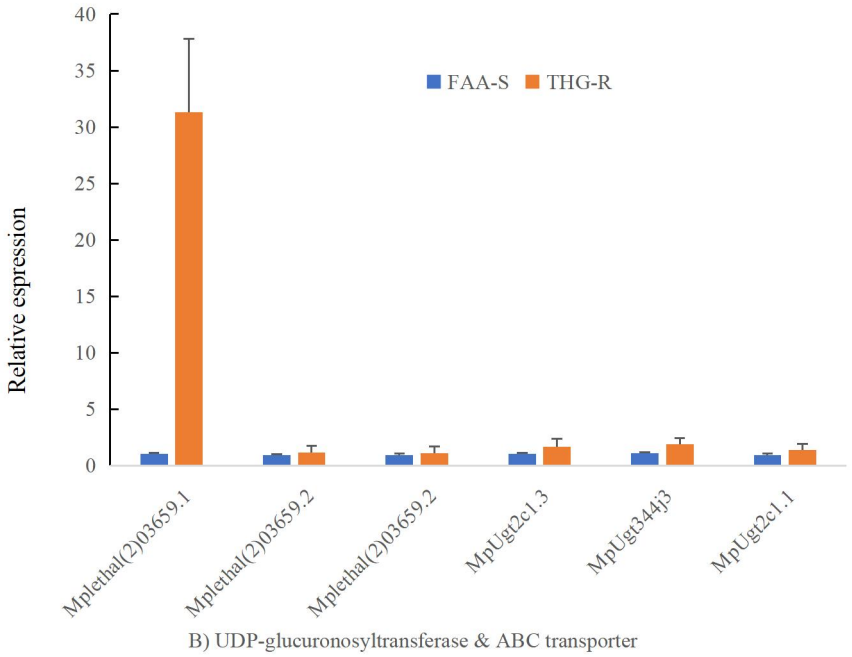

Figure 7 Quantitative Real-Time PCR (qRT-PCR) Validation of the Expression of DEGs Identified using RNA-sequencing. The Expression Levels were Normalized to the GAPDH, EF1α, and β-actin Genes. A) Expression of the Genes for P450, Esterases, GST, B) Expression of the ABCs and UGTs in each Pairwise Comparison of the Thiacloprid Resistant (THG-R) Strain and three Susceptible (FAA-S) Strains

4 DISCUSSION

Neonicotinoid resistance in GPA has become a serious worldwide problem. In this study, the susceptible GPA developed a very high-level resistance to thiacloprid (RR = 1201.2) after 50 generations of selection, which indicated a high risk of evolving thiacloprid resistance. Several studies have also documented that selection with neonicotinoids in the laboratory may result in highly resistant GPA strains. The GPA developed a 124.5-fold resistance to imidacloprid after a 20-generation selection [32], while a 75.6-fold resistance to thiamethoxam was generated after a 15-generation selection [33] and 57.5-fold acetamiprid resistance was achieved after a five-generation selection [34]. The intensity of selection in the field by neonicotinoids also causes GPA field populations to evolve a high resistance to neonicotinoids. For example, GPA in the FRC strain from southern France exhibited a 1679- and 225-fold resistance to imidacloprid and thiamethoxam, respectively [9], and strain 99H1 collected from Italy was found to have a more than 600-fold resistance to imidacloprid [35]). Risk management practices should be implemented to combat and slow thiacloprid resistance in GPA, such as resistance monitoring and rotations with different insecticides.

Laboratory bioassays were conducted to evaluate the cross-resistance in the THG-R strain between thiacloprid and other insecticides. The eight other insecticides were allocated to the IRAC Group 4 of compounds that act as nicotinic acetylcholine receptor (nAChR) competitive modulators. We found that the selection of GPA with thiacloprid after more than 50 generations in the laboratory induced a very high level of cross-resistance to imidacloprid (894.3-fold), moderate levels of resistance to acetamiprid (48.7-fold), dinotefuran (44.7-fold), flupyradifurone (24.9-fold), and sulfoxaflor (14.6-fold), and very low levels of resistance to thiamethoxam (9.4-fold) and clothianidin (6.4-fold). Although the five insecticides, imidacloprid, acetamiprid, dinotefuran, thiamethoxam, and clothianidin are neonicotinoids (Group 4A), they showed great differences in cross-resistance with thiacloprid (Group 4A). Previous studies indicated the presence of a high cross-resistance between thiacloprid and imidacloprid in GPA. Five highly imidacloprid-resistant field populations ($156 \leq RR \leq 412$) exhibited more than a 110-fold cross-resistance to thiacloprid [36]. Similarly, the FRC strain (RR > 2500 for imidacloprid) [14] exhibited > 2500-fold resistance to thiacloprid, > 80-fold resistance to acetamiprid, and 54-fold resistance to dinotefuran. However, the FRC strain also had a high (> 2,500-fold) resistance to clothianidin and > 100-fold resistance to thiamethoxam, but the THG-R strain had a low cross-resistance to the two neonicotinoids. The THG-R strain also developed a moderate cross-resistance to flupyradifurone (Group 4C) and sulfoxaflor (Group 4A), and the FRC strain also conferred a 43-fold resistance to sulfoxaflor [14]. However, the absence of cross-resistance between flupyradifurone and imidacloprid was observed in a low imidacloprid-resistant GPA strain [37]. Although cross-resistance did not occur between triflumezopyrim (Group 4D) and thiacloprid in the THG-R strain, the relatively low toxicity of triflumezopyrim against GPA limited its application. Based on our results, Group 4 insecticides cannot be used as an alteration tool for GPA thiacloprid resistance management strategies.

The toxicity of thiacloprid to THG-R GPA was enhanced by PBO and DEM, indicating that P450 and GST may be related to the decreased susceptibility to thiacloprid in GPA. The obviously increased activities of P450 and GST in the THG-R strain further supported the hypothesis of this study. Previous studies have demonstrated that increased

detoxification through metabolic enzymes significantly contributed to resistance to Group 4 insecticides in GPA, but this did not always occur. A significant synergism was detected in which the pretreatment of the FRC strain of GPA with PBO reduced the RRs from 1,679-fold to 234-fold for imidacloprid and from 225-fold to 26-fold for thiamethoxam [9], and for the clone 5191A it led to a 14.5-fold synergism of imidacloprid [38], with a much higher synergism than that observed in this study (2-fold). However, PBO synergism was not detected in acetamiprid-resistant GPA [34]. Another synergist, DEM, was also found to increase the toxicity of imidacloprid to *Rhopalosiphum padi* by 8.32-fold [39]. The activities of P450 monooxygenases and GST were reported to be 2.03- and 1.57-fold higher in thiamethoxam-resistant GPA than in a susceptible strain [33], which was similar to our result (1.91-fold). These results indicate that cytochrome P450 and GST may be involved in thiacloprid resistance in GPA. The thiamethoxam-resistant GPA also exhibited a 6.12-fold higher CarEs activity than the susceptible strain [33]. Our study yielded contrasting results in which no increase in activity was found in the THG-R strain, and DEF also had no obvious synergistic effect on the THG-R strain, which demonstrated the CarEs was not associated with thiacloprid resistance in GPA.

The molecular mechanisms governing high levels of neonicotinoid in GPA have been widely studied, but these resistant strains were collected in the field. Here, we attempted to determine the molecular mechanisms of thiacloprid resistance in GPA using an RNA-seq library approach. We discovered approximately 1,670 DEGs (1,037 up-regulated and 633 down-regulated) for susceptible and artificially selected high thiacloprid-resistant populations of GPA (THG-R). The number of DEGs was much higher than other neonicotinoid-resistant GPA strains. In the Cascade209, EastMunglinup209, and EastNaernup209 clones of GPA that are resistant to sulfoxaflor, a total of 1,033, 1,046, and 860 genes were consistently differentially expressed compared to the three susceptible clones, respectively [20]. Only 273 DEGs were identified between the insecticide resistant clone 5191A (27.5-fold to imidacloprid and 41.31-fold to thiacloprid) and the susceptible clone 4106A [40]. In general, the GO enrichment of DEGs in the THG-R strain indicated that the metabolic process was significantly enriched (Figure 2A, 2B), while the “metabolic pathway” (including drug metabolism-cytochrome P450, metabolism of xenobiotics by cytochrome P450, fatty acid metabolism, and drug metabolism-other enzymes) was also enriched in a KEGG analysis. These metabolic pathways are known to be involved in insecticide metabolism [41,42].

The most widely studied genes belonging to the three gene families that typically participate in the detoxification of metabolic resistance to insecticides are *cytochrome P450* (P450s proteins, encoded by *CYP* genes), *glutathione S-transferases* (GST), and *carboxylesterases* (CarEs). The P450s are a superfamily of enzymes that can catalyze the oxidation of steroids, fatty acids, and xenobiotics [19]. The cytochrome P450 enzymes are important in the adaptation to the detoxification of insecticides in phytophagous insects and cytochrome P450-mediated enhanced metabolism has been proven to be responsible for insecticide resistance, including neonicotinoid resistance. In this study, we showed that the enhanced transcription of two P450 genes *MpCyp4c1* and *MpCyp6a14* in the THG-R strain was due, at least in part, to an approximately 3-fold amplification, while *MpCyp4c1* was found to exhibit a 2.13-fold overexpression by qPCR verification. However, the overexpression and duplication of *CYP6CY3* contributed to the differences in neonicotinoid-resistant GPA, such as a 22-fold overexpression in the 5191A clone [40], 9-36-fold overexpression in field collected populations in Greece [10], and 2.8−6.7-fold overrepresentation with copy numbers in field collected populations in Australia [43]. Nakao et al. [44] confirmed that *CYP6CY3* showed metabolic activity against imidacloprid, as well as acetamiprid, clothianidin, and thiacloprid. Furthermore, 21−76-fold highly overexpressed *CYP380C40*, which is another P450 gene, was detected in the sulfoxaflor resistant GPA clones [20]. However, no significant overexpression of the two P450 genes was found in the THG-R strain. From the results of the P450 inhibitor experiment, it was concluded that the P450 might not be the main enzyme involved in laboratory selected thiacloprid resistant GPA. Similarly to our results, *CYP6CY3* was also found to not be upregulated in a high acetamiprid-resistant (57.5-fold) GPA strain [34]. This difference revealed the existence of another enhanced metabolic route for neonicotinoids in addition to the P450 routes in GPA. Carboxylesterase was significantly down-regulated in the THG-R strain, which was consistent with the results of a previous study that showed that the FE4 gene did not involve the detoxification of thiacloprid in the pest [45]. The GSTs exhibited no significant different expression between the THG-R and FAA-S strains, which was consistent with other studies. From our study, we found that the three detoxification enzymes did not play the key role in the thiacloprid resistance of GDP [20]. However, the esterase *MpThem6* gene exhibited a 7-fold overexpression, which indicated that it probably had an important role in thiacloprid resistance.

The UGTs are a superfamily of enzymes that catalyze the transfer of glycosyl residues from activated nucleotide sugars to hydrophobic molecules (aglycones) and are also known as biotransformation enzymes that participate in the detoxification process [46]. The UGT gene family that was found to be significantly overexpressed in the THG-R strain included *MpUgt2c1.3* (2.43-fold), *MpUgt344j3* (2.28-fold), *MpUgt2c1.1* (2.04-fold), and *UGT344P2* (1.44-fold) (Figure 2). The gene *UGT344P2* was overexpressed by 6-33-fold in the sulfoxaflor resistant GPA clones (Pym et al., 2022), which may be correlated with cross-resistance to sulfoxaflor in the THG-R strain. Another two UGTs, namely *UGT352A4* and *UGT352A5,* were found to be 2.66-fold and 1.9-fold overexpressed, respectively, compared to the susceptible strain, and the knockdown of *UGT352A5* resulted in a decrease in the thiamethoxam resistance in the thiamethoxam-resistant (THQR) *B. tabaci* [47]. In a thiamethoxam-resistant strain of *A. gossypii*, the transcripts of 13 UGTs (*UGT344J2*, *UGT348A2*, *UGT344D4*, *UGT341A4*, *UGT343B2*, *UGT342B2*, *UGT350C3*, *UGT344N2*, *UGT344A14*, *UGT344B4*, *UGT351A4*, *UGT344A11*, and *UGT349A2*) were increased by approximately 2.0-fold and the suppression of selected UGTs significantly increased the insensitivity of resistant aphids to thiamethoxam [48]. We considered that the UGTs may play an important role in the cross-resistance to Group 4 insecticides in the THG-R

strain.

The ABC transporters are responsible for the translocation of a variety of substrates (e.g., metabolites, lipids, inorganic ions, and xenobiotics) by pumping them out of the cells through the cell membrane. The ABCs involved in insecticides have received much attention. Three ABC genes, *Mplethal(2)03659.1*, *MpAbcg23.3*, and *Mplethal(2)03659.2*, were found to be overexpressed in the THG-R strain, with *Mplethal(2)03659.1* overexpressed by 30.32-fold. The suppression of five overexpressed ABCs (*ABCA2*, *ABCD1*, *ABCD2*, *ABCE1*, and *ABCG15*) significantly increased the thiamethoxam sensitivity of resistant *A. gossypii* (Pan et al., 2020), while 10 ABCs (*ABCA1*, *ABCA2*, *ABCB1*, *ABCB5*, *ABCD1*, *ABCG7*, *ABCG16*, *ABCG26*, *ABCG27*, and *MRP7*) were up-regulated and the knockdown of *ABCA1* and *ABCD1* significantly increased the sulfoxaflor sensitivity in sulfoxaflor-resistant *A. gossypii* [49]. Furthermore, the knockdown of *AgABCG7* and *AgABCG26* increased thiamethoxam and imidacloprid mortality in a field multi-resistant population of *A. gossypii* (SDR) [50]. These data also confirmed that the diverse metabolic processes of *Mplethal(2)03659.1* were involved in thiacloprid resistance.

Mplethal(2)03659.1 and *MpThem6* attracted our attention because of their strong expression in the THG-R strain, which suggested that the two genes played a vital role in thiacloprid metabolism and transport. However, the involvement of the two genes in the metabolism related to insecticides is poorly understood. *Mplethal(2)03659.1* is an ATP-binding cassette transporter C (ABCC) family protein that has been widely detected in the genomes of other aphids, such as *A. gossypii* (XM_050204743.1), *Rhopalosiphum maidis* (XM_026951384.1), and *Diuraphis noxia* (XM_015510588.1). It is a probable multidrug resistance-associated protein that is similar to the human multidrug resistance-associated protein 1 that mediates the export of organic anions and drugs from the cytoplasm (probable multidrug resistance-associated protein lethal). *Mplethal(2)03659.1* has a possible involvement in cantharidin detoxification in two blister beetle species, *Lydus trimaculatus* (Fabricius, 1775) (tribe Lyttini) and *Mylabris variabilis* (Pallas, 1781) (tribe Mylabrini) [51]. Further studies should be conducted to investigate if overexpression of the two genes is widespread in the field resistant MPA population and to determine the effects of knockdown of the two genes on the susceptibility of neonicotinoids to their resistant populations.

5 CONCLUSIONS

Our results suggested that the GPA has the potential to rapidly evolve resistance to thiacloprid under continuous selection in the laboratory. Our experiment also revealed evidence for cross-resistance to Group 4 insecticides, except for triflumezopyrim, in the THG-R strain. Group 4 insecticides were therefore not recommended for use in rotation with thiacloprid when resistance occurred in the field. Enzyme activities and synergism tests indicated that the evolution of resistance to thiacloprid in the THG-R was associated with cytochrome P450. We constructed RNA-seq libraries to investigate the DEGs between THG-R and FAA-S. A comparative analysis of the DEGs between THG-R and FAA-S revealed that genes for detoxification enzymes, including cytochrome P450, UGTs, ABCs and thioesterase, were significantly overexpressed. The *MpUgt2c1.3*, *MpThem6*, *Mplethal(2)03659.1, MpCyp4c1*, and *MpCyp6a14* genes were identified as being overexpressed in the THG-R strain by qPCR. Conversely, the genes previously reported to be responsible for neonicotinoid resistance in GPA, including *CYP6CY3*, *CYP380C40*, and *UGT344P2*, were not significantly upregulated in the THG-R strain. We considered that the ABC gene *Mplethal(2)03659.1* and the thioesterase gene *MpThem6* may play a vital role in the metabolic mechanism of thiacloprid resistance in GPA. A complete identification of the function of these genes is necessary to fully understand their role in thiacloprid resistance in GPA.

COMPETING INTERESTS

The authors have no relevant financial or non-financial interests to disclose.

FUNDING

This work was supported by Fujian Natural Science Foundation (2022J01461), the program of Fujian Provincial Department of Science & Technology (2020R10240011), program of Science and Technology Innovation Foundation of FAAS Supported by Financial Department of Fujian Government (CXTD2021002-1, XTCXGC2021017).

REFERENCES

[1] Yi XU, Gray S M. Aphids and their transmitted potato viruses: A continuous challenges in potato crops. Integr. Agric. 2020, 19: 367-375.
[2] IRAC. The IRAC Mode of Action Classification, 2023.
[3] Hlaoui A, Chiesa O, Figueroa C C, et al. Target site mutations underlying insecticide resistance in tunisian populations of Myzus persicae (sulzer) on peach orchards and potato crops. Pest Manag. Sci. 2022, 78: 1594-1604.
[4] Li Y, Xu Z, Li S, et al. Insecticide resistance monitoring and metabolic mechanism study of the green peach aphid, Myzus persicae (sulzer) (Hemiptera: Aphididae), in Chongqing, China. Pestic. Biochem. Physiol. 2016, 132: 21-28.

[5] Tang Q L, Ma K S, Hou Y M, et al. Monitoring insecticide resistance and diagnostics of resistance mechanisms in the green peach aphid, Myzus persicae (sulzer) (hemiptera: aphididae) in China. Pestic. Biochem. Physiol. 2017, 143: 39-47.
[6] Casida J E. Neonicotinoids and other insect nicotinic receptor competitive modulators: Progress and prospects. Annu. Rev. Entomol. 2018, 63: 125-44.
[7] Nauen R, Strobel J, Tietjen K, et al. Aphicidal activity of imidacloprid against a tobacco feeding strain of Myzus persicae (Homoptera: Aphididae) from Japan closely related to Myzus nicotianae and highly resistant to carbamates and organophosphates. Bull. Entomol. Res. 1996, 86: 165-171.
[8] Mota-Sanchez D, Wise JC. The Arthropod Pesticide Resistance Database. Michigan State University, 2023.
[9] Bass C, Puinean AM, Andrews M, et al. Mutation of a nicotinic acetylcholine receptor β subunit is associated with resistance to neonicotinoid insecticides in the aphid Myzus persicae. BMC Neurosci, 2011, 12(1): 51.
[10] Ch Voudouris C, Kati AN, Sadikoglou E, et al. Insecticide resistance status of Myzus persicae in Greece: long-term surveys and new diagnostics for resistance mechanisms. Pest Manag. Sci, 2016, 72: 671-83.
[11] Alptekin S, Bass C, Nicholls C, et al. Induced thiacloprid insensitivity in honeybees (Apis mellifera L.) is associated with up-regulation of detoxification genes. Insect Mol. Biol, 2016, 25:171-80.
[12] Jeschke P, Moriya K, Lantzsch R, et al. Thiacloprid (Bay YRC 2894) - a new member of the chloronicotinyl insecticide (CNI) family. Pflanzenschutz-Nachr. Bayer, 2001, 54: 147–160.
[13] Foster SP, Cox D, Oliphant L, et al. Correlated responses to neonicotinoid insecticides in clones of the peach-potato aphid, Myzus persicae (Hemiptera: Aphididae). Pest Manag. Sci, 2008, 64: 1111-1114.
[14] Cutler P, Slater R, Edmunds AJ, et al. Investigating the mode of action of sulfoxaflor: A fourth-generation neonicotinoid. Pest Manag. Sci, 2013, 69: 607-19.
[15] Le Goff G, Hilliou F. Resistance evolution in Drosophila: the case of CYP6G1. Pest Manag. Sci. 2017, 73: 493-499.
[16] Yang X, Xie W, Wang SL, et al. Two cytochrome P450 genes are involved in imidacloprid resistance in field populations of the whitefly, Bemisia tabaci, in China, Pestic. Biochem. Physiol, 2013, 107: 343-350.
[17] Chen A, Zhang H, Shan T, et al. The overexpression of three cytochrome P450 genes CYP6CY14, CYP6CY22 and CYP6UN1 contributed to metabolic resistance to dinotefuran in melon/cotton aphid, Aphis gossypii Glover. Pestic. Biochem. Physiol. 2020,167,104601.
[18] Zhang Y, Yang Y, Sun H, et al. Metabolic imidacloprid resistance in the brown planthopper, Nilaparvata lugens, relies on multiple P450 enzymes. Insect Biochem. Mol. Biol. 2016, 79: 50-56.
[19] Nauen R, Bass C, Feyereisen R, et al. The role of cytochrome P450s in insect toxicology and resistance. Annu. Rev. Entomol. 2022, 67: 105-124.
[20] Pym A, Umina PA, Reidy-Crofts J, et al. Overexpression of UDP-glucuronosyltransferase and cytochrome P450 enzymes confers resistance to sulfoxaflor in field populations of the aphid, Myzus persicae. Insect Biochem. Mol. Biol. 2022, 143: 103743.
[21] Pan Y, Tian F, Wei X, et al. Thiamethoxam resistance in Aphis gossypii glover relies on multiple UDP-glucuronosyltransferases. Front Physiol. 2018, 9, 322.
[22] Shang CC, Soderlund DM. Monooxygenase activity of tobacco budworm (Heliothis virescens) larvae: Tissue distribution and optimal assay conditions for the gut activity, Comp. Biochem. Physiol. B Biochem. Mol. Biol. 1984, 79: 407–411.
[23] Van Asperen K. A study of housefly esterase by means of a sensitive colorimetric method. Insect Physiol. 1962, 8: 401–416.
[24] Habig WH, Pabst MJ, Jakoby WB. Glutathione S-transferases the first enzymatic step in mercapturic acid formation. Biol. Chem. 1974, 249: 7130–7139.
[25] Bradford MM. A rapid and sensitive method for the quantitation of microgram quantities of protein utilizing the principle of protein-dye binding. Anal. Biochem. 1976, 72: 248–254.
[26] Anders S, Pyl PT, Huber W. HTSeq--a Python framework to work with high-throughput sequencing data. Bioinformatics. 2015, 31:166-9.
[27] Trapnell C, Williams BA, Pertea G, et al. Transcript assembly and quantification by RNA-Seq reveals unannotated transcripts and isoform switching during cell differentiation. Nat. Biotechnol. 2010, 28: 511-515.
[28] Kenneth JL, Thomas DS. Analysis of relative gene expression data using real-time quantitative PCR and the 2(-Delta Delta C(T)) Method. Methods 2001, 25: 402-408.
[29] Tang QY, Zhang CX. Data Processing System (DPS) software with experimental design, statistical analysis and data mining developed for use in entomological research. Insect Sci, 2013, 20(2): 254-260.
[30] Zhang XL, Liao X, Mao KK, et al. Neonicotinoid insecticide resistance in the field populations of Sogatella furcifera (Horváth) in Central China from 2011 to 2015. Asia Pac. Entomol. 2017, 20: 955–958.
[31] Pertea M, Kim D, Pertea GM, et al. Transcript-level expression analysis of RNA-seq experiments with HISAT, StringTie and Ballgown, Nature Protocols. 2016, 11: 1650-1667
[32] Choi BR, Lee SW, Yoo JK. Resistance development and cross-resistance of green peach aphid, Myzus persicae (homoptera: aphididae), to imidacloprid. Pestic. Sci. 2002, 6: 264-270.
[33] Zhang P, Zhou X. Metabolic mechanism of resistance to thiamethoxam in Myzus persicae. Plant Protection. 2015, 41: 39-44.

[34] Berber G, Demîrcî B, Toprak U, et al. Acetamiprid resistance in the green peach aphid Myzus persicae (Sulzer) (Hemiptera: Aphididae): Selection, cross-resistance, biochemical and molecular resistance mechanisms. JAFAG 2022, 39: 136-142.
[35] Panini M, Dradi D, Marani G, et al. Detecting the presence of target-site resistance to neonicotinoids and pyrethroids in Italian populations of Myzus persicae. Pest Manag. Sci, 2014, 70: 931-938.
[36] Mottet C, Fontaine S, Caddoux L, et al. Assessment of the dominance level of the R81T target resistance to two neonicotinoid insecticides in Myzus persicae (Hemiptera: Aphididae). Econ. Entom. 2016, 109(5): 2182-2189.
[37] Nauen R, Jeschke P, Velten R, et al. Flupyradifurone: A brief profile of a new butenolide insecticide. Pest Manag. Sci, 2015, 71: 850-862.
[38] Philippou D, Field L, Moores, G. Metabolic enzyme(s) confer imidacloprid resistance in a clone of Myzus persicae (Sulzer) (Hemiptera: Aphididae) from Greece. Pest Manag. Sci. 2010, 66: 390-395.
[39] Gong P, Chen D, Wang C, et al. Susceptibility of four species of aphids in wheat to seven insecticides and its relationship to detoxifying enzymes. Front. Physiol. 2021, 11:623612.
[40] Puinean AM, Foster SP, Oliphant L, et al. Amplification of a cytochrome P450 gene is associated with resistance to neonicotinoid insecticides in the aphid Myzus persicae. PLoS Genet. 2010, 6: e1000999.
[41] Bonizzoni M, Ochomo E, Dunn W A, et al. RNA-seq analyses of changes in the Anopheles gambiae transcriptome associated with resistance to pyrethroids in Kenya: identification of candidate-resistance genes and candidate-resistance SNPs. Parasit. Vectors. 2015, 8: 474.
[42] Safi NHZ, Ahmadi AA, Nahzat S, et al. Evidence of metabolic mechanisms playing a role in multiple insecticides resistance in Anopheles stephensi populations from Afghanistan, 2017, 16: 100.
[43] de Little SC, Edwards O, van Rooyen AR, et al. Discovery of metabolic resistance to neonicotinoids in green peach aphids (Myzus persicae) in Australia. Pest Manag. Sci, 2017, 73: 1611-1617.
[44] Nakao T, Kawashima M, Banba S. Differential metabolism of neonicotinoids by Myzus persicae CYP6CY3 stably expressed in Drosophila S2 cells. Pestic. Sci, 2019, 44: 177-180.
[45] Foster SP, Denholm I, Thompson R. Variation in response to neonicotinoid insecticides in peach-potato aphids, Myzus persicae (Hemiptera: Aphididae). Pest Manag. Sci, 2003, 59: 166-173.
[46] Brierley CH, Burchell B. Human UDP-glucuronosyl transferases: chemical defence, jaundice and gene therapy. Bioessays, 1993, 15: 749-754.
[47] Du T, Fu B, Wei X, et al. Knockdown of UGT352A5 decreases the thiamethoxam resistance in Bemisia tabaci (Hemiptera: Gennadius). Int. Biol. Macromol, 2021, 186: 100-108.
[48] Pan Y, Zeng X, Wen S, et al. Multiple ATP-binding cassette transporters genes are involved in thiamethoxam resistance in Aphis gossypii glover. Pestic Biochem Physiol, 2020, 167: 104558.
[49] Wang L, Zhu J, Cui L, et al. Overexpression of multiple UDP-glycosyltransferase genes involved in sulfoxaflor resistance in Aphis gossypii glover. Agric. Food. Chem. 2021, 69: 5198-5205.
[50] Lv Y, Li J, Yan K, et al. Functional characterization of ABC transporters mediates multiple neonicotinoid resistance in a field population of Aphis gossypii Glover. Pestic. Biochem. Physiol, 2022, 188: 105264.
[51] Fratini E, Salvemini M, Lombardo F, et al. Unraveling the role of male reproductive tract and haemolymph in cantharidin-exuding Lydus trimaculatus and Mylabris variabilis (Coleoptera: Meloidae): a comparative transcriptomics approach. BMC Genomics, 2021, 22: 808.

Eurasia Journal of Science and Technology
ISSN: 2663-1016
DOI: https://doi.org/10.61784/ejst3034

EXPLORING THE APPLICATION OF GENERATIVE AI IN TPRS INTERNATIONAL CHINESE LANGUAGE TEACHING PRACTICE: A CASE STUDY OF INTERNATIONAL STUDENTS WITH ELEMENTARY CHINESE PROFICIENCY

Qing Tang
International School, Wuhan University of Science and Technology, Wuhan 430065, Hubei, China.
Corresponding Email: tangqing0319@163.com

Abstract: Under the wave of global changes in educational intelligence triggered by generative AI technology, this paper aims to explore six strategies for TPRS international Chinese language teaching to realize digital reforms relying on generative AI by taking international students with elementary Chinese language proficiency as the teaching target, with a view to promoting the innovation and practice of artificial intelligence in the field of international Chinese language education.
Keywords: Generative; AI; TPRS; International Chinese language

1 INTRODUCTION

Under the background of rapid globalization, more and more foreign students choose to learn Chinese. For beginner level students, it is a challenge to learn Chinese effectively. In this process, the accelerated application of advanced generative artificial intelligence tools such as GPT-4.0 in international Chinese language teaching is objectively giving rise to innovations and changes in teaching methods, providing new possibilities for international Chinese language teaching. TPRS (Teaching Proficiency through Reading and Storytelling) is a story-based language teaching method that emphasizes the improvement of language proficiency through interesting stories and situations. This paper will explore in detail how generative AI tools can be integrated into TPRS international Chinese language teaching to help foreign students with elementary Chinese proficiency master Chinese more effectively.

2 SPECIFIC STRATEGIES OF GENERATIVE AI ENABLING TPRS PEDAGOGY

TPRS is a teaching method that emphasizes comprehension and communication, which is mainly realized through the steps of establishing meanings of vocabulary, establishing context, story inquiry, interactive practice, and combining reading and writing. The development of artificial intelligence technology provides many new tools for TPRS, and using these tools can optimize the TPRS teaching process and make learning more convenient, efficient and immersive. The following six aspects are selected to show the specific strategies of generative AI assisting instructional design.

2.1 Generating Word Lists

When the teacher creates a vocabulary list for a lesson's preparation, the target words in the lesson are selected, and ChatGPT-4 automatically and quickly labels these words with Pinyin and adds foreign translations according to the teacher's instructions, as shown in Figure 1. This greatly saves the teacher's workload of lesson preparation, compared with the previous manual input of Pinyin and translation and adjusting the format one by one[Case 1].

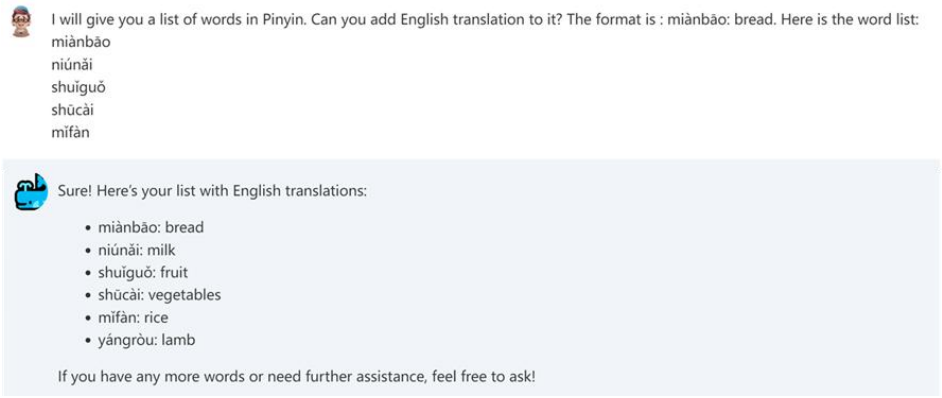

Figure 1 Vocabulary List by ChatGPT-4

2.2 Conversational Pre-teaching of Vocabulary

With the launch of the ChatGPT API, Quizlet released Q-Chat, a chatbot with the help of generative AI technology that specializes in helping students learn and memorize words. It provides students with a natural communication environment that allows them to interact with AI through a question-answer mode, as shown in Figure 2. In this mode, the teacher creates pre-study tasks before class, and students, according to their Chinese level choose their activity options from five items through the chat interface: teach me, practice with sentences, quiz me, story mode, and ask a question. Students will be able to practice and consolidate the vocabulary as if they were having a conversation with a friend, with real-time feedback and instant error correction. This mode greatly enriches the learning process, allowing students to memorize vocabulary in an easy and interesting chatting experience, fully prepared for participation in class activities and improving class learning efficiency[Case 2].

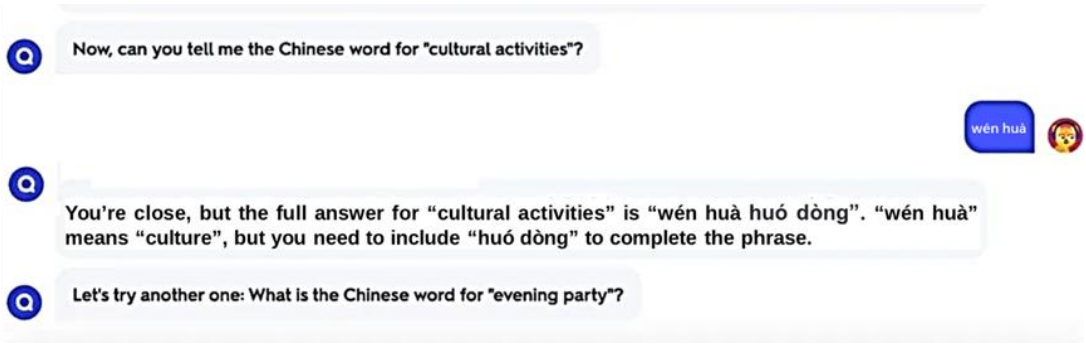

Figure 2 Conversational Pre-teaching of Vocabulary by Q-Chat

2.3 Real-Time Voice

In the tide of rapid development of artificial intelligence technology, in May 2024 OpenAI released an iterative version of GPT-4 - GPT-4o. It realizes a comprehensive processing enhancement of text, image, and speech on the basis of maintaining the same level of intelligence as that of GPT-4, especially the introduction of real-time speech function, which is able to realize seamless voice conversation, can respond to the conversation within the shortest 232 milliseconds, the average response time of 320 milliseconds, and is almost the same as human reaction speed, and support being interrupted at any time. In addition, it can identify different emotions, put them into context-appropriate conversations and responses, and "feel" the way of language organization and expression of emotions without a "mechanical" and "stuttering" sense. This is a revolutionary breakthrough in intelligent interaction capability, making the communication between AI and humans more natural and smoother, and moving towards the goal of "more like a human being", indeed. In August 2024, Iflytek benchmarked against the voice function of GPT-4o, by creating a Chinese interaction mode. It released the "Starfire Extreme Hyper-Anthropomorphic Interaction" technology, or "Starfire" for short. As the first product in China that directly realizes speech-to-speech end-to-end modeling, this technology is of great help in the field of education, providing new possibilities for speech interaction teaching, including the application of TPRS listening and speaking sessions.

2.3.1 Circular questioning

Circular questioning is one of the most effective ways to provide a large amount of comprehensible input for target language items in the TPRS story inquiry session. The teacher first says a sentence containing the target language, and then raises questions for different components of the sentence. For each component, the teacher usually uses four questions in three types of questioning: two general questions with affirmative and negative answers respectively, one alternative question, and one special question. By repeating the cycle in this way, the students' mastery of the target language is constantly reinforced, thus providing them with a large amount of comprehensible input. Circular questioning requires the teacher to be 100% enthusiastic in driving the students, to act like an actor, to attract students' attention and curiosity with exaggerated gestures, and this state needs to be sustained throughout the whole lesson. In addition, the teacher is required to do continuous, extensive, repetitive questioning of target sentences in the story within the limited class time, as many as tens or hundreds of questions asked, with the questions' keys repeated and "reported" to the whole class in a loud voice. This is undoubtedly a great challenge to the teacher's physical strength and throat. Meanwhile, for students, the high-density and similar circular questioning for the same vocabulary or language point can easily create fatigue or contempt [1]. Starfire can take over this heavy work in class, freeing the teacher partially or completely, and keeping students' attention by making it more interesting and dramatic. See case 3 for more details on how to do this[Case 3].

(1) Define the target sentence: the teacher says a target sentence, e.g., "Xiao Mei likes to eat dumplings," and asks Starfire to initiate questions about different components of the sentence.
(2) Comprehension: Starfire will use its natural language comprehension skills to understand the sentence. It will recognize the main elements of the sentence (e.g., "Xiao Mei", "likes", and "dumplings") and the relationships between these elements.

(3) Generate questions: Starfire generates audio questions based on the understanding of the sentence. For example, for "Xiao Mei", it can generate the following questions: "Does Xiao Mei like eating dumplings?" "Does Dasan like to eat dumplings?" and "Does Xiao Mei or Dasan like to eat dumplings?" and "Who likes dumplings?".
(4) Generate feedback: Starfire generates feedback based on the student's oral responses. If the student's answer is correct, Starfire can generate confirming feedback, and if the answer is wrong, it can correct the error.
(5) Circular Questioning: after completing one round of questioning and feedback, Starfire can start the following two rounds of questioning for "like" and "dumplings" respectively, thus realizing the goal of circular questioning.
Starfire's emotion expression is very rich and flexible, and it can control dozens of emotions, styles, dialects, and adjust the speed of speech according to the user's command in communication. Teachers can make choices from them, such as "ask the question in a sarcastic way" or "speak faster", and Starfire will ask students questions according to the teacher's instructions, thus increasing students' interest and motivation in answering questions.
Teachers should have a high level of control over the classroom in this session, pay attention to the command degree of students all the time, and change the way of questioning according to the actual situation. If the students in the creation of the story process are too chaotic, teachers have to maintain order in the classroom, and pull their thoughts back to class [2].

2.3.2 Reading aloud activities

In the TPRS reading session, in order to provide sufficient visual input and memorization time for the students' brain, students have to do a lot of reading aloud practice based on the story built by teachers and students, so as to complete the linguistic connection of sound, meaning, and writings, deepen their memorization of the three parts, and form their Chinese thinking way. In traditional class, teachers use various ways of reading aloud, such as teacher-led reading, whole class reading, group reading, relay reading, etc. However, such traditional ways are rather dull and rigid and it is difficult for students to have a happy experience. In order to cultivate students' interest in reading aloud, and then guide them to do longer reading and deeper understanding, teachers can implement the following reading aloud steps with the help of Starfire technology:
(1) Starfire leads the reading and students follow. Starfire can imitate the tone of characters such as the Monkey King, Crayon Shin-chan, and Peppa Pig, etc. This kind of free and flexible voice switching breaks the previous single form of only teacher-led reading, and greatly improves the students' participation and interest in reading aloud.
(2) When students are able to read aloud fluently, then change to the following forms of reading aloud:
i. Opposite voice state method: the opposite state held between Starfire and the students includes fast vs. slow, loud vs. low voice, clapping vs. stomping. For example, if Starfire reads a sentence quickly, the students should read the sentence slowly; if the teacher claps after Starfire reads a sentence, the students should stomp their feet after reading the sentence.
ii. Keyword emphasis method: when Starfire reads a certain sentence, it emphasizes the keywords of the sentence. The students have to recognize the keywords that are emphasized, and clap their hands when they read these keywords in the follow up reading.
iii. Sentence break method: students are to recognize where Starfire breaks a sentence and clap their hands at the breaks.
iv. Singing method: in March 2024, AI startup Suno introduced the V3 music generation model. The teacher enters a story text or target sentence, along with a simple song description, and then Suno generates a beautiful and catchy song. Starfire, the teacher and students can interpret the song by singing in unison, in duet, and in relays.

2.4 Intelligent Tests and Assessments

2.4.1 Generate tests

Teachers can use ChatGPT to make out a test and specify the problem requirements around the story content. For example, teachers can let ChatGPT automatically generate a number of test problems of reading comprehension or gap-filling, as well as answers to the them. More multidimensional problem types can be generated by adding supplemental prompts, e.g., reading comprehension problems contain three detail problems, one inference problem, and one main idea problem [3].
In addition to objective questions, ChatGPT can also make out open-ended questions that guide students to answer independently or in collaborative groups for discursive learning [4].

2.4.2 Automatic scoring and reviewing

Through artificial intelligence technology, teachers can understand the overall test performance within a few seconds after the test, keep track of students' learning in real time, check their weak points, and accordingly adjust the teaching strategy and carry out intensive training in class timely.
Whether subjective or objective problems, they can be automatically corrected with artificial intelligence tools. For objective problems, the teacher can input problems through the WeChat test applet, and then ask students to answer them within the specified time. When the answering time is over, the applet automatically scores the students and statistically analyzes the answering data of the whole class, and at the same time generates visual data charts, grade distribution and ranking lists; for subjective problems, the teacher can first initiate a group note in the WeChat class group, ask students to input their answers in the group note, then copy and paste the students' answers into ChatGPT, and issue instructions for ChatGPT to select the best few students and explain the reasons [5].

2.5 Generating Parallel Stories

ChatGPT can overcome the disadvantages of TPRS itself and assist teachers in generating parallel stories in large numbers. The TPRS pedagogy itself has the disadvantage of relying too narrowly on co-constructed stories, which results in two major pedagogical difficulties: (1) in terms of difficulty, as students' language proficiency rises, story building becomes more difficult, and the average teacher lacks the ability to consistently construct story outlines of ever-increasing difficulty. (2) Quantitatively, TPRS emphasizes comprehensibility, interest, and repetition, which cannot be achieved through traditional class instruction alone. Students need to receive a lot of comprehensible input and read a lot of interesting stories, and it is difficult for teachers to bear such a heavy burden individually [6]. As a language model for instant text output, ChatGPT can help teachers quickly and efficiently generate parallel stories with controllable difficulty and in line with students' characteristics by limiting vocabulary, sentence patterns, and stylistics according to students' answering test levels, interactions, and learning styles on the basis of existing reading materials. This largely solves the problems faced by TPRS Chinese teaching, such as the lack of teaching resources, the pressure on teachers to prepare lessons, and the high degree of flexibility in class.

2.6 Automatic Coloring

In order to address the difficulty of native speakers of English in grasping the tones and their relative pitches of Chinese characters, the TPRS method developed the TOP Pinyin spelling system. Teaching experience has shown that native speakers of English who consistently use the TOP Pinyin Spelling System to learn Chinese tones are more responsive and sensitive to the four tones of Chinese language, and are able to grasp the tonal range better and correct the foreign accents and tones effectively [8]. Teachers can use the online tool of conversion of characters into Pinyin to generate five different colors for Chinese characters in the reading materials based on different tones according to the color-coding principle of the TOP Pinyin method, so as to remind students to pay attention to reading the tones of the Chinese characters accurately and keep teachers away from the trouble of manually color-coding Chinese characters one by one[Case 4].

Huánghé yuǎn shàng bái yún jiān, yí piàn gū chéng wàn rèn shān.

3 CONCLUSIONS

This paper takes the example of using the TPRS pedagogy to teach international students with elementary Chinese proficiency in the information age, preliminarily explores the effective methods of generative AI tools promoting the enhancement of the effectiveness of international Chinese language teaching, and tries to establish an intelligent pathway and strategy of international Chinese language education and teaching, to ensure that the students get a high-quality Chinese language education experience, and to realize the cultivation goal of improving learners' Chinese language proficiency. The iterative updating of generative AI technology has accelerated, allowing the educational concepts of "adapting teaching to the student's ability" and "student-centeredness" to become a reality. Only by keeping abreast of the digital reforms, taking the initiative to seek changes and opportunities, paying close attention to the learners' spiritual and personalized needs with the help of intelligent technology, and returning to the nurturing focus, can international Chinese teachers become the guides of intelligent technology and the leaders of Chinese language teaching, and help our country move forward from being a big country in language service to a strong country in language service.

COMPETING INTERESTS

The authors have no relevant financial or non-financial interests to disclose.

REFERENCES

[1] Xu Wanhua. A Study on the Application of TPRS Teaching Method in Adult Intermediate Online Chinese Language Classes: A Case Study of Shanghai University of Political Science and Law Intermediate Online Chinese Language Classes for Foreign Students. 2021: 36.
[2] Ma Xiaofei. A Study on the Application of TPRS Teaching Method in Adult Elementary Chinese Speaking Classes: An Example of Chinese Language Teaching in Xi'an Samsung Company. 2021: 57.
[3] Xu Juan, MA Ruiling. The Technological Transformation of International Chinese Language Education Under the ChatGPT Wave. Journal of International Chinese Teaching, 2023(2): 46.
[4] Song Fei, Guo Jiahui, Qu Chang. The Application System and Practice of ChatGPT in Teaching Chinese as a Foreign Language. Journal of Beijing International Studies University, 2023(6): 120.
[5] Chen Jiang. AI-Powered Teaching Interaction. www.yuketang, 2024.
[6] Liu Yaqian. Action Research on TPRS for Online Elementary Chinese in Ecuador. 2022: 51.
[7] Xu Wanhua. A Study on the Application of TPRS Teaching Method in Adult Intermediate Online Chinese Language Classes: A Case Study of Shanghai University of Political Science and Law Intermediate Online Chinese Language Classes for Foreign Students. 2021: 14.

Eurasia Journal of Science and Technology
ISSN: 2663-1016
DOI: https://doi.org/10.61784/ejst3035

RENEWABLE ENERGY OUTPUT FORECASTING BASED ON DEEP LEARNING

LinYing Tang, JingXuan Liu*
School of Information Engineering, Hunan Automotive Engineering Vocational University, Zhuzhou 412001, Hunan, China.
Corresponding Author: JingXuan Liu, Email: 316301806@qq.com

Abstract: To address the challenge of decreased prediction accuracy caused by the significant uncertainty and volatility of renewable energy sources, this paper proposes a data-driven forecasting model that leverages an improved deep learning algorithm to enhance accuracy. First, data mining techniques are used to preprocess collected data, minimizing the impact of poor-quality data on forecasting outcomes. Then, Complete Ensemble Empirical Mode Decomposition with Adaptive Noise (CEEMDAN) is applied to separate the data into high- and low-frequency components. A Gated Recurrent Unit (GRU) model is employed for predicting high-frequency data to capture short-term fluctuations, while a Kalman Filter (KF) model is used for low-frequency data to extract long-term trends. The final forecast is obtained by combining the high- and low-frequency predictions. Simulation results demonstrate that the proposed data preprocessing effectively removes poor-quality data, improving subsequent forecast accuracy. Additionally, the combined forecasting approach effectively captures both high-frequency fluctuations and low-frequency trends, meeting the accuracy requirements for renewable energy forecasting.
Keywords: Deep Learning; Forecast; Load; Complete Ensemble Empirical Mode Decomposition with Adaptive Noise

1 INTRODUCTION

Accurate forecasting of renewable energy output has become increasingly critical for the reliable operation and planning of modern power systems. As countries transition towards greener energy sources, the integration of intermittent renewable energy like wind and solar power has accelerated significantly. Unlike traditional energy sources, renewable generation is inherently variable and influenced by numerous environmental factors, making it difficult to predict with precision [1]. These fluctuations can destabilize the grid, posing challenges to maintaining a consistent balance between supply and demand. For instance, unexpected weather changes can lead to sudden decreases in renewable generation, necessitating costly compensatory actions through conventional power sources, which are often less environmentally friendly [2]. Therefore, effective forecasting is essential for reducing the costs associated with these measures and optimizing grid stability and efficiency. Accurate predictions enable grid operators to better manage reserve power allocations, avoid over-reliance on fossil fuels, and minimize environmental impact. Additionally, improved forecasting supports better scheduling and dispatch of energy resources and enhances demand response mechanisms [3]. In the broader context of sustainable development, advancements in renewable energy forecasting play a pivotal role in achieving carbon reduction goals and building a resilient, low-carbon energy infrastructure for the future.

Traditional forecasting methods for renewable energy can be broadly divided into two main categories: model-based approaches and data-driven approaches. Model-based methods rely heavily on physical models and domain-specific knowledge, incorporating factors such as meteorological inputs, power generation characteristics, and system constraints to generate predictions [4]. These methods often use deterministic or stochastic models based on physical laws and engineering principles. For instance, PVs [5] forecasting might rely on models of solar radiation that take cloud cover, atmospheric conditions, and solar angle into account, while WTs [6] forecasting may depend on models that simulate wind flow and turbine dynamics. The first group references [5]-[8] show how to improve the model of the WTs, PVs, and other renewable energy. Model-based approaches are generally effective when environmental conditions are relatively stable and predictable, allowing them to produce accurate results by simulating the underlying physical processes [9]. However, they are limited in their ability to handle the high uncertainty and variability inherent in renewable energy sources, which are highly sensitive to rapid and unpredictable changes in weather patterns and environmental conditions.

In contrast, data-driven approaches have gained popularity for renewable energy forecasting due to their ability to analyze large datasets and automatically extract patterns. These methods employ machine learning or data mining algorithms that analyze historical data without requiring detailed knowledge of the physical processes involved. Instead of relying on deterministic models, data-driven methods identify statistical relationships and trends within the data [10], making them particularly useful for capturing complex, nonlinear dynamics in renewable energy output. Techniques such as neural networks [11], decision trees [12], and clustering algorithms [13] allow data-driven models to adapt to new information, effectively learning from recent observations. Unlike model-based methods, data-driven approaches can automatically adjust to emerging patterns and anomalies, making them highly adaptable to the rapidly fluctuating nature of renewable energy sources [14]. This flexibility makes data-driven forecasting particularly advantageous for managing the intermittency and variability of renewable energy, as it can more readily capture short-term fluctuations

and seasonal patterns. As a result, data-driven forecasting is increasingly viewed as a future trend in the field, offering a promising alternative to traditional methods and paving the way for more accurate and resilient renewable energy integration into the grid.

Although data-driven methods provide advantages like capturing nonlinear relationships and adapting to changing conditions, they face significant challenges due to the high uncertainty and short-term fluctuations in renewable energy generation. Sudden weather changes, equipment malfunctions, and fluctuating energy demand complicate accurate forecasting. While data-driven approaches can learn from historical patterns, they often struggle with the dynamic nature of renewable sources, particularly during peak load times or extreme weather events when precise predictions are critical for grid stability. To address these issues, researchers have focused on algorithmic improvements, as highlighted in Reference [15], which discusses enhancements such as hybrid models, ensemble learning, and advanced neural networks. Techniques like ensemble learning combine multiple models to reduce individual biases, while recurrent neural networks and long short-term memory networks (LSTMs) are effective for time-series predictions [16]. Despite these advancements detailed in References [17]-[20], there remains a crucial need for further improvements in prediction accuracy. Enhanced models are vital for optimizing power system operations and facilitating the integration of renewable energy sources into the grid, thereby supporting the transition to a sustainable energy future.

This paper introduces a novel forecasting approach that combines data preprocessing with a frequency decomposition model. First, data preprocessing removes poor-quality data, minimizing their impact on the model. Second, the proposed method utilizes a hybrid frequency-combination approach that separately models high-frequency and low-frequency components to effectively capture both short-term fluctuations and long-term trends in renewable energy data. This dual approach demonstrates the potential to significantly improve forecast accuracy by addressing both data quality and frequency-specific modeling challenges.

2 DATA PREPROCESSING

The chapter begins by using Graph Neural Networks (GNNs) to detect and filter abnormal data, ensuring data quality for subsequent processing. Then, the Complete Ensemble Empirical Mode Decomposition with Adaptive Noise (CEEMDAN) is applied to separate the data into high- and low-frequency components, providing a foundation for further analysis and prediction across different frequency bands.

2.1 Abnormal Data Detection Using

Graph Neural Networks (GNNs) [21] have recently gained prominence in anomaly detection, particularly in datasets with complex interdependencies, such as social networks and power system sensor networks. In such datasets, traditional anomaly detection methods may fall short as they often ignore the relationships between data points. GNNs, however, excel at modeling these relationships by constructing a graph structure where nodes represent data points, and edges represent relationships. This makes GNNs highly effective in detecting anomalies that deviate from expected patterns, especially those related to the network's structural properties.

In a GNN model, data is often represented as a graph $G = (V, E)$, where V is the set of nodes and E is the set of edges. Each node $v \in V$ represents a data point, and each edge $(u, v) \in E$ represents a relationship between nodes u and v. GNNs update the features of each node by aggregating information from its neighbors. A common update formula is:

$$h_v^{(k)} = \sigma(W^{(k)} \cdot AGG(\{h_u^{(k-1)}: u \epsilon N(v)\} \cup h_v^{(k-1)})) \quad (1)$$

where $h_v^{(k)}$ is the feature vector of node v at layer k,$N(v)$ denotes the neighbors of node v,W^k is the weight matrix at layer k,$\sigma$is an activation function, and $AGG$is an aggregation function (such as mean or weighted average).

After training, the GNN model assigns anomaly scores to nodes, based on how much a node's behavior or connections deviate from the learned patterns. Nodes with high anomaly scores are considered outliers or "bad data." By removing these high-scoring nodes, it is possible to eliminate erroneous or unrepresentative data from the dataset, which improves data quality and enhances the accuracy of downstream tasks, such as predictive modeling or pattern recognition.

2.2 Steps in Data Frequency Division Preprocessing

After processing with the GNN, clearly abnormal data is removed to prevent common interference. Next, the CEEMDAN method is applied to perform frequency division on the GNN-processed data. The steps are as Figure 1 shows.

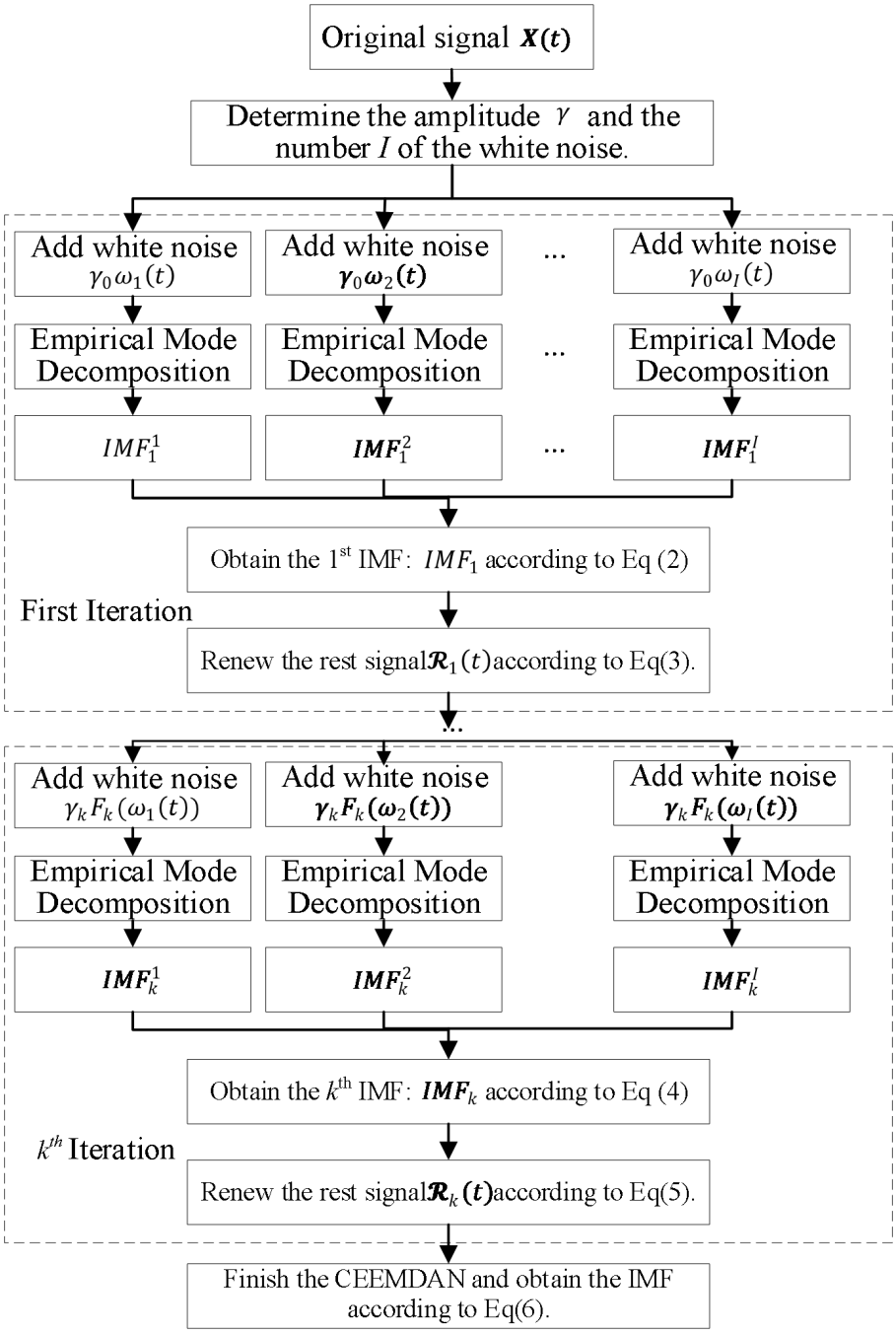

Figure 1 Flow Chat of the CEEMDAN

1. Generate the *i*-th signal sequences:

$$X_{new}(t) = X(t) + \gamma_0\omega_i(t), (i = 1,2, ..., N) \quad (1)$$

2. Extract the first IMF and the residual signal using the CEEMDAN method:

$$IMF_1 = \frac{1}{N}\sum_{i=1}^{N} IMF_1^i \quad (2)$$

$$\mathcal{R}_1(t) = X(t) - IMF_1 \quad (3)$$

3. Extract the (*k*+1)-th IMF after adding white noise $\omega_i(t)$ to the residual signal:

$$IMF_{k+1} = \frac{1}{N}\sum_{i=1}^{N} F_1[\mathcal{R}_k(t) + \gamma_k F_k(\omega_i(t))] \quad (4)$$

$$\mathcal{R}_k(t) = \mathcal{R}_{k-1}(t) - IMF_k \quad (5)$$

4. Continue with step 3 until $r_k(t)$ becomes either a monotonic function or a constant. At this stage, the signal is represented by Equation (6), assuming that there are *m* IMF after step 3.

$$X(t) = \sum_{k=1}^{m} IMF_k + \mathcal{R}_m(t) \quad (6)$$

The IMF components decomposed by CEEMDAN exhibit varied characteristics, including components that capture instantaneous fluctuations and others that represent tends. Using a single prediction model for all components is neither specific nor efficient in terms of computational resources. Therefore, the IMF components are classified and

reorganized into high- and low-frequency components, each assigned to an appropriate prediction model. The classification process uses sample entropy to assess the complexity of each IMF, as shown in reference [22].

3 DIFFERENT FORECASTING MODEL FOR DIFFERENT FREQUENCE COMPONENTS

This chapter forecasts the preprocessed high- and low-frequency data. The Gated Recurrent Unit (GRU) is applied to predict the high-frequency data, while the Kalman Filter (KF) is used for the low-frequency data. Finally, the predictions are combined to produce the final forecast.

3.1 High- frequency Data Forecasting Based on GRU

The framework of the GRU is as Figure 2 shows.

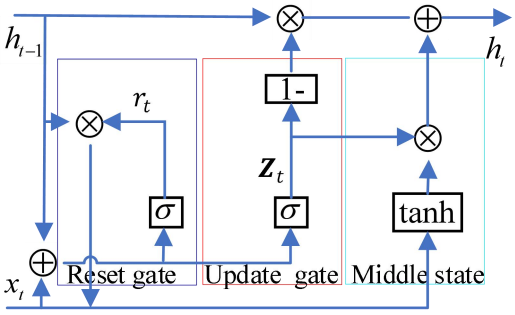

Figure 2 Structure of GRU

As shown in Figure 2, using GRU (Gated Recurrent Unit) to predict high-frequency data can capture short-term and long-term dependencies in sequence data. GRU is an improved version of recurrent neural network (RNN), which controls the transmission of information through "reset gate" and "update gate", which helps solve the gradient disappearance problem of traditional RNN.

The "reset gate" controls whether the state of the previous time step has an impact on the current state as follow:

$$\boldsymbol{r}_t = \sigma(\mathbf{W}_t \cdot [\boldsymbol{h}_{t-1}, \boldsymbol{x}_t] + \mathbf{b}_t) \tag{7}$$

The "update gate" is the update $\mathbf{z}_t$ that calculates the current time t:

$$\mathbf{z}_t = \sigma(\mathbf{W}_z \cdot [\boldsymbol{h}_{t-1}, \boldsymbol{x}_t] + \mathbf{b}_z) \tag{8}$$

The candidate hidden state $\widetilde{\boldsymbol{h}}_t$ is calculated as follows:

$$\widetilde{\boldsymbol{h}}_t = \tanh\,(\mathbf{W} \cdot [\boldsymbol{r}_t * \boldsymbol{h}_{t-1}, \boldsymbol{x}_t] + \mathbf{b}) \tag{9}$$

The hide state $\boldsymbol{h}_t$ renew as follows:

$$\boldsymbol{h}_t = \boldsymbol{z}_t * \boldsymbol{h}_{t-1} + (1 - \boldsymbol{z}_t) * \widetilde{\boldsymbol{h}}_t \tag{10}$$

Through the above GRU, the high-frequency data can be forecasted accurately.

3.2 Low- frequency Data Forecasting Based on KF

The low-frequency data can be predicted by the KF, which is an optimal state estimation method for linear dynamic systems. KF estimates the optimal value of state variables through iteration based on the dynamic system model and observation data and it is divided into a prediction step and an update step.

Assume that the state $\boldsymbol{x}_k$ is as follows:

$$\boldsymbol{x}_k = \boldsymbol{A}\boldsymbol{x}_{k-1} + \boldsymbol{w}_{k-1} \tag{11}$$

Where $\boldsymbol{x}_k$ is the hidden true state at time *t*. $\boldsymbol{A}$ is the state transfer matrix. $\boldsymbol{w}_{k-1}$ is the noise.

Thus, the low-frequency data $\boldsymbol{X}_{low}$ is as follows.

$$\boldsymbol{X}_{low} = \mathbf{H}\boldsymbol{x}_k + \mathbf{v}_k \tag{12}$$

Where $\mathbf{H}$ is the observation matrix, that influence the state to observation. $\mathbf{v}_k$ is the observation noise.

1. Prediction Step

State prediction is as follows:

$$\widehat{\boldsymbol{x}}_{k|k-1} = \boldsymbol{A}\widehat{\boldsymbol{x}}_{k-1|k-1} \tag{13}$$

Covariance prediction is as follows:

$$\mathbf{P}_{k|k-1} = \boldsymbol{A}\mathbf{P}_{k-1|k-1}\boldsymbol{A}^T + Q \tag{14}$$

2. Update Step

After receiving a new observation $\boldsymbol{z}_t$, the KF updates its state estimate and error covariance.

Kalman Gain Calculation is as follows:

$$\mathbf{K}_T = \mathbf{P}_{k|k-1}\mathbf{H}^T(\mathbf{H}\mathbf{P}_{k|k-1}\mathbf{H}^T + \mathbf{R})^{-1} \tag{15}$$

Where $\mathbf{K}_T$ is the Kalman Gain, which determines the weight given to the observation vs. the prediction.
State Update is as follows:

$$\hat{\boldsymbol{x}}_{k|k} = \hat{\boldsymbol{x}}_{k|k-1} + \mathbf{K}_k(\boldsymbol{z}_t - \mathbf{H}\hat{\boldsymbol{x}}_{k|k-1}) \tag{16}$$

Where $\hat{\boldsymbol{x}}_{k|k}$ is the updated state estimate after incorporating the new observation $\boldsymbol{z}_t$.
Covariance Update is as follows:

$$\mathbf{P}_{k|k} = (\mathbf{I} - \mathbf{K}_k\mathbf{H})\mathbf{P}_{k|k-1} \tag{17}$$

Where $\mathbf{P}_{k|k}$ is the updated error covariance matrix.

4 SIMULATION

The article employs data from January 1 to December 31, 2019, collected from a specific region in Xinjiang, to make predictions. It utilizes a sliding window approach for single-point forecasting, as illustrated in Figure 3.

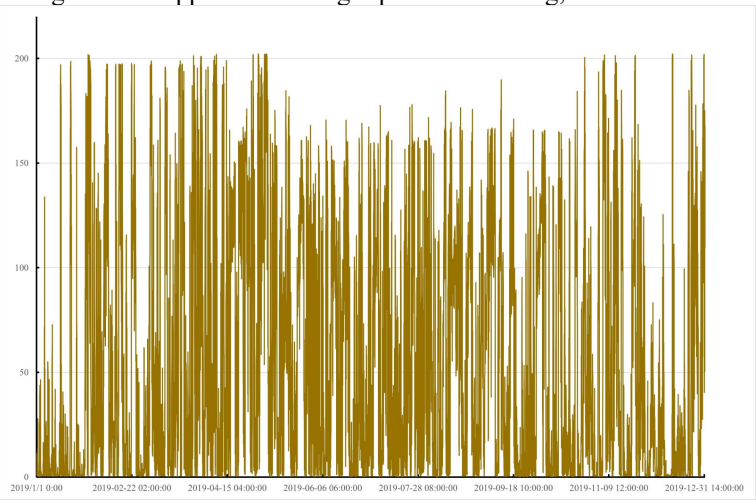

Figure 3 The Output of the WTs in Xinjiang Province

The data was decomposed using CEEMDAN, resulting in 11 IMF values, which were grouped into high- and low-frequency bands. Various models, as discussed in the article, were applied to these bands for prediction. The forecast results were then recombined, yielding the outcomes displayed in Figure 4, which also includes comparisons with other standard algorithms. The statistical comparison of these results is presented in Table 1.

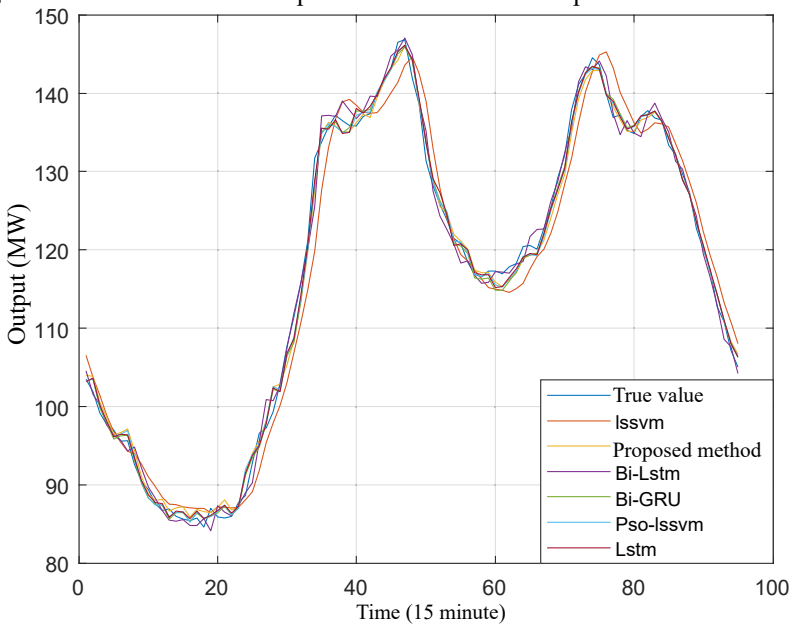

Figure 4 The Forecast Results in Different Methods

Table 1 Statistics in Different Methods

	RMSE	MAE	MAPE

Proposed method	1.0817	0.8097	0.80503%
Lssvm	1.5355	1.1235	0.96216%
Bi-lstm	1.1785	0.91779	0.8066%
Bi-GRU	1.1777	0.92081	0.8161%
Pso-lssvm	1.171	0.93537	0.82399%
Lstm	3.1757	2.5535	2.1448%

The analysis results indicate that the prediction method outlined in the article achieves the highest accuracy, effectively forecasting the output trend of wind turbines (WTs) with greater precision than existing algorithms. This superior performance can be attributed to the use of CEEMDAN for frequency division processing, which allows for separate consideration of short-term fluctuations and long-term trends. The GRU algorithm excels in capturing the accuracy of short-term fluctuations, while the KF algorithm effectively extracts long-term trends. By combining the strengths of both algorithms, the prediction accuracy achieved is significantly superior to that of other methods.

5 CONCLUSION

This paper presents a data-driven prediction model that utilizes frequency division techniques to separate short-term fluctuations from long-term trends in wind turbine (WT) output. The model employs the GRU algorithm to predict short-term fluctuations and the Kalman Filter (KF) algorithm to capture periodic changes in long-term trends. This approach effectively avoids the mutual interference of multimodal data, leading to improved prediction accuracy. Simulation results demonstrate that the proposed prediction model performs well, showcasing its potential for further development and broader application.

FUNDING

This work was supported by Intelligent control technology based on hybrid enhanced intelligence and big data processing methods and its application in new power systems (No. HQZYKY2022B12).

COMPETING INTERESTS

The authors have no relevant financial or non-financial interests to disclose.

REFERENCE

[1] Del Ser, J, Casillas-Perez, D, Cornejo-Bueno, L, et al. Randomization-based machine learning in renewable energy prediction problems: Critical literature review, new results and perspectives. Applied Soft Computing, 2022, 118(8): 108526. DOI:10.1016/j.asoc.2022.108526.

[2] van Wijk, J, Fischhendler, I, Rosen, G, et al. Penny wise or pound foolish? Compensation schemes and the attainment of community acceptance in renewable energy. Energy Research & Social Science, 2021, 81, 102260. DOI: https://doi.org/10.1016/j.erss.2021.102260.

[3] Chen, JJ, Qi, BX, Rong, ZK, et al. Multi-energy coordinated microgrid scheduling with integrated demand response for flexibility improvement. Energy, 2021, 217, 119387. DOI: https://doi.org/10.1016/j.energy.2020.119387.

[4] Willard, J, Jia, X, Xu, S, et al. Integrating scientific knowledge with machine learning for engineering and environmental systems. ACM Computing Surveys, 2022, 55(4): 1-37. DOI: https://doi.org/10.1145/3514228.

[5] Ahmed, R, Sreeram, V, Mishra, Y, et al. A review and evaluation of the state-of-the-art in PV solar power forecasting: Techniques and optimization. Renewable and Sustainable Energy Reviews, 2020, 124, 109792. DOI: https://doi.org/10.1016/j.rser.2020.109792.

[6] Bilal, B, Adjallah, KH, Sava, A, et al. (2023). Wind turbine output power prediction and optimization based on a novel adaptive neuro-fuzzy inference system with the moving window. Energy, 2023, 263, 126159. DOI: https://doi.org/10.1016/j.energy.2022.126159.

[7] Azad, A, Shateri, H. (2023). Design and optimization of an entirely hybrid renewable energy system (WT/PV/BW/HS/TES/EVPL) to supply electrical and thermal loads with considering uncertainties in generation and consumption. Applied Energy, 2023, 336, 120782. DOI: https://doi.org/10.1016/j.apenergy.2023.120782.

[8] Sadeghi, D, Amiri, N, Marzband, M, et al. Optimal sizing of hybrid renewable energy systems by considering power sharing and electric vehicles. International Journal of Energy Research, 2022, 46(6): 8288-8312. DOI: https://doi.org/10.1002/er.7729.

[9] Hu, Z, Gao, Y, Ji, S, et al. Improved multistep ahead photovoltaic power prediction model based on LSTM and self-attention with weather forecast data. Applied Energy, 2024, 359, 122709. DOI: https://doi.org/10.1016/j.apenergy.2024.122709.

[10] Ji, C, Sun, W. A review on data-driven process monitoring methods: Characterization and mining of industrial data. Processes, 2022, 10(2): 335. DOI: https://doi.org/10.3390/pr10020335.

[11] Rahman, MM, Shakeri, M, Tiong, SK, et al. Prospective methodologies in hybrid renewable energy systems for

energy prediction using artificial neural networks. Sustainability, 2021, 13(4): 2393. DOI: https://doi.org/10.3390/su13042393.

[12] Costa, VG, Pedreira, CE. Recent advances in decision trees: An updated survey. Artificial Intelligence Review, 2023, 56(5): 4765-4800. DOI: https://doi.org/10.1007/s10462-022-10275-5.

[13] Ikotun, AM, Ezugwu, AE, Abualigah, L, et al. K-means clustering algorithms: A comprehensive review, variants analysis, and advances in the era of big data. Information Sciences, 2023, 622, 178-210. DOI: https://doi.org/10.1016/j.ins.2022.11.139.

[14] Ahmad, T, Madonski, R, Zhang, D, et al. Data-driven probabilistic machine learning in sustainable smart energy/smart energy systems: Key developments, challenges, and future research opportunities in the context of smart grid paradigm. Renewable and Sustainable Energy Reviews, 2022, 160, 112128. DOI: https://doi.org/10.1016/j.rser.2022.112128.

[15] Kordzadeh, N, Ghasemaghaei, M. Algorithmic bias: review, synthesis, and future research directions. European Journal of Information Systems, 2022, 31(3): 388-409. DOI: https://doi.org/10.1080/0960085X.2021.1927212.

[16] Lv, SX, Peng, L, Hu, H, et al. Effective machine learning model combination based on selective ensemble strategy for time series forecasting. Information Sciences, 2022, 612, 994-1023. DOI: https://doi.org/10.1016/j.ins.2022.09.002.

[17] Choudhary, K, DeCost, B, Chen, C, et al. Recent advances and applications of deep learning methods in materials science. npj Computational Materials, 2022, 8(1): 59. DOI: https://doi.org/10.1038/s41524-022-00734-6.

[18] Zhang, L, Wen, J, Li, Y, et al. A review of machine learning in building load prediction. Applied Energy, 2021, 285, 116452. DOI: https://doi.org/10.1016/j.apenergy.2021.116452.

[19] Sapoval, N, Aghazadeh, A, Nute, MG, et al. Current progress and open challenges for applying deep learning across the biosciences. Nature Communications, 2022, 13(1): 1728. DOI: https://doi.org/10.1038/s41467-022-29268-7.

[20] Yan, X, Wang, W, Xiao, M, et al. Survival prediction across diverse cancer types using neural networks. In Proceedings of the 2024 7th International Conference on Machine Vision and Applications, 2024, 134-138. DOI: https://doi.org/10.1145/3653946.3653966.

[21] Wu, Y, Dai, HN, Tang, H. Graph neural networks for anomaly detection in industrial Internet of Things. IEEE Internet of Things Journal, 2021, 9(12): 9214-9231. DOI: 10.1109/JIOT.2021.3094295.

[22] Shi, J, Teh, J. Load forecasting for regional integrated energy system based on complementary ensemble empirical mode decomposition and multi-model fusion. Applied Energy, 2024, 353, 122146. DOI: https://doi.org/10.1016/j.apenergy.2023.122146.

Eurasia Journal of Science and Technology
ISSN: 2663-1016
DOI: https://doi.org/10.61784/ejst3036

GOALS AND HABITS: LOCAL MANAGEMENT MODEL CHOICE IN CHINA — COMPARATIVE ANALYSIS OF THE PREVENT CHOICE FOR THE COVID-19

YanRunYu Liang, ShiYu Xie*
School of Elderly Care Services and Management, Nanjing University of Chinese Medicine, Nanjing 210023, Jiangsu, China.
Corresponding Author: ShiYu Xie, Email: 540001@njucm.edu.cn

Abstract: Chinese administration exhibits a tension between inherent contradictions and effective management. When policy goals are rigid, as seen in COVID-19 prevention, local authorities often cannot rely on 'muddling through' strategies and must adopt campaign-style responses. However, cities like Shanghai developed precise, multi-target prevention models. This paper uses a framework of task attributes and management habits to analyze these differences across selected cities, finding that management habits are crucial in shaping responses when flexibility is limited. Localities with high specialization, autonomy, and coordination capacity tend to employ delegated management, balancing "political and professional responsibilities" to create targeted prevention mechanisms. In contrast, other areas resort to direct command and layered campaign-style responses. Overall, China's epidemic prevention reflects a feedback-adjustment process between central policy goals and local implementation outcomes.
Keywords: Management model; Task difficulty; Management habits; Precision prevention

1 INTRODUCTION

The COVID-19 pandemic has presented significant global challenges [1], prompting varied responses from public authorities. Some countries implemented strict containment measures immediately, while others opted for minimal intervention or herd immunity strategies [2]. Unlike many nations, China maintained a rigorous anti-contagion policy focused on achieving zero community transmission, reflecting its national policy and administrative structure.

China's National Health Commission divides its epidemic response into four stages. The first, "emergency containment," aimed at halting the spread at all costs, with national-level, campaign-style measures. The second, the "exploration of normalized prevention and control," focused on "preventing importation and internal rebound" through isolation and widespread PCR testing. In the third stage, "dynamic zeroing with precise control," regions began to integrate regular, targeted prevention with emergency responses [3]. Throughout, the goal of "zero transmission" has remained, evolving from a broad, static approach to a precise, dynamic model [4].

City vaccination practices show commonalities, with community- and grid-based management forming the foundation of epidemic prevention nationwide [5]. As the focus of prevention shifted to blocking external imports and controlling local spread, measures like isolation [6], health QR codes, and PCR testing were widely used to interrupt transmission.

However, distinct local approaches have emerged. Most regions adhere to centralized leadership, mass mobilization, and stringent quarantine to achieve zero COVID at any cost. In contrast, cities like Shanghai use a precise model with rapid tracing, targeted testing, and limited closures around confirmed cases rather than extensive PCR testing and large-scale lockdowns. This precise, normalized approach is increasingly standardized in practice.

These observations reveal two key aspects of China's zero COVID-19 policy: the central administration’s evolving targets across different stages, and the varied prevention models adopted by city public authorities. What, then, drives the shifts in national goals and the diverse local responses? The “black box” of China's COVID-19 response still warrants investigation, particularly concerning public sector operations and decision-making logic.

Recent research on public sector behavior and management has made significant progress, offering valuable insights for understanding China's management mechanisms [7]. This article aims to shed light on the "black box" of China's COVID-19 response by analyzing goal attributes and management habits within local policy implementation frameworks.

2 THEORETICAL FRAMEWORK

2.1 Patterns of Local management Behavior in Policy Implementation

In recent years, China's national management and local public sector behavior have become academic hotspots, with growing research enriching our understanding of management models.

This has resulted in a series of achievements such as "Pressure System" [8], "Tournament System" [9], "Administrative Contracting System" [10], "Campaign-style Management" [11], " Loose-coupling" [12] and so on.According to the distribution of“Control rights”, Zhou and Lian categorized different management models into "Highly Connected", "Administratively Contracted", and "Loosely Connected" and observed that these three models alternated at different

points in time [13]. For example, in the areas of family planning, environmental protection, and stability maintenance, as the intensity of target setting, inspection and acceptance, and incentive design of higher authorities changes, local public authorities will loosen their policy implementation efforts under the "high-pressure posture", and policy implementation appears to alternate between the three different modes of management mentioned above [14].Yao. et al. introduced the task attribute dimension to the “Control rights” analysis framework, and provided an analytical framework for the rational choice of static selection and dynamic transformation of management mode. According to its model, the management model depends on the difficulty of the task and assessment, and the intermediate public sector as the manager and the basic public sector of the executor will take consistent actions due to the optimal strategy when faced with the same task [15]. In fact, this is a common assumption of such studies. Normally, under the institutional structure of "pressure-based institutions" and "administrative contracting", management patterns appear as "loosely connected" patterns, and when the central administration is highly focused on specific goals and tasks, management patterns shift from "loosely connected" to "highly connected" patterns, often in the form of campaign management. When the central administration is highly focused on a specific goal, the management pattern shifts from "loosely connected" to a "highly connected" pattern, often in the form of campaign-based management.

However, there is a contradiction between "unified system and effective management" in the requirement of unified task objectives [16]. Evans (2010) has noted that for employees, discretion can be seen as the extent of freedom he or she can exercise in a specific context [17]. Related to this, local public authorities have similar discretion to street-level bureaucrats when it comes to completing tasks given by the central administration [18-19], and the more difficult the task, the greater the possibility of policy alienation and "Muddling Through" [20-22]. The essence of policy alienation is the local administration’ s ambiguous treatment of "impossible tasks" and the policy implementation behavior of constantly adjusting between standardization and feasibility [23].

2.2 Institutions and Mechanisms for Emergency Management of Epidemic Prevention

Studies have been conducted to explain the effects and causes of fighting against COVID-19 in China from an emergency management perspective. Studies on total-control management consider it to be the result of the rapid downward shift of the center of gravity of social management and the innovation of grassroots social management, reflecting the unique institutional advantages of China's national management [24]. It is manifested in authorities were confident in their capacity to mobilize people and concentrate resources in the face of catastrophes characterized by suddenness, urgency, severity, unpredictability, and sociability [25].

Efficient implementation and group prevention and control are the characteristics and advantages of China's emergency management [26]. Grid-based and community-based closed management has "basic and coverage advantages" and has played a significant role in the management effectiveness of the community-based epidemic response system [27]. The grid-based management model is not a pre-determined part of China's emergency management system, but rather a control system that combines management and services by using institutional organizations and technology to reorganize disembedded individuals whose mobility properties are becoming more and more prominent. Grid-based management is the basic community management model in China, which is conducive to breaking down departmental barriers, subsuming the phenomenon of compartmentalization under the traditional section hierarchy, and building a seamless service-oriented public sector [28]. The main purpose is to ensure the top-down penetration of national public policy intentions with a three-dimensional section hierarchy, and to guarantee the unity, stability and standardization of grassroots operation, which played a fundamental institutional role during prevent COVID-19.

The province-city-district-community-grid management structure provides an organizational foundation for rapid, extensive, and cohesive social mobilization, enabling "wartime" readiness and effective epidemic control through localized closures and checkpoints [29]. This integrated urban emergency management system enhances grassroots management coordination, ensuring smooth information, resource, personnel, and technology exchange between municipal and district levels for operational synergy. Advanced technologies like data monitoring, communication systems, AI, and urban management platforms further enable the emergency management system to deeply penetrate metropolitan management.

The above study focuses on the all-pervasive prevention models and analyzes the mechanisms that make them effective. In terms of local management, these models can be categorized as campaign-based management.Campaign management is the usual local practice in the face of unconventional management, characterized by the process of special focus on certain emergencies by elevating special tasks to political tasks required by the leadership committee and public sector, and by breaking institutional, conventional, or professional boundaries to concentrate effective resources with comprehensive political mobilization [30]. This approach can solve social problems thoroughly and quickly by mobilizing available resources extensively and is the preferred tool for extraordinary management. Under the general situation of epidemic prevention and control, local public authorities, as responsible subjects, tend to choose the campaign mode of management based on path dependence for total prevention and control.

There are alternative to campaign-style public sector for epidemic prevention, and comprehensive control-style epidemic prevention has a negative impact on socioeconomic development. When rigid tasks like preventing epidemics, local public authorities must address several goals of epidemic prevention and control, as well as local development. Various management models may develop in different places depending on the characteristics of different policy aims, local economic conditions, and public sector capacity [31]. It has been found by scholars that there are differences in

policy measures and intensities across regions [32], and their formation mechanisms are dependent on time and space [33].

The local context of the policy implementer in a given field is crucial for understanding the logic of policy implementation [34]. When faced with high task pressures, local-specific contexts not only lead local public authorities to develop adaptable behaviors, but also make it form different task execution modes, and the task attributes and local context jointly affect the local task execution mode [35].

3 GOALS AND HABITS: AN ANALYTICAL FRAMEWORK FOR LOCAL PUBLIC SECTOREPIDEMIC PREVENTION MODELS

Under the Pressure System, local public sector behavior is shaped by both policy mandates and local contexts. Most studies on policy adaptation focus on negative behaviors under "command-resistance," with Maynard-Moody identifying discretion as a key factor in policy deviations [36]. Increasing top-down mandates have limited bottom-up adaptation, leading instead to proactive grassroots adaptations [37]. In epidemic prevention, local public authorities face clear targets and accountability, with minimal discretion, making effective adaptation to local contexts essential [38]. Epidemic control, a core element of emergency management, depends on the administration's institutional management capacity, with differences in strategy reflecting variations in local management during normalization [39].

This management style can be defined as a management habits. Management habits are the institutional methods wherein cities are managed on a regular basis, causing the formation of management habits over time.

Gao notes that Shanghai's precise epidemic prevention reflects its urban management system and the modernization of management capacity, classifying the system into proactive, scientific, and accurate prevention models, and defining modernization as leadership, execution, smart management, and adaptability [40]. Shanghai's model derives from the city 's established management concepts and the competencies of its civil servants. This suggests that Shanghai's routine management mechanisms support its distinctive, precise prevention approach [41]. While Chinese cities share similar management structures, differences in decision-making, implementation, and resources lead to varied modernization capacities, resulting in diverse local responses to crises.

China's public sector structure exhibits a high degree of uniformity in functions, responsibilities, and organization across different levels, known as "isomorphic responsibility" [42]. The professional sector brings specialized expertise, while the administrative sector oversees regional development, managing and coordinating broadly [43]. This interplay between professionalism and administration presents a common challenge for modern public authorities, as they must balance adherence to professional standards with administrative pressures. Local public authorities, as duty bearers, face political evaluations and must decide whether to rely on the professional sector or delegate specific management tasks [44].

The intricate relationship between the administration and the professional sectors is reflected in the configuration of supervising and being supervised, controlling and being controlled, assisting and cooperating. Liu et al. quantitatively examine the professional background of the Health Commission's leadership and organizational structure to determine the role of insider leadership in epidemic prevention and control [45], suggesting that professional sector are the primary decision.When it comes to special tasks, such as the prevention and control of epidemics, however, the municipal leader bears main duty, and the specialist leader's professional role is contingent on the authorization of his or her special department by the executive branch.

Wilson notes that public authorities with a high capacity for moderation are more flexible in their behavior, more likely to delegate authority in professional matters to professional departments acting in accordance with professional concepts and technical norms, more likely to believe in the effectiveness of their management than in the autocratic command of the executive branch, and more likely to embrace the risk of accountability [46]. With clear authorities and responsibilities and a standard operating procedure, the former can develop delegated management practices. It is rule-based, discretionary, and professional, with a strict distinction of functions and authority. While the latter expresses itself in the approaches of unified control and direct command, the administration keeps on doing tasks that should be performed through administrative and professional work divisions. The division of functions is unclear, as are the authorities and responsibilities, and there is a lack of understanding of regulations and management autonomy, and uses political campaigns to enhance enforcement [47].

Faced with demanding and difficult tasks such as epidemic prevention and control (Chinese dynamic zero-Covid policy), public authorities with authorised management practices respect the professionalism of the functionaries and develop initiatives for epidemic prevention based on professional studies and varying levels of social mobilization. Local public authorities, habituated to administrative centralization, are path-dependent on political campaigns, in which administration forms an emergency hub to give direct commands, optimize mobilization of all forces to achieve particular, and demonstrate progress is being made.

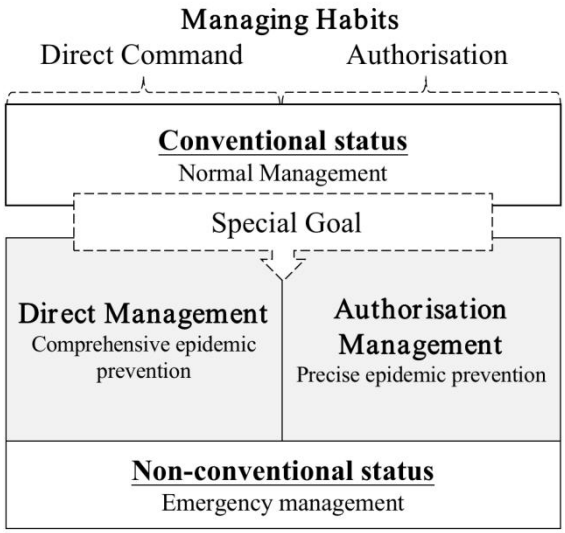

Figure 1 A Double Constraint Model of Local Public sector Epidemic Prevention Model Choice in China

A dual constraint model for local public sector epidemic preparedness in China can be outlined (see Figure 1). When COVID-19 control becomes a central strategy, the primary focus of local management shifts to effective epidemic prevention. This leads to two distinct management models: one combines regular and emergency management without disrupting normal institutional functions, while the other adopts a political campaign approach, where specialist departments serve only in advisory roles.

4 CASE STUDY：TOTAL CONTROL VERSUS PRECISION VACCINATION MODELS

This study compares two epidemic prevention models in China post-normalization, focusing on Shanghai's precision approach and using other regions for comparison. Nanjing and Shaoxing, which implemented multiple rounds of universal PCR testing, are compared with Tonghua, Manzhouli, and Xi'an, where city-wide lockdowns were enforced.

4.1 Task: Two Modalities of Positive Behavior Prevention

The political campaign and precision models of epidemic prevention both stem from local public authorities' proactive responses to policy challenges. The key differences lie in: first, whether epidemic prevention goals are balanced with social development objectives, and second, the scope and intensity of control measures (such as lockdowns, PCR tests, and personnel restrictions).

The political campaign model focuses heavily on epidemic prevention, with multiple rounds of universal PCR testing, widespread closures, and lockdowns becoming central to urban development. Even with the classification of risk zones, cities maintain universal PCR testing to meet the "dynamic zero" target. In cities like Xi'an and Tonghua, once case numbers reach a few hundred, entire districts are sealed off, halting city traffic and market activities, severely disrupting the economy and daily life.

On 18 January 2021, nearly 400,000 people were quarantined at home for 36 days throughout the city of Tonghua ; a total of 836 industrial enterprises were shut down in Shangyu District and Yuecheng District of Shaoxing City, Zhejiang Province on 8 December 2021 due to epidemic prevention and control after the outbreak; the city of Xi'an was closed in December 2021 and 13 million people were quarantined at home in the city; in 19 December 2022, there were still cities such as Yinchuan and Xining that were still fully closed due to the epidemic [48].

Shanghai, despite its high risk of importation from internationally and strong population movements, has maintained normal socioeconomic order till March 2022 without any control measures such as city closure, state of war declaration, or universal screening [49]. Based on flow survey data, it restricted the blockade region to high-risk neighborhoods, buildings, etc., in order to maximize the scope, reduce the duration, and minimize the socioeconomic impact.

4.2 Mechanism Distinctions between Two Epidemic Prevention Models

In terms of similarities among the two epidemic prevention models, the multi-level public sector management structure provides the institutional foundation for the construction of a three-dimensional epidemic prevention and control system as part of a comprehensive emergency response to the CODIVE19 outbreak, and the advancement of technological advances has facilitated joint epidemic prevention and control in different regions.

Firstly,the combination of a public sector management system with a grid-based community management model provides the rapid construction of a wide-coverage, seamless, and unified social mobilization system in addition to the severance of the virus transmission chain through obligatory social isolation.The community grid management model is

the institutional fundamental basis for the public sector to obtain personal information, and the netting and carpeting of health conditions improves the effectiveness of tracing the chain of infection and tracing the close contacts, isolating or treating the detected cases in time to prevent the spread of the epidemic within the community.

Additionally, the technological advancement has facilitated the unified prevention and control of epidemics in various cities.Basic technical measures for epidemic control, such as controlling the population by color classification using health QR code, conducting epidemiological surveys and tracing utilizing communication big data localize, trip codes, and place codes, and conducting universal PCR tests, have been implemented with incredible ripening [50].

The main distinction among the two models of epidemic prevention measures is whether the contact tracing is utilized as the primary method. The comprehensive prevention and control model is based on China's "Level 1 response to major public health emergencies" in which society is transformed from a normal state to an emergency state concentrating on epidemic prevention, with specialty epidemiological investigations playing a supporting role. The normal protocol is to declare an emergency situation as soon as a case is discovered in a city, with centralized management and unified command by the administration, and to interrupt the chain of transmission of the virus through mass suspension of work and schooling, total control of population movement, and closure of neighborhoods through grid-based management, as well as multiple rounds of universal PCR tests. In essence, the goal was to achieve a speedy zero number of confirmed cases through a disease-prevention political campaign (see Figure 2).

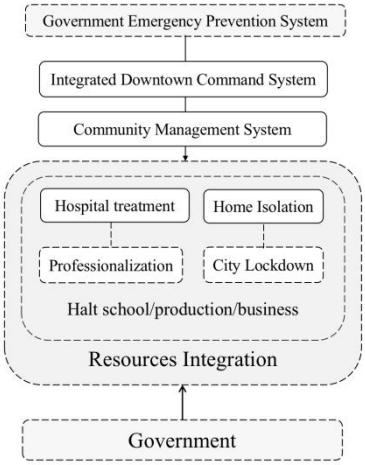

Figure 2 Comprehensive Epidemic Prevention

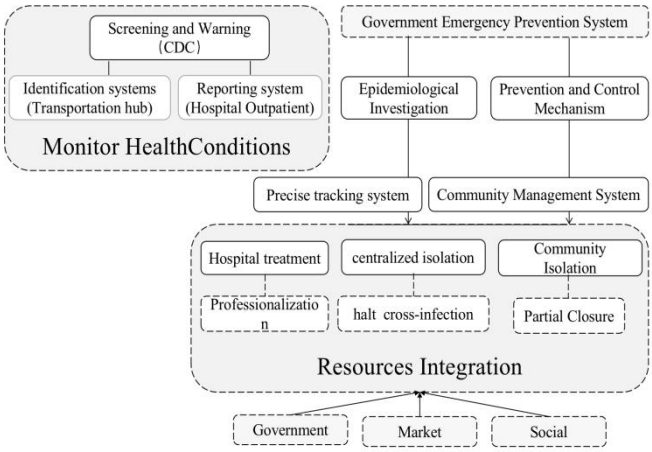

Figure 3 Precision Epidemic Prevention Model

Three characteristics distinguish the Shanghai precision vaccination model. The first is proactive detection, which creates a defense line against the epidemic before it occurs. Through proactive screening of critical populations in a hospital, a number of confirmed cases were reported in Shanghai at the beginning of 2021. Second, quick reaction. Once a new confirmed case is identified, the emergency management method identifies sites, cases, and identifiers. Third, exact and organized. The public health system scientifically identifies the three levels of close contacts, sub-close contacts, and high-risk groups and enforces closed-loop management strategies to prevent simplification and expansion.

Three elements are required for effective implementation of the precision prevention model (see Figure 3). Firstly, a system for sensitive and exhaustive information collection and early warning.Epidemic prevention will be most efficient once identified, reported, managed, and treated early. In Shanghai, 127 fever clinics in hospitals, 225 in community health service centers, screening of high-risk personnel, food cold chain monitoring, and pharmacy monitoring of

high-risk drug consumers(those who buy cold or fever-reducing medication are considered to be at risk of a confirmed CODIVE19) create a traceable monitoring and tracking system [51].

Secondly, a technological epidemiological investigation and traceability system supports accurate epidemic prevention. Shanghai has over 3,100 epidemiologists with structured operating methods to quickly identify and target the right population and environment in the event of an epidemic using professional testing technology. In Shanghai, epidemiological investigations follow the "2+4+24" principle: a flow investigation team comes within 2 hours and conducts rapid sampling and testing; core information, including close contacts and sub-close contacts, is distributed; temporary control measures are implemented within 4 hours; track checks, personnel control, and premises cleaning are finished within 24 hours; and a flow investigation report is completed.Then, a press conference is organized to inform the community with official relevant information [52].

Thirdly, an effective combination preventative and control mechanism is created. This broad coordination method includes daily precision prevention, localized epidemic emergency response, parallel disposal, and tidy reaction from multiple sectors. Precision prevention and control avoids authoritative resource allocation in a comprehensive control model and establishes a coordinated working model with a linkage system among actors. Shanghai's communication management and public security departments work with the CDC and flow investigation team to undertake virus tracing and close connection precision identification with full empowerment, multiple rounds, and high communication feedback frequency. These mechanisms have been modified and implemented in the city's daily process-based management system to prevent epidemics.

4.3 Managing Habits—the Formation of a Precise Vaccination Model in Shanghai

As was evident from the preceding analysis, the main distinction between the two models is whether to implement total disease prevention and control in the style of a campaign or regular and precise disease prevention when new instances occur.The construction of a permanent and standardized model of precision prevention in involves coordination of the leaders, and it is the management philosophy and practice of all levels of Shanghai's public sector and administrations to let the professionals do there jobs. The separation of tasks between politics and professionals necessitates a clear definition of responsibility and professionalism, as well as the construction of an effective framework for cooperation and trust between the professional and administrative sectors.Therefore, precise pandemic prevention is a highly professional approach. Accurate epidemic prevention likewise necessitates an effective implementation mechanism, which is based on a regular management system and is reflected in a coordination mechanism with distinct authority and responsibility, each with specific responsibilities and compliance of regulations [53].

4.3.1 Professional decision-making: scientific foundation for precise vaccination

Professionalism is the foundation of precise epidemic prevention, which requires both a plan based on scientific analysis into the characteristics of the virus and the progression of the epidemic and a professional team capable of utilizing big data and other technology means for rapid flow and detection.Shanghai helped contribute 66 public health experts and infectious disease control specialists to form two municipal expert groups for public health and medical treatment, with experts from the Centre for Disease Prevention and Control responsible for epidemic prevention. Both expert groups have dual team leaders, and clinical cases will be first discussed in the public health group, where specialists collaborate to create preventive actions [54].Shanghai established a specialist consulting system. The mayor and related officials convened specialists and professional organizations to compile a situation report on epidemic prevention and control and hear expert research and recommendations [55]. The scope of the control area and the population, the disposal precautions, are determined by the expert after an in-depth evaluation and study based on the results of the epidemiology, and thus providing professional and technical support for the prevention of CODIVE19 [56].

The emergence of Zhang Wenhong, a national network expert in epidemic prevention in Shanghai, is not entirely due to his ability, but to the way Shanghai treats its experts. The emergence of Zhang Wenhong, a national network expert in epidemic prevention in Shanghai, is not entirely due to his ability, but to the way Shanghai treats its experts [57]. He mentioned that "There are specialist groups in all of the province's cities, some of whose leaders are more specialized than I am. I am famous because they are in a different position than I am, and the way in which I communicate with the public is recognized by the public sector; yet, I am picked by society [58]. "The role of experts is contingent upon their autonomy, and, as indicated previously, the management techniques of responsible leadership and expert reliance are context-dependent. Between the tensions of administration and professionalism, a city with the philosophy of empowering specialists to execute professional tasks and trusting specialists will develop the habit of professional management. When it comes to unexpected events, professionals have a greater power of discourse , rather than leaders taking decisions instead of experts.

It has been a tradition for Shanghai to lean forward professionally and to emphasize the management practices of experts. When responding to SARS in 2003, the Shanghai group then built an expert advisory group led by the city's Health Bureau and consisting of 20 experts from the fields of infection, respiratory medicine, epidemiology and critical care emergencies [59]. The role of specialists is highly valued throughout the entire process of precision vaccination，

They have constructed a flat Epidemic Prevention and Control Command that functions in the front and sinks down to the Center for Disease Control and Prevention, where the Command and experts work in the same space and make scientific decisions based on expert research.

4.3.2 Integration and coordination: organizational foundation for precision immunization

Precise epidemic prevention also relies on clear responsibility, authority and coordinated management practices developed during regular management. This covers two aspects: on the one hand, daily monitoring and management of the epidemic, as well as testing the standardized and refined management strategy and normalized management's efficacy. Responsibility for the entire control of the epidemic lies with all levels of public sector, network and information centres, civil affairs, police, and transport authorities. The city has designed a "three-tier system" and a "five-pack system" at the level of the community. A "five packs and one grid" approach has been implemented in shopping malls, supermarkets, and vegetable farms, requiring grassroots staff to work in small groups and conduct daily inspections to assist communities with their inspection work.

On the other hand, it is the complementary management of precision vaccination that tests the daily management practices and effectiveness of co-ordination and individual responsibility.This requires not only the expertise of the public health system, but also the efficient cooperation of the regional integrated management and logistical support system, and the management of the post-tracking process necessarily requires the coordination of multisectoral resources, the coordinated distribution of materials, and the communication of information.

For example, on 25 January 2021, during the 10-hour closure of the Red House, the administration ' s logistics department quickly followed up by arranging marching beds for pregnant women and the elderly, distributing meals, bedding and rechargeable batteries, arranging shuttle buses to take patients home after the closure, and waiving parking fees for those who drove to the hospital. 31 October 2021 At 18:00, Shanghai received a notice from an out-of-town Disneyland with a close pick-up and arranged for 220 temporary shuttle buses to be on standby at the Disney West bus hub within four hours, and by 23:00, PCR tests for tens of thousands of people had been completed.

5 DISCUSSION AND CONCLUSIONS

This study extended further than the 'command-and-resist' viewpoint of the principal-agent model to analyze the strategies of public authorities when discretion is constrained . It develops a framework for analyzing task attributes and management practices, compares case studies of behavioral differences in epidemic prevention policy choices across Chinese cities, and responds to the reasons for the overall policy shift in practice and the emergence of two epidemic prevention models.

Firstly, in terms of the task, local public authorities must be proactive when faced with tasks such as epidemic prevention that have a high degree of accountability and limited discretion. Currently, local contexts demand distinct implementation strategies for local policies. In contrast, city public authorities with limited managerial capacity and a lack of autonomy tend to exert administrative power and adopt a direct command model when confronted with the tension between politics and professionalism, utilizing political campaigns for comprehensive control to achieve a zero community transmission policy through high payouts in the short term and to convey to the central public sector the importance that city leaders attach to epidemic prevention and to reduce the risk of being held accountable.

Secondly, if COVID-19 is a transient virus similar as SARS or if the mission is targeted at a natural disaster such as an earthquake, a "one-size-fits-all" campaign type of management could be deemed effective. The constant evolution of the COVID-19 variation necessitates that the public sector strike a balance between its goals of epidemic prevention, economic development, and social development, which is why precise epidemic prevention is gaining national recognition. It standardizes epidemic prevention and integrates it into the city's regular management process, establishing a combination of normal and emergency management mechanisms in response to alterations in the epidemic situation, and continually improving them.

In this framework, the attributes of the mandate are decisive, and the central mandate determines the boundaries of local discretion, like Shanghai's exploration of precise epidemic prevention cannot deviate from the strict criterion of "zero" without authorization. The mandate of the central public sector defines the boundaries of local autonomy. The pursuit of precise prevention cannot circumvent the strict constraints of zero community transmission policy without authorization, but the upward mobility of the Tiao/Kuai mechanism can drive the central public sector to adapt to the mandate's objectives.

As COVID-19 continues to mutate, the specific approach and efficacy of precision vaccination may be challenge [60], but the central vaccination policy and local vaccination models will be modified accordingly. As recent studies find that local public authorities in China, an authoritarian country, also exhibit a substantial level of responsiveness to local citizens' requests and concerns [61-62]. For instance, since 2022, the central administration has consistently expressed its opposition to "cascading," "one-size-fits-all," "city lockdown," and "traffic restrictions," and the new standards of the epidemic prevention strategy contain the phrases "precise" and "dynamic" being used more frequently [63]. This is precisely the type of policy fine-tuning that the central administration is summarizes nationwide experience.

This continual interaction between goals and local discretion is both the foundation of China's policy for preventing COVID-19 and a mechanism for China's adaptive management [64-65]. Such a mechanism requires both a strong, binding central mandate and sufficient autonomy and modern management capacity for local public authorities.

COMPETING INTERESTS

The authors have no relevant financial or non-financial interests to disclose.

FUNDING

This research was sponsored by the Special Research Project of School of Elderly Care Services and Management, Nanjing University of Chinese Medicine (NJUCM), "Research on the Risk Avoidance Mechanism of the House-for-Pension Scheme in the Context of Social Governance for the Elderly(2024YLFWYGL006)".

REFERENCES

[1] Atkeson A. What will be the economic impact of COVID-19 in the US? Rough estimates of disease scenarios. National Bureau of Economic Research, 2020.
[2] Qi J, Zhang D, Zhang X, et al. Short- and medium-term impacts of strict anti-contagion policies on non-COVID-19 mortality in China. Nat Hum Behav 6, 2022: 55–63. DOI: https://doi.org/10.1038/s41562-021-01189-3
[3] Xu TL, Ao MY, Zhou X, et al. China's practice to prevent and control COVID-19 in the context of large population movement. Infect Dis Poverty 9, 115 (2020).
[4] Andrew C, Goldsmith M. From local government to local governance—and beyond? International Political Science Review, 1998, 19(2): 101-117.
[5] Rhyne C S. The Law of Local Government Operations. Law of Local Government Operations Project, 1980.
[6] Kirchgässner G. On the theory of optimal government behaviour. Journal of Economic Dynamics and Control, 1984, 8(2): 167-195.
[7] Ledger T. The logic of appropriateness: understanding non-compliance in South African local government. Transformation: Critical Perspectives on Southern Africa, 2020, 103(1): 36-58.
[8] Joseph Fewsmith, Xiang Gao. Local Governance in China: Incentives & Tensions. Daedalus. 2014, 143 (2): 170–183.
[9] Zhou L A. Research on the promotion tournament of local cadres in China. Economic Research, 2007, 15: 36–50.
[10] Zhou L A. The administrative subcontract: Significance, relevance and implications for intergovernmental relations in China. Chinese Journal of Sociology, 2016, 2(1): 34-74.
[11] Feng S. Formation and transition of Chinese national campaign: The integrated explanation based on regimes. In: Zhou X, Liu S, Zhe X (eds) State Building and Government Behavior, Beijing: China Social Sciences Press, 2012: 33–70.
[12] WEICK O. Loosely coupled systems: a reconceptualization. Academy of management review, 1990, 15(2): 203-223.
[13] Zhou X, Lian H. Modes of governance in the Chinese bureaucracy: A "control rights" theory. The China Journal, 2020, 84(1): 51-75.
[14] Yang, Xuedong. A pressure system: a brief history of a concept. Social Science, 2012: 4-12.
[15] YAO Dongmin, CUI Lin, ZHANG Pengyuan, et al. Choice and Transformation of China's Governance Modes: A Formal Model. Social, 2021, 41(6): 41-74.
[16] Zhou X. The institutional logic of collusion among local governments in China. Modern China, 2010, 36(1): 47-78.
[17] Evans T. Professional Discretion in Welfare Services: Beyond Street-Level Bureaucracy. London: Ashgate, 2010.
[18] Ying X. Petitions and Power: A Story of the Migrants of a Dam in China. Routledge, 2018.
[19] Chŏng C, ho Jeong C, Chung J H, et al. Central control and local discretion in China: Leadership and implementation during post-Mao decollectivization. Oxford University Press on Demand, 2000.
[20] Lindblom Charles. The Science of Muddling Through. Public administration review, 1959, 19(2): 79-88
[21] Zhou X. The institutional logic of collusion among local governments in China. Modern China, 2010, 36(1): 47-78.
[22] Vadapalli D K. Barriers and Challenges in Accessing Social Transfers and Role of Social Welfare Services in Improving Targeting Efficiency: A Study of Conditional Cash Transfers. Vulnerable Children and Youth Studies, 2009.
[23] Tummers L, Bekkers V. Policy implementation, street-level bureaucracy, and the importance of discretion. Public Management Review, 2014, 16(4): 527-547.
[24] Zhao T, Wu Z. Citizen–State Collaboration in Combating COVID-19 in China: Experiences and Lessons From the Perspective of Co-Production. The American Review of Public Administration, 2020, 50(6–7): 777–783.
[25] Borokh O. China: Interpreting the Economic Impact of the COVID-19 Pandemic in the Context of National Goals//Economists and COVID-19. Palgrave Macmillan, Cham, 2022: 9-25.
[26] Mei C. Policy style, consistency and the effectiveness of the policy mix in China's fight against COVID-19. Policy and Society, 2020, 39(3): 309-325.
[27] Cheng Y, Yu J, Shen Y, et al. Coproducing responses to COVID-19 with community-based organizations: lessons from Zhejiang Province, China. Public Administration Review, 2020, 80(5): 866-873.
[28] Linden R M, Linden R M. Seamless government: A practical guide to re-engineering in the public sector. Jossey-Bass, 1994.
[29] Kraemer M U G, Yang C-H, Gutierrez B, et al. The effect of human mobility and control measures on the COVID-19 epidemic in China. Science, 2020, 368(6490): 493–497.

[30] Zhao Y, Zhang X, Wang Y. Evaluating the effects of campaign-style environmental governance: evidence from Environmental Protection Interview in China. Environmental Science and Pollution Research, 2020, 27(22): 28333-28347.
[31] Chen J, Pan J, Xu Y. Sources of authoritarian responsiveness: A field experiment in China. American Journal of Political Science, 2016, 60(2): 383-400.
[32] Cheng Y, Yu J, Shen Y, et al. Coproducing responses to COVID-19 with community-based organizations: lessons from Zhejiang Province, China. Public Administration Review, 2020, 80(5): 866-873.
[33] ChenW, ZhangHb, GaoR. Spatial-Temporal Relationship between Control Policiesand COVID-19 Epidemic Distributionin Emergency Management: A CaseStudy of Response Strategies of Municipalities in Hubei Province during the Spring Festival 2020. Public Administration and Policy Review, 2020, 9(3): 16-28.
[34] Bifulco L, Centemeri L, Salvati M. La partecipazione nei Piani sociali di zona: geometrie variabili di governance locale. 2007.
[35] Bifulco L, Centemeri L. Governance and participation in local welfare: The case of the Italian Piani di Zona. Social Policy & Administration, 2008, 42(3): 211-227.
[36] Maynard-Moody S, M Musheno, D Palumbo. Street-Wise Social Policy: Resolving the Dilemma of Street-Level Influence and Successful Implementation. The Western Political Quarterly, 1990, 43(4).
[37] Guo J. Policy Learning and Policy Implementation in China: A Case Study of the Grain for Green Project. The University of Hong Kong, PhD Thesis, 2010.
[38] Mei C. Policy style, consistency and the effectiveness of the policy mix in China's fight against COVID-19. Policy and Society, 2020, 39(3): 309-325.
[39] Howlett M, Ramesh M, Perl A. Studying public policy: Policy cycles and policy subsystems. Oxford: Oxford university press, 2009.
[40] Gao Enxin. The Balanced Governance: How the TCE Strategy Succeed to Prevent and Control the COVID-19?—A Case Study of a Chinese Megacity. Journal of Public Management, 2022, 19(1): 1-12.
[41] Gao Enxin. Why can Shanghai's permanent epidemic control? 2022. https://mp.weixin.qq.com/s/kELQUGGqpsX3diiH0ey5hQ.
[42] Jujun Z, Zhirui W. Strong negative incentive and weak implicit negotiation: the campaign-style environment governance in China. Journal of Global and Area Studies, 2019, 3(2): 45-67.
[43] Mertha A. China's “Soft” centralization: Shifting Tiao/Kuai authority relations. China Quarterly, 2005, 184: 791–810.
[44] Kohn M L. Bureaucratic man: A portrait and an interpretation. American Sociological Review, 1971: 461-474.
[45] Mastrangelo A, Eddy E R, Lorenzet S J. The importance of personal and professional leadership. Leadership & Organization Development Journal, 2004.
[46] Wilson J Q. Bureaucracy: What government agencies do and why they do it. Hachette UK, 2019.
[47] Shi C, Guo F, Shi Q. Ranking effect in air pollution governance: Evidence from Chinese cities. Journal of environmental management, 2019, 251: 109600.
[48] Based on official public information detailing the epidemic since 2021, which including Shanghai Release, Shaoxing Release, Nanjing Release, Xi'an Release, People's Daily, etc. 2021.
[49] Xiaoxiang Morning Post. How can Shanghai forcefully avoid full nucleic acid? Wu Fan: Ultra-long incubation period is not a scientific conclusion, one more not one less not. https://baijiahao.baidu.com/s?id=1718459110620700834&wfr=spider&for=pc.
[50] Cheng Y, Yu J, Shen Y, et al. Coproducing responses to COVID-19 with community-based organizations: lessons from Zhejiang Province, China. Public Administration Review, 2020, 80(5): 866-873.
[51] Xiaoxiang Morning Post. How can Shanghai forcefully avoid full nucleic acid? Wu Fan: Ultra-long incubation period is not a scientific conclusion, one more not one less not. 2021. https://baijiahao.baidu.com/s?id=1718459110620700834&wfr=spider&for=pc.
[52] People's Information. "Fast, accurate, strict, and early"! A team of more than 3,000 people is on the frontline of epidemic prevention in Shanghai. 2021.
[53] People's Information. "Fast, accurate, strict, early"! A team of more than 3,000 people is standing firm at the forefront of epidemic prevention in Shanghai. 2021. https://baijiahao.baidu.com/s?id=1717588774258499214&wfr=spider&for=pc.
[54] He A J, Shi Y, Liu H. Crisis governance, Chinese style: Distinctive features of China 's response to the Covid-19 pandemic. Policy Design and Practice, 2020, 3(3): 242-258.
[55] The Paper. Zhang Wenhong: Shanghai is the most tolerant place, and the integration of the medical prevention system has made me a "weblebrity". 2020. https://m.thepaper.cn/baijiahao_7780785.
[56] CN-HEALTHCARE. What makes a city with the highest GDP in the country and which never does full nucleic acid testing commended by the National Health Commission. 2021. https://www.cn-healthcare.com/articlewm/20210930/content-1269631.html.
[57] Gao Enxin. The Balanced Governance: How the TCE Strategy Succeed to Prevent and Control the COVID-19? -- A Case Study of a Chinese Megacity, Journal of Public Management, 2022, 19(1): 1-12.
[58] The Paper. Zhang Wenhong: Shanghai is the most tolerant place, and the integration of the medical prevention system has made me a "weblebrity". 2020. https://m.thepaper.cn/baijiahao_7780785.

[59] South Reviews. Zhang Wenhong: I'm just a doctor. 2021. https://baijiahao.baidu.com/s?id=1709537448894734734&wfr=spider&for=pc.
[60] Shanghai Observer. C conversation with Zhang Wenhong's mentor, Weng Xinhua, who gave "Zhang Dad" this scor. 2021. https://www.jfdaily.com/news/detail?id=232303.
[61] Hu Xijin. Mocking and criticising Shanghai for being short-sighted. 2022. http://www.3xol.com/xw/1172.html.
[62] Chen J, Pan J, Xu Y. Sources of authoritarian responsiveness: A field experiment in China. American Journal of Political Science, 2016, 60(2): 383-400.
[63] Distelhorst G, Hou Y. Constituency service under nondemocratic rule: Evidence from China. The Journal of Politics, 2017, 79(3): 1024-1040.
[64] New China News Agency (NCNA). Many places are "cascading" with regulation. 2022. https://mp.weixin.qq.com/s/0zHa6Fw8Qk5K-TWzBhkwmA.
[65] Duan T, Sun Z, Shi G. Sustained Effects of Government Response on the COVID-19 Infection Rate in China: A Multiple Mediation Analysis. International Journal of Environmental Research and Public Health, 2021, 18(23): 12422.

Eurasia Journal of Science and Technology
ISSN: 2663-1016
DOI: https://doi.org/10.61784/ejst3037

RECONSTRUCTION OF CHARACTER IMAGES IN TRANSLATED LITERARY WORKS FROM THE PERSPECTIVE OF MEDIO-TRANSLATOLOGY: A CASE STUDY OF THE CHINESE VERSION OF TWO YEARS' VACATION

Rui Qi*, ShuangShuang Xiao
School of Foreign Languages, Fuyang Normal University, FuYang 236037, Anhui, China.
Corresponding Author: Rui Qi, Email: 928185592@qq.com

Abstract: The construction of character images in translated literary works directly influences whether the translation can successfully integrate into the target language's cultural system, thus facilitating effective cross-cultural communication. This paper, from the theoretical perspective of Medio-translatology, takes the sole female character in the French novel The *Two Years' Vacation* as a focal point, analyzing the rewriting of her character in the Chinese version and exploring the underlying reasons for such changes. Through this analysis, the paper aims to provide new perspectives and insights for the translation of literary works and cross-cultural exchange.
Keywords: Translated literature; Character image reconstruction; Medio-translatology; *Two Years' Vacation*

1 INTRODUCTION

The French writer Jules Verne is renowned for his unique imagination of science, exploration, and the future in his literary works. His books have been translated into numerous languages and are popular worldwide. The *Two Years' Vacation* (Deux ans de vacances) is an adventure novel published by Verne in 1888. The novel, with its captivating storyline and profound character portrayals, tells the story of a group of students from France who, while traveling across the Pacific, are forced to survive on a deserted island after being struck by a sudden storm. The *Two Years' Vacation* was translated into Chinese in the early 20th century by Liang Qichao and Luo Pu, making its debut to Chinese readers. The first ten chapters were translated by Liang Qichao, while the remaining eight chapters were translated by Luo Pu. The Chinese version was titled *Fifteen Little Heroes*, which caused a strong reaction in society at the time. After its release in 1902, the novel was repeatedly reprinted, and by 1930, the Shanghai Bookstore had issued the fifth edition. "… The young Zhou Zuoren, before beginning his literary activities, was a youth profoundly moved by Xinmin Congbao and Fifteen Little Heroes…"[1] As a representative work of French adventure novels, *Fifteen Little Heroes* has attracted scholarly attention. Current research on this work mainly focuses on the translation strategies chosen by the translators and, through analysis of the translated text, explores the translators' purposes. For example, Yao Dadui, from the perspective of comparative literature, has deeply analyzed the phenomenon of inserting political discourse and removing colonial discourse in the translation version;[2] Wang Jin'an and others, using the theory of translation purpose, have elaborated on the characteristics of the target-language readers reflected in the novel.[3] Novels are a narrative literary genre centered on the creation of characters. The portrayal of characters is an important path through which both the author and the translator realize their creative intentions. In a sense, the success or failure of creating typical characters determines the success or failure of the work.[4] However, existing research has rarely treated the translated work as an independent entity. There is little comparison of how character images are shaped in the Chinese translation versus the original French text, how translators have reshaped the characters during the translation process, and which factors influence the reshaping of characters' images. This article, starting from the theory of Medio-translatology, focuses on the only female character (Kate) in the French novel *Two Years' Vacation*. It analyzes the differences in the portrayal of this character between the original French version and the Chinese version translated by Liang and Luo. It also explores the social and cultural reasons behind the translators' re-shaping of Kate's character image, and, by doing so, discusses the social attributes and social value of translated literary works. This approach aims to facilitate the entry of literary works into the target-language cultural system, thus enabling effective cross-cultural communication.

2 RECONSTRUCTION OF CHARACTER IMAGES IN TRANSLATED LITERARY WORKS

Translation broadens the scope of literary works' dissemination and promotes interaction and exchange between different languages and cultures. "The so-called foreign literary works that Chinese readers generally read are, in fact, foreign literature translated by Chinese translators, that is, 'translated literature.' It is clearly a new work independent of the original, derived from the original, but by no means identical to it…"[5]Literary works often focus on the creation of character images, reflecting social life through narrative plot and environmental descriptions. Translating literary works requires translators to possess deep literacy in language, culture, and literature to ensure that the target audience can experience the most faithful representation of the original. Among these, the reshaping of character images by the translator can significantly affect the transmission and reception of the translated work in the target language world. As

an independent literary work, the character images in a translated work also undergo a journey across languages and cultures, facilitated by the bridge built by the translator. In this process, what changes occur in the portrayal of characters, why these changes happen, and what impact they have are important issues for comparative literature and cultural studies to address. This also aligns with what later people referred to as the "cultural turn"[6] in translation studies, and "liberated the discipline of translation from the limitations of previous theories."[7] Professor Xie Tianzhen steps beyond the linguistic aspects of translation studies and proposes a theory of Medio-translatology with a focus on literary or cultural research. "Medio-translatology involves a descriptive study of translated works, not concerned with evaluating the quality of translations, nor passing judgment on their merits. Instead, it treats the translated work as a given fact and then explores and analyzes the issues of literary exchange, influence, dissemination, and reception on this basis."[8] "Creative rebellion" is a fundamental concept in Medio-translatology, which includes the creative rebellion of the translator, the creative rebellion of the receiver, and the creative rebellion of the reception environment. Among these, "the creative rebellion of the translator takes precedence, referring to the various 'rewriting' actions the translator might take under the constraints of translation norms, such as translation concepts and the translation environment."[9] "Creative rebellion is an objective phenomenon in translation, revealing a rule in cross-linguistic and cross-cultural communication and reception. It helps us to understand more profoundly the essence of translation."[10] The adventure novel *Two Years' Vacation* by Jules Verne features fifteen young boys as the main characters, with the only female character, Kate, appearing outside of this group of boys. By comparing the original French version of the novel with the Chinese version translated by Liang and Luo, it becomes evident that the translator significantly reworked and reshaped the character of Kate. Changes can be observed in her age, identity, and fate, with notable alterations. Kate, having crossed the seas from France to China, had already assumed an entirely new identity.

3 RECONSTRUCTION OF FEMALE CHARACTERS IN CHINESE VERSION OF *TWO YEARS' VACATION*

3.1 From a Middle-Aged Woman to a Young and Beautiful Girl

In the original French version of the novel, Kate officially appears in Chapter 22. The protagonist, Briant, discovers Kate, who is on the brink of death, while searching for his friends who had left due to disagreements. "Une femme était étendue là, immobile comme unemorte, une femme dont les vêtements – jupe de grosseétoffe, corsage pareil, châle de laine brune, noué à saceinture – paraissaient encore en assez bon état. Safigure portait des traces d'excessives souffrances, bienqu'elle fût de constitution robuste, n'étant d'ailleursâgée que de quarante à quarante-cinq ans. Épuisée defatigues, de faim peut-être, elle avait perduconnaissance, mais un léger souffle s'exhalait de seslèvres."[11] (A woman lay there, motionless like a dead person, a woman whose clothes—a heavy fabric skirt, a matching bodice, a brown wool shawl tied at her waist—still appeared to be in fairly good condition. Her face bore traces of extreme suffering, although she was of robust constitution, being only around forty to forty-five years old. Exhausted from fatigue, perhaps from hunger, she had lost consciousness, but a faint breath escaped from her lips.-Translated by the author). In Chapter 13 of the Chinese version, Kate appears: "The lifeless body was dressed in luxurious clothes, with a half-cloak draped over her shoulders. Although her complexion was pale and her face showed traces of sorrow, she was a stunning beauty, a flawless sixteen-year-old girl."[12] As can be seen, in the original French version, Kate is a middle-aged woman in her forties or fifties. She is described as being sturdy in build, dressed simply, and there is little detail given about her appearance, other than a mention of her painful expression. However, in the Chinese version, the translator reimagines her as a sixteen-year-old girl, dressed in luxurious clothing, and particularly emphasizes that she is a very beautiful young woman.

3.2 From a Maid to a Student

In the French original, after being rescued by the boys, Kate recounts her background: "Elle était d'origine américaine, avait longtemps vécusur les territoires du Far-West aux États-Unis. Elle senommait Catherine Ready, ou plus simplement Kate. Depuis plus de vingt ans, elle remplissait les fonctions de femme de confiance, au service de la familleWilliam R. Penfield, qui habitait Albany, capitale del'État de New York."[11] (She was of American origin and had lived for a long time in the territories of the Far West in the United States. Her name was Catherine Ready, or more simply, Kate. For over twenty years, she had served as a trusted woman in the service of the William R. Penfield family, who lived in Albany, the capital of the state of New York.-Translated by the author). From the above, it is clear that Kate's profession is that of a servant. However, in the Chinese version, Chapter 14, the translator reimagines her as an educated student: "The boys carefully inquired about her background and learned that her name was Jia Zhilan… She had been studying for a long time in the capital of New York."[12]

3.3 From a Caring Mother to An Romantic Partner

In Jules Verne's original, Kate is portrayed as a maternal figure to the fifteen boys stranded on the island. After meeting the children, she takes on the responsibility of caring for them. Not only does she help them find food on the island, but she also offers them nurturing, motherly affection. For example, in Chapter 22, after Kate is rescued and learns of the boys' plight, it is written: "L'excellente femme ne pensait plus à elle pour nepenser qu'à eux. S'ils devaient rester ensemble sur l'île Chairman, elle serait leur servante dévouée, elle les soignerait, elle les aimerait comme une mère."[11] (The excellent woman no longer thought of herself, but only of them. If they were to remain together on Chairman

Island, she would be their devoted servant, she would care for them, she would love them as a mother. -Translated by the author). And in Chapter 23, it is further described: “l’excellente créatureavait reporté sur les plus jeunes enfants de la colonietout ce que son cœur contenait de tendressesmaternelles, et jamais elle ne leur marchandait sescaresses.”[11] (The excellent woman had transferred to the younger children of the colony all the tenderness that her heart contained, and never withheld her affection from them. -Translated by the author). Additionally, at the end of the French novel, after Kate and the fifteen boys escape the island and return to New Zealand, the children treat her as a member of their family: “elle fut réclamée, 609 disputée, par les Briant, les Garnett, les Wilcox et biend’autres. Finalement, elle se fixa dans la maison deDoniphan, dont elle avait sauvé la vie par ses soins.”[11] (She was claimed, contested over, by the Briants, the Garnetts, the Wilcoxes, and many others. Finally, she settled in the house of Doniphan, whose life she had saved with her care. -Translated by the author). However, in the Chinese version, the translator alters Kate's maternal role and transforms her character into a romantic figure. She develops a love story with one of the main characters, a young boy named Duban. Due to Duban's injury, Kate is responsible for his care: “…Therefore, while taking care of Duban, Kate felt an infinite sympathy and affection for him, truly considerate in every way. For a whole month, she never left Duban’s sickbed. Duban also felt her deep affection, and after returning to their homeland, the two eventually became a couple…”[12] By comparing the French and Chinese versions, it can be seen that Kate's character undergoes significant changes in terms of age, appearance, identity, and fate. For details, refer to Table 1.

Table 1 Comparison of Kate's Character Traits in the French and Chinese Versions

Kate's character traits	French version	Chinese version
Age	Forty to fifty years old	Sixteen years old
Appearance	Not mentioned	Beautiful
Style of dress	Dressed simply	Luxurious clothing
Identity	Maid	Student
Fate	Family member	Romantic partner

4 REASONS FOR THE RECONSTRUCTION OF FEMALE CHARACTERS IN CHINESE VERSION OF *TWO YEARS’ VACATION*

4.1. Adaptation to Traditional Novel Genres

During the Late Qing period, traditional Chinese novels were still primarily based on stories of “talented scholars and beautiful women.” In classical Chinese literature, this type of narrative—focused on the talented scholar and the beautiful woman—was a very common literary tradition. The “talented scholar” is typically portrayed as a person with profound knowledge and quick wit, while the “beautiful woman” is often depicted as not only physically beautiful but also gentle, wise, and virtuous. The connection between the two characters is not just physical but also intellectual and cultural, reflecting a deep compatibility in spirit and taste. These stories often carry a strong cultural and intellectual background, embodying the scholarly class's admiration for knowledge, talent, and moral integrity. The “talented scholar” in these novels represents the cultural elite and an idealized male figure, while the “beautiful woman” symbolizes an elegant, virtuous, and beautiful female ideal. From an artistic creation perspective, presenting the female character as a “beautiful woman” serves to heighten the drama and appeal of the narrative. Traditional Chinese novels emphasize emotional expression, and the image of the "beautiful woman" is often a key driver of conflict and tension in the plot. Through the portrayal of the female character's beauty and emotional depth, the storyline is propelled forward. In *Two Years' Vacation*, the main characters are fifteen brave, intelligent boys, which aligns with the traditional elements of the “talented scholar” genre. However, as the only female character in the novel, Kate's original portrayal as a middle-aged woman does not fit the traditional expectations of the genre, nor does it align with the cultural conventions of such novels. This would diminish the narrative tension and dramatic conflict in the story, especially in a translation intended to appeal to readers familiar with traditional Chinese novels. Consequently, the translator reimagined Kate’s character, transforming her from a middle-aged woman into a beautiful young girl, ultimately becoming an ideal companion for one of the boys. This reshaping of Kate’s character reflects the translator’s adaptation to the literary conventions of Late Qing period fiction and the desire to maintain the traditional appeal and dynamics of “talented scholar and beautiful woman” narratives.

4.2 Adaptation to the Audience and Mode of Dissemination

The translation of literary works is often adjusted according to the needs of the target audience. The intended readership of the Chinese version of *Two Years' Vacation* primarily consisted of male intellectuals during the late Qing Dynasty. This group had high expectations for literary works, particularly in terms of character development and plot construction. They were more inclined to appreciate dramatic elements, emotional conflict, and social symbolism. In this context, the translator’s adaptation of female characters became one of the key factors that contributed to the appeal

of the translated text. In the original version, Kate is portrayed as a middle-aged woman; however, in the translation, the translator reimagines her as a beautiful girl and even incorporates a romantic subplot involving the protagonist. This adaptation reflects the translator's deep understanding of the target audience and their preferences. The male intellectuals of the late Qing Dynasty were not only concerned with the philosophical content of the work, but also with the emotional resonance and the attractiveness of the characters. By youthfulizing Kate's character and introducing a romantic element, the translator catered to the readers' preference for romantic plots and idealized female figures, further enhancing the readability and emotional appeal of the translation. Although this alteration deviated from the original characterization, it was a strategic decision based on considerations of the translation's dissemination and acceptance within a new cultural and social context. The goal was to ensure that the translated version would attract broader attention and recognition in its new environment. Additionally, the translation was initially serialized in the newspaper Xinmin Congbao. The serial format of publication posed specific demands on the structuring of the story's plot. The serial format required frequent reading and sustained attention from the audience, compelling the translator to focus on maintaining tension and suspense in the narrative to keep readers engaged. In this mode of dissemination, the translated version needed to be structured in a way that ensured strong readability and dramatic appeal in order to retain the audience's interest and enhance the work's dissemination effect.

4.3 Translation Purpose of the Translator

As a leading figure in the late Qing Dynasty's reform movement, Liang Qichao's translation philosophy and practice were always aimed at guiding China toward national strength through reforms. "His translation activities and ideas are closely linked with his reformist, improvement-oriented, and patriotic endeavors."[5] As Liang Qichao's student, Luo Pu similarly attached great importance to the social function of novels, advocating the use of literature to promote social reform and cultivate a "new citizen" with independent thinking, adventurous spirit, and the capacity for self-governance, who would take on the responsibility of national revival. This vision is most clearly embodied in his reimagining of the "new woman" in his translations. Under the traditional male-centered worldview, women's education and development had long been neglected. Luo Pu, however, reinterprets Kate's role from that of a maidservant in the original text to a female student in the Chinese version. This change not only critiques and rebels against traditional educational values but also conveys a translation purpose that hopes for women to receive modern education and develop an independent, upward-oriented spirit. Moreover, the storyline involving free love in the Chinese version also reflects the translator's breakthrough and transcendence of traditional views on marriage. In traditional Chinese culture, women's marriage choices were almost entirely subject to family arrangements. By introducing a free-love subplot, the translator grants women the right to choose their own partners, advocating for women's freedom in marriage as part of the "new citizen" ideology. This plot not only overturns the traditional arranged marriage system but also embodies respect for women's individual will and freedom. Through the creation of an independent and self-determined "new woman" character, the translation guides the awakening of contemporary women and promotes their autonomy and status in social, marital, and familial contexts. On this level, Kate's reimagined character not only aligns with Luo Pu's educational vision for the "new citizen," but also reflects his deep concern and hopes for the enhancement of Chinese women's social standing.

5 CONCLUSION

The translation of literary works is not merely a linguistic conversion; it is a deep adaptation to the target culture, the needs of readers, and the translator's motivation. In this process, the characters in the original work often undergo rewriting and reshaping. In *Two Years' Vacation*, Kate, the only female character, undergoes significant transformations in her age, appearance, social status, and even fate upon moving from France to China. This shift reflects not only the translator's "creative rebellion" but also the cumulative influence of the target culture's social and cultural factors. From the perspective of translated Literature, although the rewriting of the character diverges from the original, it gives new life to the original text within the target culture and fosters the exchange and interaction between different social and cultural contexts. Therefore, literary translation is not just a reproduction of the text but also a process of cross-cultural understanding and creative transformation.

FUNDING

This article was supported by the General Research Project in Humanities and Social Sciences at Fuyang Normal University (2021FSSK20).

COMPETING INTERESTS

The authors have no relevant financial or non-financial interests to disclose.

REFERENCES

[1] Han Yiyu. Study on the Chinese Translation of French Literature in the Late Qing and Early Republic Periods. Beijing: China Social Sciences Press, 2008.

[2] Yao Dadui. Verne's Eastern Journey: Political Discourse in "The Fifteen Little Heroes". Literary Criticism, 2020, (01): 216-223.
[3] Wang Jin'an, Shi Juping. Looking at Liang Qichao's Translation of "The Fifteen Little Heroes" from the Perspective of the Target Language Audience. Science and Technology Information, 2012, (27): 196.
[4] Wang Bin. The Dream of Home and Country in Sci-Fi Adventure: An Ethical Construction in Liang Qichao's Translation of "The Fifteen Little Heroes". Chinese Translators Journal, 2016, 37(01): 40-43.
[5] Meng Zhaoyi, Li Zhaidao. A History of Chinese Translated Literature. Beijing: Peking University Press, 2005.
[6] Hermans Theo. Translation in Systems: Descriptive and System-oriented Approaches Explained. Manchester: St, Jerome, 1999.
[7] Gentzler Edwin. Contemporary Translation Theories. Clevedon: Multilingual Matters, 2001.
[8] Bao Xiaoying. A View of the Translation of Chinese Culture in the Field of Medio-translatology: A Study of Professor Xie Tianzhen's Views on the Translation of Chinese Culture. Foreign Language Studies, 2015, 32(05): 78-83.
[9] Xie Tianzhen. Medio-translatology. Shanghai: Shanghai Foreign Language Education Press, 1999.
[10] Xie Tianzhen. Translation Studies: Innovative Concepts and Academic Prospects. Foreign Language Journal, 2019, (04): 95-102.
[11] Jules Verne. Two Years' Vacation. Primento Editions, 1962.
[12] Yin Bingzi, Pi Fasheng, trans. The Fifteen Little Heroes. Shanghai: Shanghai Culture Press, 1956.

Eurasia Journal of Science and Technology
ISSN: 2663-1016
DOI: https://doi.org/10.61784/ejst3040

DESIGN OF A REMOVABLE CYLINDER WASHING MACHINE STRUCTURE BASED ON TRIZ AND QFD

YiMing Zhang[1], RuiSu Yang[1], Yi Sun[1*], ChenRui Liu[1], JiaYi Gao[2]
[1]*School of Management Science and Engineering, Beijing Information Technology University, Beijing 100000, China.*
[2]*School of Architecture and Urban Planning, Beijing University of Architecture and Architecture, Beijing 100044, China.*
Corresponding Author: Yi Sun, Email: 1066482686@qq.com

Abstract: There are various solutions for the development of cleaning methods for the inner drum of a drum washing machine, in which the design and development of the drum structure is difficult because of its many influencing factors and low efficiency and quality assurance, this paper will be through a questionnaire survey, innovative design for the drum structure of the inner drum of a washing machine, and analyze the correlation of the structural functions of a washing machine through the negative correlation characteristics in the quality house, and build an ideal solution. The paper will analyze the interrelationship of the structural functions of the washing machine through the negative correlation characteristic in the quality house to construct the ideal solution. Secondly, through the TRIZ theory of technical contradictions, physical contradictions to analyze the feasibility of the program, after screening to determine the final program, so as to complete the simple disassembly of the internal drum, so as to complete the user more convenient than the traditional washing machine thorough cleaning and maintenance.
Keywords: Inner drum removable washing machine; Contradiction matrix; TRIZ; QFD

1 PROBLEM DESCRIPTION

1.1 Project Overview

1.1.1 Project source

In modern family life, washing machine has become an indispensable household appliance, its cleaning function is directly related to the user's clothing hygiene and health. However, after using for a period of time, dirt will accumulate inside the washing machine. With the cleaning process, the dirt will fall off and mix into the wrinkles of the clothes, and then pollute the clothes. As shown in Figure 1, Figure 2.

Figure 1 Drum Seal Strip of the Washing Machine

Figure 2 Outer Wall of the Washing Machine Drum

1.1.2 Problem description

In order to solve the cleaning problem of the washing machine itself and ensure the clean effect of laundry, some washing machines have added the procedure of "self-cleaning" through detergent soaking, heating and repeated spraying to remove the stains of the washing machine itself. However, the clearance effect can not be completely cleaned up.

The best way of cleaning is still to cleaning. As shown in Figure 3:

Figure 3 Cleaning Effect Diagram of the Washing Machine

This group chooses the creative direction to solve the cleaning problem of washing machine, designed a new washing machine structure, and meet the following limitations:

① The manufacturing of the washing machine should not be too complex, and the cost should not exceed a certain proportion of the price of the existing washing machine (this proportion will be understood through the questionnaire);

② The washing machine does not need a high cost of the overall disassembly and cleaning method;

③ The self-cleaning method of the washing machine should be simple and easy to operate;

④ The service performance, reliability and service life of the washing machine itself should not be affected.

1.2 Initial Situation Analysis of Problems

1.2.1 Main problems exist

The non-disassembly and cleaning of the washing machine can not achieve the purpose of thorough cleaning. The common disassembly methods of mechanical structure can be divided into strike unloading method, pull unloading method, pressure unloading method, temperature difference method and destructive disassembly method. The disassembly method of the washing machine is complex, and the disassembly of the inner bucket needs to be made by professional technical workers to book the door-to-door service. And according to the assembly structure of the unique design of different brands of washing machines, the use of strike and unloading method, through the screwdriver, wrench, flat mouth pliers and other tools, to complete the disassembly. This disassembly cleaning method is difficult to meet the needs of users (see Table 1).

Table 1 Introduction of the Disassembly Method

Technical approach	Disassembly tool	Applicable parts/parts
Knock-off method	Hammers or other heavy objects	Small, medium and large parts/parts
Pull-and-unload method	Dedicated ejector	Disassemble parts that require high accuracy and are not allowed or can not be tapped
Pressure discharge method	Hand presses, hydraulic presses	Status quo simple interference fittings
Temperature difference method	Utilize the thermal expansion and contraction of materials	Larger sizes and hot-loaded parts
Destructive dismantling method	Machine tools such as turning, sawing, drilling, cutting, etc	Fixed connectors, shafts and sleeves have been bitten to each other, and the core value parts have not been preserved and must be destroyed

1.2.2 Current Solutions

After inquiry, the current relatively novel related patents and designs include the following types:

(1)Way to strengthen the water flow cleaning capacity.

According to the author of Beijing industrial and commercial university and other papers, "based on TRIZ ideal solution of automatic washing machine self-cleaning structure innovation design optimization" description, the design is mainly

to improve water valve, in and out of water access components, increase on the automatic washing machine washing machine dehydration tube outer wall and bucket wall self-cleaning function[1].
(2)Add cleaning tools.
According to the invention patent (invention application no.: 201010160548.4) description, disclosed a flexible particles between the washing machine and method, the washing machine with flexible particles between the inside and outside the bucket, through the regular flow of water through the flexible particles impact and friction washing machine, realize the cleaning between the bucket inside and outside the washing machine. Flexible particle materials can be added to sterilization substances, cleaning between the internal and external buckets at the same time, but also for clothing and
(3)washing machine sterilization.
Washing machine that can remove / replace the drum as a whole.
According to the description of the invention patent (invention application number: 201810184251.8), a drum washing machine with a removable washer is disclosed. It can easily take out the washing cylinder from the mouth of the outer cylinder and clean the washing cylinder outside the machine for convenient installation and no need to remove the washing machine.
(4)Non-hole inner drum washing machine.
According to the description of the invention patent (invention application no.: 201410215346.3), a drum washing machine with a non-porous inner cylinder is disclosed, where the washing water is stored in the inner cylinder and there is no water in the outer cylinder, solving the problems of water storage between the inner cylinder and the outer cylinder and the accumulation of dirt between the inner cylinder and the outer cylinder.
(5)The washing machine cleaning the brush
The design of a long handle toothbrush, suitable for cleaning the gap of the drum mouth.

1.2.3 Study objectives

This study aims to explore and propose innovative improvements for the internal cleaning function of washing machines through in-depth analysis of user pain points and needs. The goal is to improve the internal cleaning ability of the washing machines, and enhance the user satisfaction and the market competitiveness of the products.

2 SYSTEMATIC ANALYSIS

2.1 System Analysis

2.1.1 User survey and QFD analysis of drum washing machine

In order to understand users' consumption satisfaction and pain points of drum washing machines, the team made a questionnaire and released it through the "Tencent Questionnaire" to collect data. Survey content includes the basic situation of household washing machine (style, laundry frequency, washing machine capacity), the user view of washing machine since cleaning (use frequency, whether can clean the washing machine), the user view of the pain points of washing machine importance (washing poor, power consumption, noise, complex operation, maintenance difficulties), the user is willing to pay for washing machine additional function project (except mites, intelligent interconnection, drying function, self-cleaning function), etc.
After the recovery and analysis of the questionnaire, we can understand that the main usage of users is the frequency of once every 3 days, the average duration is about 60 minutes, and the service life of most washing machines is more than 5 years. In terms of satisfaction, the use of special functions (such as mite removal, sterilization) are not satisfied with the cleanliness and service life of the washing machine. Users pay more attention to the problem of self-cleaning first, and the problem of mobile convenience. In the cleaning method, the proportion of asking special personnel to dismantle and clean is low, 20 and 20.6% and 23.4% respectively. Based on the analysis and realistic scenarios, the needs of users are derived, created as shown in Figure 4.

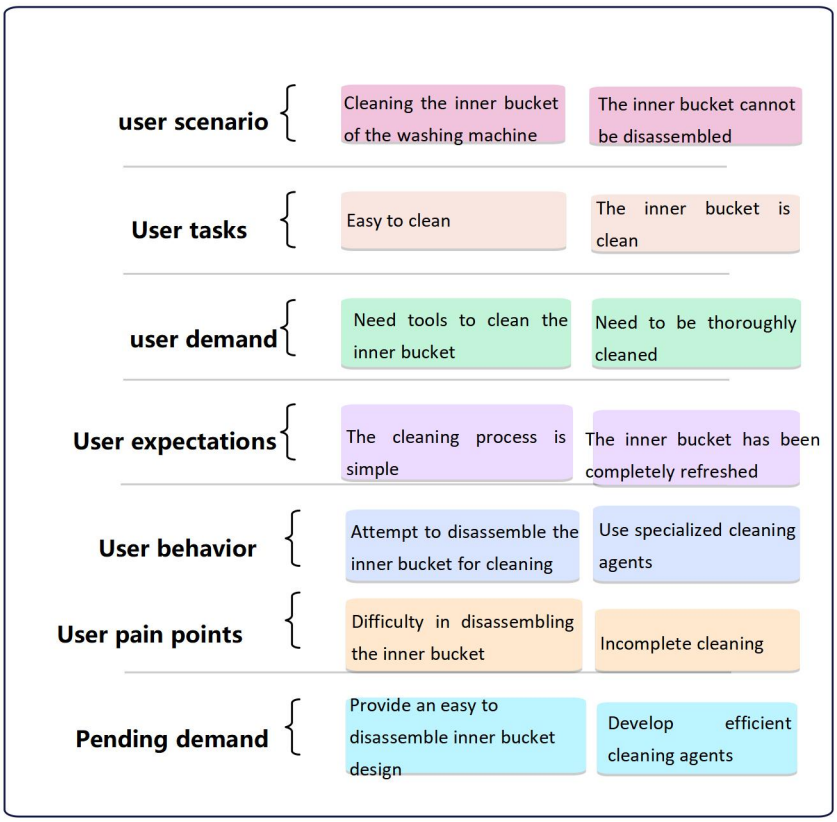

Figure 4 User Story Diagram of Cleaning the Bucket inside the Washing Machine

According to the variance test and T test results, there is no significant difference in the average price of the washing machine for consumers who choose to manually remove the inner cylinder of the washing machine. For the consumers who choose to manually remove the inner cylinder of the washing machine, the average price of the washing machine receiving the cleaning is CHY2707.17, and the standard deviation is 1403.392. Among the consumers who consider the manual disassembly, the average price of the washing machine that accepts the removable inner cylinder is 2CHY558.82, and the standard deviation is 1309.608. We considered no significant difference in the mean of acceptable price between the two groups of users.

According to the user survey results of washing machine and the product structure and function requirements of drum washing machine, QFD design is conducted, as shown in Figure 5. After analysis, the team found that there is a positive correlation between the technical characteristics, such as shock absorption and weight, sealing parts and sealing rust treatment; there is also a negative correlation between the technical characteristics; the vibration will be increased in order to strengthen the washing effect. For energy conservation and environmental protection, consumers and society require water saving and electricity saving, the drum washing machine can use relatively little water to achieve the purpose of environmental protection, but will increase the washing time and reduce customer satisfaction on the other hand. The washing machine in low temperature environment will reduce the solubility of the detergent, so the heating function, adding the drying function, resulting in the deterioration of "energy saving" characteristics; the service life and safety of the washing machine, the machine structure requires good integrity, the assembly way to ensure the tight seal, to achieve waterproof, vibration prevention, insulation and other properties, on the other hand, in order to disassemble, washing machine box, drum, piping system, circuit control system, should be removed, tested and replaced.

Among them, the pain point that is difficult to completely clean is the goal of this study, which requires the structural design and assembly design of the purpose of future maintenance and disassembly, and the convenience of maintenance window and disassembly tools to be considered in advance. The improvement of maintainability has a negative impact on the performance of rust prevention and insulation. The design of opening the window will destroy the integrity of the box and the drum. The existence of this contradiction requires further analysis using TRIZ related theory.

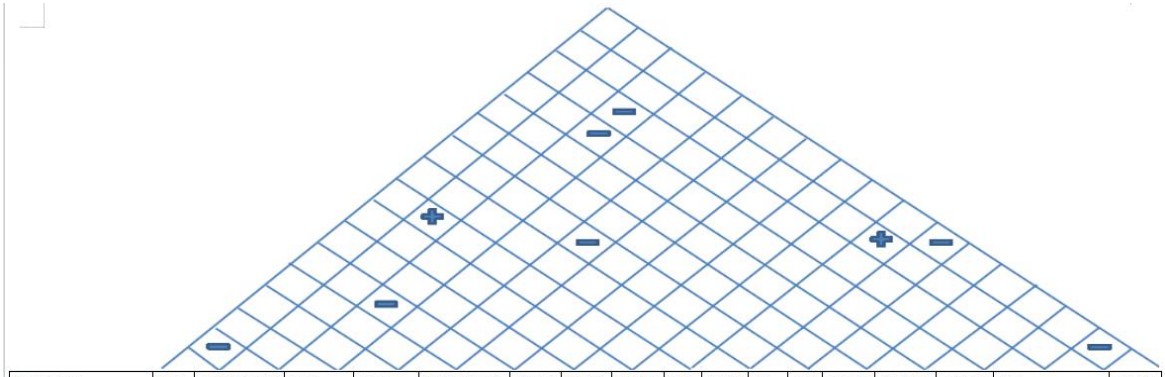

Characteristic customer demand	Speed	Shock absorption system	Power consumption	water consumption	Washing/dehydration capacity	Heating/Drying	operation panel	Washing program	Weight	Sealing element	Box body	Door body	Pipeline system	UV/ozone/silver ions	Intelligentization	Rust prevention/insulation	Assembly method
Clothing cleanliness	5		2	2		2		5						2	2		
Noise level		5							2	4							
Ease of operation							5								5		
energy conservation			5	5		5									4		
Appearance design							5				5	4					
service life		4								4						5	5
Degree of automation								5							5		
Washing time	5				3			4							4		
Special functions (such as sterilization, disinfection, etc.)						3								5			
Price	3	3	4	4	5	3	3	1	1	1	1	1	1	4	1	1	1
Security																4	5
Maintenance and upkeep (washing machine self-cleaning)	3									1	3			3			5

Figure 5 Analysis Diagram of Drum Washing Machine

2.1.2 Final ideal solution (see Table 2)

Table 2 Final Ideal Solution Analysis Table

Question	Analyze the results
The end goal of the design?	The washing machine can be thoroughly cleaned. The outside of the drum can be cleaned without disassembly as a whole.
Idealize the end result?	The structure of the washing machine is not complicated and the cost does not increase.
What are the obstacles to achieving the ideal solution?	The washing machine is operated in a tightened and sealed state.
What is the result of this disorder?	The disassembly of the washing machine requires specialized tools and personnel.
What are the conditions for not having such an obstacle?	The structure and assembly of the washing machine box and drum are simplified.
What are the resources used to create these conditions?	Electricity, air, intelligent systems.

3 USE THE TRIZ TOOL TO SOLVE PROBLEMS

3.1 The TRIZ Tool

3.1.1 Analysis of technical contradictions

In order to increase the cleaning convenience of the washing machine (maintainability), the improvement of the washing machine mechanism, whether it is to increase the window, or expand the gap, or split the drum, will affect the reliability of the washing machine, constitute the technical contradiction between the two parameters.

The improved parameters were maintainability and the deteriorated parameters were reliability. The principle of the invention is found by the contradiction matrix table (see Table 3):

Table 3 Contradiction matrix Table 1

Improved parameters	reliability
Maintainability	11、10、1、16

Principle 11: Pre-prevention principle. For systems with high risk and high cost failure, prepare and compensate in advance to improve the reliability of the system.
Principle 10: Pre-action principle. Act in advance to improve effectiveness and safety and make things simpler before procedures occur.
Principle 1: segmentation principle. Divide an object into separate parts; divide it into easy assembly (or combination) and disassembly; increase the degree of the object segmentation.
Principle 16: deficiency or excessive principle. The desired result is achieved with more or less quantities in situations where controlled precise quantities cannot be achieved.
We use the invention principle 1 (segmentation principle) to open the window or split in the drum wall, so that the cleaning tool can be cleaned or the parts can be removed.
The second step is to consider that opening the window or splitting will destroy the integrity of the drum and reduce the strength of the drum. In order to increase the intensity, the window area will reduce (deteriorate), forming the contradiction between the intensity of the object and the area of the moving object.
The improved parameter is the intensity of the object, and the deteriorated parameter is the area of the moving object. The invention principle is obtained from the contradiction matrix table (see Table 4):

Table 4 Contradiction matrix Table 2

Improved parameters \ deterioration of parameters	The area of the moving object
The strength of the object	3、34、40、29

Principle 3: local characteristics principle —— make different parts of the object should have different functions;
Principle 34: Self-abandonment and regeneration principle. This is the combination of self-abandonment and regeneration. Once a useful function is completed, remove it from the system immediately, or regenerate it immediately for reuse.
Principle 40: Principles of composite materials. Changing the uniform material structure into composite structures to obtain new properties or functions.
Principle 29: Air pressure and hydraulic structure principle. Using air pressure or hydraulic pressure to replace the components or functions of the system often enhances the reliability and controllability of the system.
We use the invention principle 3 (local characteristic principle), so that the different parts of the object should have different functions.
According to the innovative principle found out in the above contradiction matrix, and combined with the requirements of the inner barrel disassembly design of the drum washing machine, the "1 division" and "3 local quality principle" are determined to be in line with the innovation direction of the design through the specific analysis.

3.1.2 Analysis of physical contradiction and separation principle

The more functions the drum washing machine needs to meet, its structure will be more complex, which conflicts with the design requirements of simple washing machine structure and easy to manufacture. Therefore, TRIZ's conflict theory analysis shows that the conflict is a physical conflict and can be directly used to solve[2].
The core idea of solving this physical contradiction in TRIZ theory is to use the separation method to separate the mutually exclusive requirements of a certain characteristic of the research object and meet them separately[3]. In TRIZ theory, the separation principle is used to solve the physical contradictions. The separation parties are divided into four principles: spatial separation, temporal separation, conditional separation, and integral and partial separation. In this design, the spatial separation square and the condition separation are selected (see Table 5).

Table 5 Table of Correspondence between Spatial and Conditional Separation and 40 Invention Principles

	Spatial separation
The corresponding principle of invention	1.Segmentation principle 2.Principle of extraction 3.Principle of local mass 17.Principle of spatial dimensionality change 13.Principle of reverse action 14.The principle of curvature addition 7.Nesting principle 30.Flexible shell or film principle 4.Add the principle of asymmetry 24.With the help of the intermediary principle 26.Replication principle

The spatial separation method corresponds to the 40 inventions, as shown in Table 5. The principles related to mechanical structure design are selected from the invention principle corresponding to the spatial separation principle: 1.

Separation principle; 2. extraction principle; 3. local mass principle; 17. spatial dimension change principle; 13. reverse action principle; 14. curvature increase principle; 7. nested principle; 30. flexible shell or film principle; 4. increased asymmetry principle; 24. assisted agent principle; 26. replication principle. Through the selection of principles, we choose 1. segmentation principle; 3. local quality principle, the following to explain these principles.

The segmentation principle is the first principle in the invention principle of TRIZ, which divides a system into multiple parts in a virtual way or in a real way, so as to decompose (separate, separate, extract) or merge (combine, integrate, combine) a beneficial or harmful system attribute. In most cases, multiple parts of the separation are reorganized (or integrated) to present certain new functions and (or) eliminate harmful effects. With the improvement of the segmentation degree, the technical system gradually develops to the micro level. Its guidelines are: divide an object into multiple separate parts; divide it into parts that are easy to assemble (or combine) and dismantle; and increase the degree of object segmentation[4].

Therefore, in view of the conflict of the drum washing machine, the separation principle of whole and part can be used to divide the cleaning function of the washing machine into independent working content one by one, so as to reduce the difficulty of innovative design[5]. In order to realize the total function of cleaning the outer wall of the inner cylinder of the drum washing machine, the drum of the washing machine can be divided by the principle of separating the whole and the part into several independent parts to achieve. Use the mechanical structure and related modeling knowledge to design the components that can realize each function, and finally get a set of feasible solutions that can meet the needs[6].

4 DETERMINATION OF THE TECHNICAL SCHEME

In the process of this design, the group discussed and analyzed various schemes for cleaning the drum and the outer wall with simple and feasible methods without increasing the cost.

Scheme 1: Rapid disassembly structure of rear plane / side plate of washing machine

This scheme is initially generated according to the idea of dismantling the washing machine, which makes the disassembly process more convenient. Without passing special tools and personnel, it only needs to simply open the side of the wall, open a large enough window, and extend into the cleaning tools, so as to achieve the purpose of cleaning[7].

The advantage of this scheme is that it has little impact on the original structure of the washing machine and does not increase the cost. However, the disadvantage is the size of the window selection, which will increase the risk of leakage, and then produce leakage danger; too small window will produce the cleaning tools can not contact more area, the cleaning purpose can not be realized.

Scheme 2: Expand the front door of the washing machine

This scheme is based on the idea of washing the inner cylinder brush of the washing machine, that the reason why cleaning is not convenient is that the gap is too small, by magnifying the gap and improving the cleaning brush, you can be more convenient in the case without disassembly[8].

After discussion, it is believed that this method has some problems such as affecting the sealing effect and sacrificing the inner cylinder space (and use space), and it cannot guarantee that all the outer and outer walls of the inner cylinder can be completely cleaned[9].

Scheme 3: Opening of the inner wall of the washing machine drum

This scheme is to combine the two ideas of cleaning from the outer opening and the brush, open the "window" in the inside of the drum, open from the inner wall, and extend the cleaning tool. Carry on the cleaning of the outer wall of the inner wall and the outer wall by using the curve Angle of the cleaning brush[10].

The technical focus of this scheme is in the size and number of window sizes. The number of Windows, small size, it is difficult to clean all the position, the expansion of the window, will affect the structural strength of the drum.

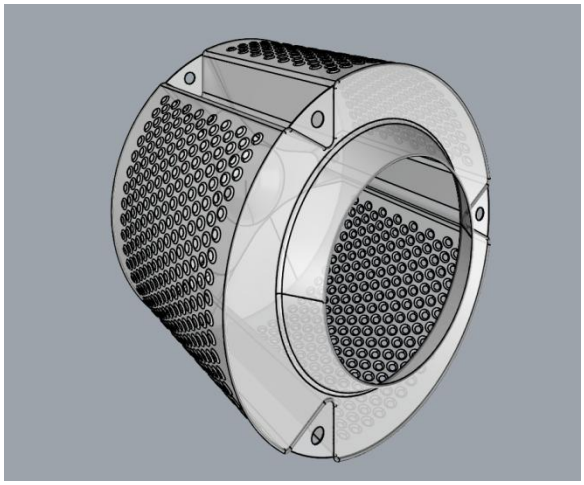

Figure 6 Design Drawing of the Removable Washing Machine Drum

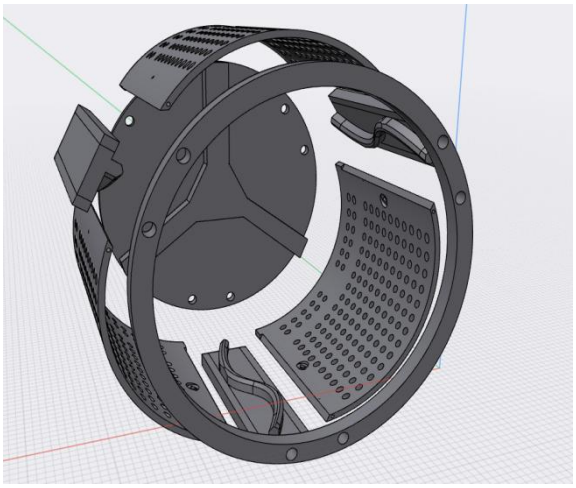

Figure 7 Schematic Diagram of the Drum Parts of the Removable Washing Machine

As shown in Figure 6 and Figure 7 is the drum structure of the washing machine. The washing machine in this design adopts the innovative easy disassembly design, which enables users to easily assemble and assemble the inner drum of the washing machine at home, eliminating the complexity and inconvenience of the traditional professional disassembly method[11]. To achieve this, we have made significant improvements to the internal structure of the washing machine, so that the inner drum will no longer use the overall stainless steel plate design, but is optimized into three distinct uneven plates, reinforcement and bottom plate.

In designing the engagement mode of these components, we introduce the protruding and concave lock and buckle mechanism. This is also used as an error-proof feature to ensure the user's intuitive operation in the disassembly process, reducing the possibility of misoperation, and also guarantee the accuracy of disassembly and assembly. This intuitive and easy to understand design can reduce the risk of error during use.

Despite the ease of easy disassembly design, we recognize that it may bring challenges to the sealing and waterproof performance of washing machines[12]. For this reason, we believe that the washing machine needs to use waterproof and anti-rust steel, so that it can not only improve the durability of the bucket in the washing machine, but also effectively resist rust and wear, to ensure that the washing machine can maintain the best performance in all kinds of environments.

COMPETING INTERESTS

The authors have no relevant financial or non-financial interests to disclose.

FUNDING

This article is supported by the funding of the Undergraduate Innovation and Entrepreneurship Training Program Project of Beijing Information Science and Technology University.

REFERENCE

[1] Wang Z, Luo H, Chen L, et al. Structural improvement of propeller impellers of high-temperature and high-pressure reactor based on TRIZ theory. Proceedings of the Institution of Mechanical Engineers, Part C: Journal of Mechanical Engineering Science, 2024, 238(7): 2602-2615.

[2] Wu D, Fang Y, Du M, et al. Intelligent improvement of gear hobbing process based on the TRIZ method. Journal of Physics: Conference Series, 2024, 2862(1): 012001-012001.

[3] Sarpong S Y N, Akowuah O J, Amoah A E, et al. Enhancing cassava grater design: A customer-driven approach using AHP, QFD, and TRIZ integration. Heliyon, 2024, 10(16): e36167-e36167.

[4] Shengqiao W, Dongyang B, Jianguo Z, et al. Optimization Study of Porosity Problem in Hand Gluing Process Based on TRIZ Theory. International Journal of Frontiers in Engineering Technology, 2024, 6(4).

[5] AI-Powered Laundry Revolution: How Smart Technologies are Transforming Washing Machines and Dryers in 2024. M2 Presswire, 2024.

[6] Amin A M, Baldacci R. QFD-based optimization model for mitigating sustainable supply chain management adoption challenges for Bangladeshi RMG industries. Journal of Cleaner Production, 2024: 472143460-143460.

[7] Liu T, Lv B, Zhu W, et al. Optimisation design of water-fertiliser infiltration device based on TRIZ theory. Journal of Physics: Conference Series, 2024, 2827(1): 012028-012028.

[8] Super Clean Machine - Long Island Power Washing & Paver Sealing Announces Premier Power Washing Services for Homes and Businesses. M2 Presswire, 2024.

[9] Super Clean Machine Offers Expert Low Pressure House Washing for Delicate Surfaces. M2 Presswire, 2024.

[10] Hagan A K N, Talburt R J. SparkDWM: a scalable design of a Data Washing Machine using Apache Spark. Frontiers in Big Data, 2024, 71446071-1446071.
[11] Duy Q B, Hung Q N ,Vuong L H. A control system for MR damper-based suspension of front-loaded washing machines featuring magnetic induction coils and phase-lead compensator. Journal of Intelligent Material Systems and Structures, 2023, 34(6):631-641.
[12] Laura P T, Beatriz F G ,Xavier D I G .Investigating a repair workshop: The reuse of washing machines in Barcelona. Sustainable Production and Consumption, 2022, 29171-179.